R. H. C. LIBRARY
CLASS No. CCE Whe
ACC. No. 85,561
DATE ACQ Dec. 1968.

Absolute Infrared Absorption Intensities in Some Aromatic Systems

by Winston Wheatley, B.Sc., M.Sc.

A thesis presented to the Faculty of Science of the University of London in candidature for the degree of Doctor of Philosophy.

Chemistry Department,
Royal Holloway College,
(University of London)
Englefield Green,
Surrey.

September 1968.

ProQuest Number: 10096747

All rights reserved

INFORMATION TO ALL USERS
The quality of this reproduction is dependent upon the quality of the copy submitted.

In the unlikely event that the author did not send a complete manuscript
and there are missing pages, these will be noted. Also, if material had to be removed,
a note will indicate the deletion.

ProQuest 10096747

Published by ProQuest LLC(2016). Copyright of the Dissertation is held by the Author.

All rights reserved.
This work is protected against unauthorized copying under Title 17, United States Code.
Microform Edition © ProQuest LLC.

ProQuest LLC
789 East Eisenhower Parkway
P.O. Box 1346
Ann Arbor, MI 48106-1346

To my parents

Acknowledgements

The author wishes to express his sincere gratitude to Dr. D. Steele for advice and guidance during the preparation of this thesis and for the personal interest he has taken in the work.

Thanks are also due to Mr. E. Smethurst for invaluable technical assistance and to Drs. P.N. Gates and K. Radcliffe for many hours of helpful discussion.

Financial assistance from the Institute of Petroleum, Hydrocarbon Research Group is gratefully acknowledged.

Abstract

The π electron rehybridization accompanying deformation of an aromatic substituent out of the plane of the ring has been invoked in the past to explain differences between the effective CH dipoles of benzene as deduced from intensity studies of in-plane and out-of-plane vibrations. As such rehybridization is likely to make a considerable contribution to intermolecular forces between aromatic systems an attempt has been made to verify the rehybridization theory. The magnitude of the rehybridization moment should be independent of the substituents on the aromatic ring.

An analysis of the vapour phase band intensities of hexafluorobenzene has established that the difference between the effective CF dipoles as deduced from the in-plane and out-of-plane vibrations is 0.3 D. in the sense compatible with the fluorine atom being at the negative end of the dipole. This rehybridization moment of 0.3 D. is equal to that deduced for benzene. Refinement of the analysis is achieved by the determination of Coriolis coupling coefficients and absolute intensities from band shape calculations. A computer program has been written for this purpose.

The intensities of all infrared active fundamental bands of hexafluorobenzene have been measured in solution in carbon disulphide, cyclohexane and benzene. The intensity changes are satisfactorily correlated on the basis of dielectric theories except for the A_{2u} fundamental of hexafluorobenzene in benzene.

Benzene interacts with many weak electron acceptors to form weakly bound complexes. The weak complexes formed between benzene and hexafluorobenzene and benzene and boron tribromide have been investigated.

R. H. C.
LIBRARY

A high pressure system has been developed to study the pressure and temperature dependence of the infrared absorption intensities of the fundamental vibrations of benzene.

Contents

General Introduction

Vibrational band intensities are intimately related to the movement of electronic charge which occurs during the associated vibrational quantum transitions. Consequently, in principle, the interpretation of infrared absorption intensities can provide information concerned with the charge distribution in molecules and on the redistribution of charge which occurs during molecular deformations. Progress in this line of research has been somewhat restricted by the need for more exact experimental intensity data and also by the fact that the interpretation of the data in terms of bond electrical properties has proved to be a complex and vexing problem.

In the double-harmonic bond-moment approximation the absolute intensity of a vibrational fundamental is directly proportional to the square of the gradient of the dipole vector with respect to the associated normal coordinate, $\frac{\partial \mu}{\partial Q_i}$, and several approaches have been made to relate this quantity to bond electrical properties. The various interpretations have been based largely on the concepts of individual bond moments and bond dipole derivatives. It has been generally concluded that in the simple bond moment hypothesis the deduced bond parameters are not generally transferable between molecules and rarely even transferable from one vibrational species to another in the same molecule. The elementary treatment has been supplemented in recent years by the inclusion of additional (cross) terms into the theory. However, such a scheme is tedious and increases the number of bond parameters by a factor of three. Nevertheless, Sverdlov has applied the second-order bond-moment hypothesis to a variety of molecules and the deduced bond parameters are generally

transferable. An appreciation of the results necessitates careful assessment of the relative importance of the additional terms. Indeed Gribov has criticized the Sverdlov theory on the grounds that quite often the additional parameters cannot be determined even for the simplest system thereby reducing the value of the theory without adding anything to an understanding of the dynamics of the problem.

Physical chemists prefer to treat the properties of molecules as the sum of a set of bond properties and the inherent assumptions of the simple bond-moment hypothesis produce the desired simplification. In spite of the shortcomings of the hypothesis, a careful analysis of many of the inconsistencies in the deduced bond parameters has provided a great deal of information concerning molecular structure. Many of the 'apparent' discrepancies in the deduced bond parameters can be readily understood - at least qualitatively - to be a consequence of hybridization changes which accompany bond length and bond angle deformations. In principle, the variations in bond dipoles and bond dipole gradients for particular bonds in a series of related molecules may be of even greater interest as they may indicate the magnitude of the electron displacement.

If the rehybridization phenomena is really significant then it is expected to manifest itself in certain modes of any π electron system. Furthermore, since rehybridization changes are determined almost exclusively by the angle between the bond linking the substituent atom to the atom involved in the π system and the plane of the molecule, a similar magnitude of the effect is anticipated for the same deformation in a series of related molecules.

The first section of this thesis is concerned with the vibrational intensities of hexafluorobenzene in the vapour phase. The data are interpreted on the basis of the simple bond-moment hypothesis and critically compared with reported data for related molecules. Support for the concept of a rehybridization moment associated with certain modes is obtained from the study.

It is possible that the concept may also be responsible for many of the glaring discrepancies that exist between condensed and solution phase infrared intensities and the values that can be predicted from vapour phase data using simple dielectric theories. Absolute infrared intensities offer many advantages for the study of environmental effects, specific interactions, weak complexes and intermolecular interactions. The rehybridization phenomena may be important in such studies.

The later chapters of this thesis are concerned with the solution phase infrared intensities of hexafluorobenzene and intensity data on the complexes formed between hexafluorobenzene and benzene and between benzene and boron tribromide.

CHAPTER ONE

Absolute Infrared Intensities - General Theory

A complete understanding of the absolute intensities of infrared absorption bands requires a close look at the mechanism by which electromagnetic radiation interacts with matter. There is a finite probability that a molecule will exchange energy with a radiating field and undergo a transition between an initial and a final quantum state. This process gives rise to a spectral line of finite width and intensity at a particular frequency, ν, given by the Bohr frequency rule

$$\nu_{n'',n'} = \nu_{n',n''} = \frac{E' - E''}{h} \qquad 1.1$$

where E refers to the energies of the n" and n' quantum states and h is Planck's constant. If $E'' < E'$ radiation is absorbed by the molecule giving rise to an absorption spectrum and if $E'' > E'$ radiation is emitted by the molecule giving rise to an emission spectrum.

The intensity of the resulting spectral line is determined by the probability of the transition which gives rise to the line. It can be shown that the probability of a randomly oriented molecule being promoted from a state n" to a state n' is

$$\frac{8\pi^3}{3h^2} \langle n''/\mu/n' \rangle^2 . (\rho\nu_{n'',n'}) \qquad 1.2$$

where $\langle n''/\mu/n' \rangle$ is the quantum mechanical matrix element of the dipole moment of the molecule with respect to the wave functions of the respective states and $(\rho\nu_{n'',n'})$ is the radiation density for the particular frequency of transition. The probability of induced emission is given by the same expression with the primes reversed and thus the net absorption probability is given by:

$$\frac{8\pi^3}{3h^2} \langle n''/\mu/n' \rangle^2 . (\rho \nu_{n'',n'})(N''_n - N'_n) \qquad 1.3$$

where N_n represents the number of molecules per unit volume in each state.

Each such transition reduces the energy of the field by an amount $h\nu_{n'',n'}$ so that the net loss of energy for a differential element of absorbing material of length dl and of unit cross-sectional area will be

$$- dI = \nu_{n'',n'} \frac{8\pi^3}{3h} \langle n''/\mu/n' \rangle^2 . (\rho \nu_{n'',n'})(N''_n - N'_n)\, dl \qquad 1.4$$

The radiation flux intensity is related to the radiation density by

$$I = c\rho \qquad 1.5$$

where c is the velocity of light. Substitution for ρ followed by integration yields.

$$\log_e \frac{I_0}{I} = \nu_{n'',n'} \frac{8\pi^3 l}{3hc} . \langle n''/\mu/n' \rangle^2 . (N''_n - N'_n) \qquad 1.6$$

At equilibrium, the Boltzmann expression represents the relative populations of the states n" and n'

$$N'_n = N''_n\, e - (E' - E'')/_{kT} \qquad 1.7$$

hence

$$N''_n - N'_n = pN \left[\frac{e^{-E''/kT} - e^{-E'/kT}}{\sum_i e^{-E_i/kT}} \right] \qquad 1.8$$

where N is Avagudra's number and p is the molar concentration. Substitution is 1.6 and subsequent rearrangement gives

$$\alpha(\nu) = \frac{1}{pl} \log_e \frac{I_0}{I} = \nu_{n'',n'} \frac{8\pi^3 N}{3hc} \langle n''/\mu/n' \rangle^2 \left[\qquad \right] \qquad 1.9$$

The left hand side of 1.9 defines an experimentally observable quantity, the absorption coefficient, $\alpha(\nu)$, of the spectral line.

It is well known both from experiment and theory[1] that an absorption line has a finite width so that it is more realistic to write

$$\int_{\text{line}} \alpha(\nu)d\nu = \nu_{n'',n'} \frac{8\pi^3 N}{3hc} \langle n''/\mu/n' \rangle^2 \left[\quad \right] \qquad 1.10$$

This defines the total integrated line absorption coefficient.

An infrared absorption band is assigned to transitions between two vibrational states and a fundamental band corresponds to a single vibrational transition from the state V = 0 to the state V = I. Due to accompanying rotational transitions a fundamental infrared absorption band has many rotational components and the total integrated intensity is obtained by summing the rotational fine structure over the whole band.[2]

$$\Gamma_\nu = \frac{1}{pl} \int_{\text{BAND}} \log_e \frac{I_0}{I} d\nu = \frac{8\pi^3 N}{3hc} \langle o/\mu/1 \rangle^2 \qquad 1.11$$

The factor $\left[\quad \right]$ is usually close to unity and is therefore omitted. The frequency is slightly different for each rotational component so that it is more correct to write[2]

$$\Gamma_{0,1} = \frac{1}{pl} \int_{\text{BAND}} \log_e \frac{I_0}{I} d(\log\nu) = \frac{8\pi^3 N}{3hc} \langle o/\mu/1 \rangle^2 \qquad 1.12$$

This defines the integrated intensity of a vibrational fundamental.

Equation 1.12 is exact for a single transition between the ground vibrational level V = 0 and an upper vibrational level V = I. However, such a transition can seldom be studied in practice, for most spectral bands consist of a main band with a number of overlapping hot bands. The increased absorption due to the hot bands is exactly compensated by the increase in induced emission and the experimental intensity is determined by integrating over a fundamental and all the associated hot bands.[3,4]

The summation can be carried out exactly to yield

$$\Gamma_{OBS.} = \frac{8\pi^3 N}{3hc} \langle o/\mu/1 \rangle^2 \qquad 1.12a$$

which is the same as 1.12.

When the vibration is degenerate the expression applies to each of the components of the degeneracy so that it is necessary to introduce a degeneracy factor, g, into the expression,

$$\Gamma = \frac{8\pi^3 Ng}{3hc} \langle o/\mu/1 \rangle^2 . \qquad 1.13$$

In this derivation rotational quantization has so far been neglected. It can be shown that an exact summation over the associated rotational components in the case of symmetric top molecules requires a correction factor which is equivalent to multiplying the right hand side by the factor[5]

$$1 + \frac{2Bc}{\nu_o} \frac{1 + e^{-h\nu_o/kT}}{1 - e^{-h\nu_o/kT}} \qquad 1.14$$

where B is the rotational constant, $B = \frac{h}{8\pi c I_B}$ and I_B is the moment of inertia perpendicular to the symmetry axis. Neglect of rotational quantization introduces an error of less than a few percent.

At this point it is convenient to develop the quantum mechanical matrix element of the dipole moment in terms of quantities which can be related to bond properties.

$$\langle o/\mu/1 \rangle = \int \psi_o^* \, \mu \, \psi_1 \, d\tau \qquad 1.15$$

where ψ_o^* is the complex conjugate of the complete wave function for the ground state, μ is the electric moment of the system, ψ_1 is the wave function for the state V = I and $d\tau$ is the volume element of configuration space. The electric moment of a molecule is a vector quantity having

components μ_x, μ_y and μ_z which can be expressed

$$\mu_x = \sum_i e_i X_i, \quad \mu_y = \sum_i e_i Y_i \text{ and } \mu_z = \quad e_i Z_i \qquad 1.16$$

where e_i is the charge on the i-th particle and X_i, Y_i and Z_i are the space-fixed cartesian coordinates of the i-th particle, the sum being over all particles. In general, the electric moment can be expanded as a power series in the coordinates of the atoms. A Taylor series expansion in terms of normal coordinates is most convenient

$$\mu_x = \mu_x^o + \sum_{k=1}^{3N-6} \frac{\partial \mu_x}{\partial Q_k} Q_k + \text{higher order terms} \quad . \qquad 1.17$$

Similar expressions describe μ_y and μ_z. The term μ_x^o is the x component of the permanent electric moment of the molecule, $\frac{\partial \mu_x}{\partial Q_k}$ is the dipole moment derivative with respect to the normal coordinate Q_k and the summation is over the 3N-6 normal coordinates used to describe the motion of a system of N particles. If "higher order terms" are neglected and if the vibrational wave function ψ_v is the product of harmonic oscillator functions then we write

$$\int \psi_{v'}^* \mu_x \psi_{v''} d\tau_v = \mu_x^o \int \psi_{v'}^* \psi_{v''} d\tau_v + \sum_{k=1}^{3N-6} \frac{\partial \mu_x}{\partial Q_k} \int \psi_{v'}^* Q_k \psi_{v''} d\tau_v$$

1.18

The first term on the right hand side vanishes unless v" = v' because of orthogonality of the functions ψ_v and therefore the permanent electric moment μ^o has no influence on the intensity of vibrational transitions. The integral in the second term can be expressed as product-type wave functions

$$\int \psi_{v'}^* Q_k \psi_{v''} d\tau_v = \int \psi_{v_1'}^* (Q_1) \psi_{v_1''}(Q_1) dQ_1 \int \ldots\ldots \int \ldots\ldots \qquad 1.19$$

and again because of orthogonality of the functions ψ_v the integral will vanish unless $v_1' = v_1''$, etc. with the exception of v_k' and v_k''. If the integral $\int \psi^*_{v_k'} (Q_k)\, Q_k\, \psi_{v_k''} (Q_k)\, dQ_k$ is to differ from zero then it must be true that $v_k'' = v_k' + 1$ or $v_k'' = v_k' - 1$. The conclusion is reached that only linear terms in the electric moment expansion influence the intensity of vibrational transitions and that the only vibrational transitions which can occur with emission or absorption of radiation are those in which only one quantum number changes and that by one unit only.

With these selection rules we can write

$$\langle 0/\mu_x/1 \rangle = \frac{\partial \mu_x}{\partial Q_k} \int \psi_0^*\, Q_k\, \psi_1\, dQ_k \,. \qquad 1.20$$

The integral involving the harmonic oscillator wave functions is expressed in explicit form by

$$\int \psi_0^*\, Q_k\, \psi_1 dQ_k = \left(\frac{h}{8\pi^2 \nu_i}\right)^{\frac{1}{2}} \qquad 1.21$$

hence

$$\langle 0/\mu_x/1 \rangle^2 = \frac{h}{8\pi^2 \nu_i} \left(\frac{\partial \mu_x}{\partial Q_k}\right)^2 \qquad 1.22$$

where ν_i is the harmonic frequency of the i-th mode. Substitution for $\langle 0/\mu/1 \rangle$ in 1.15 yields the relationship

$$\Gamma = \frac{N\pi^2}{3c\nu_i} \sum_{x,y,z} \left(\frac{\partial \mu}{\partial Q_k}\right)^2 \qquad 1.23$$

between the integrated intensity of a fundamental infrared absorption band and the derivative of the molecular dipole moment with respect to a normal coordinate. For molecules of high symmetry, all except one of the components of the dipole derivative will vanish for vibrations of a particular symmetry class provided that the axes are chosen to coincide with the symmetry axes, i.e. the change in dipole moment will be oriented

along a fixed direction in the molecule for all vibrations of that symmetry class.

At this point it is convenient to discuss the most commonly used intensity units. It follows immediately from 1.12 that the units of are (concentration x length)$^{-1}$ and Crawford[2] has suggested that the most appropriate units are therefore mol^{-1}.cm^{2}. Vibrational intensities are often expressed in terms of a quantity, A

$$A = \frac{1}{pl}\int \log_e \frac{I_0}{I}\, d\nu \qquad 1.24$$

which has the units of frequency x (concentration x length)$^{-1}$. The units of frequency most commonly used in the infrared region are cm^{-1}. All expressions derived so far have expressed frequency in units of cycles/sec. It is convenient to use the cm^{-1} frequency unit and from the definitions of Γ and A it follows that they are related by the approximate expression

$$A = \Gamma \bar{\nu}_o \qquad 1.25$$

where $\bar{\nu}_o$ is the frequency of the band origin in cm^{-1}. Re-writing 1.23 with the frequency in cm^{-1} units we obtain

$$\Gamma = \frac{N\pi\alpha}{3c^2\bar{\nu}_i} \cdot \sum_{x,y,z}\left(\frac{\partial\mu}{\partial Q_k}\right)^2 \qquad 1.26$$

hence

$$A = \frac{\bar{\nu}_o}{\bar{\nu}_i} \cdot \frac{N\pi\alpha}{3c^2} \cdot \sum_{x,y,z}\left(\frac{\partial\mu}{\partial Q_k}\right)^2 . \qquad 1.27$$

Whenever the intensity is expressed in terms of A, the absorption frequency $\bar{\nu}_o$ is assumed to be constant over the whole band and equal to the harmonic frequency $\bar{\nu}_i$ so that many authors use the simplified expression

$$A = \frac{1}{pl}\int \log_e \frac{I_0}{I}\, d\tilde{\nu} = \frac{N\pi g}{3c^2} \sum_{x,y,z}\left(\frac{\partial\mu}{\partial Q_k}\right)^2 \qquad 1.28$$

The units of A are therefore $mol^{-1}.cm.$ Whiffen has expressed absolute intensities in units of $mol^{-1}.cm^2.sec^{-1}.$ which is equivalent to expressing an A value as $\frac{N\pi g}{3c} \sum_{x,y,z}\left(\frac{\partial\mu}{\partial Q_k}\right)^2$. For consistency we will quote intensities in terms of $mol^{-1}.cm^2.sec^{-1}$.

In the double harmonic oscillator approximation the square of the dipole moment derivative with respect to the normal coordinate is directly proportional to the integrated absorption intensity. Normal coordinates and internal symmetry coordinates are related by linear transformations of the type

$$Q_k = \sum_{k'} \left(L^{-1}\right)_{kk'} S_{k'} \qquad 1.29$$

$$\text{or} \quad S_{k'} = \sum_k L_{kk'} Q_k$$

where $L_{kk'}$ are the elements of the L matrix obtained by solution of the secular equation, so that it is convenient to express dipole moment derivatives with respect to internal symmetry coordinates. From 1.29 it follows that

$$\frac{\partial\mu}{\partial S_{k'}} = \sum_k \frac{\partial\mu}{\partial Q_k}\cdot\frac{\partial Q_k}{\partial S_{k'}} = \sum_k \frac{\partial\mu}{\partial Q_k}\left(L^{-1}\right)_{kk'} \qquad 1.30$$

and

$$\frac{\partial\mu}{\partial Q_k} = \sum_{k'} \frac{\partial\mu}{\partial S_{k'}}\cdot L_{kk'} \quad . \qquad 1.31$$

The calculation of any particular $\frac{\partial\mu}{\partial S_{k'}}$ requires the knowledge of all $\frac{\partial\mu}{\partial Q_k}$ values for the particular symmetry species.

The question of the sign of the square root of the intensity

introduces a serious uncertainty into the interpretation of the dipole moment derivative in terms of bond properties. In general, if there are n fundamental vibrations in a particular symmetry class then there will be 2^n different sign combinations leading to 2^n distinct solutions for the bond parameters. A choice is made between the values on the basis of lack of credulity of the authors to certain of the derived gradients. Where isotopic data is available the principal method of eliminating certain sign combinations is the failure of the $\frac{\partial \mu}{\partial S}$ to transfer. Occasionally the chosen set can be confirmed by vibration-rotation interaction studies.[6]

If the molecule has a high degree of symmetry the matrix factorises into diagonal blocks and $_{kk'}$ vanishes unless $S_{kk'}$ and Q_k belong to the same irreducible representation. Further, since normal coordinates and matrix vectors are calculated from the vibrational secular equation, reliable values of $\frac{\partial \mu}{\partial Q_k}$, can be obtained for molecules which have been the subject of intensive force constant calculations.

It is convenient to develop the theory of infrared absorption intensities further and to show how they can be interpreted in terms of quantities which are related to bond parameters.

In order to reduce dipole moment derivatives to quantities which are characteristic of individual bonds it is necessary to introduce a set of assumptions that will allow molecular properties to be represented by the sum of a set of bond properties. The assumptions of such a hypothesis are:

i) the stretching of a bond by dr produces a dipole moment change

directed along the bond of $\left(\frac{\partial \mu}{\partial r}\right) dr$;

ii) the deformation of a bond through an angle $d\Theta$ produces a dipole moment change perpendicular to the bond and in the plane of movement of $\frac{\partial \mu}{\partial \Theta} \cdot d\Theta$

iii) a change in one bond does not result in changes in another bond, except when this is geometrically necessary.

With these assumptions, the total moment resulting from an arbitrary distortion is the vector sum of the moments produced by each individual bond. The great value of such a hypothesis, the independent bond moment hypothesis, lies in the fact that data on many molecules is reduced to a common basis. There have been several critical reviews of the IBMM[7,8] and a large number of bond moments and effective charges have been tabulated.[7,8] The general conclusion is that, although there is a certain amount of consistency between values for similar molecules, some glaring discrepancies exist and it seems that in the double harmonic-bond moment approximation, the deduced bond moments are not transferable between molecules and rarely even transferable from one vibrational class to another of the same molecule. Qualitatively many of the inconsistencies may be reconciled by allowing for the presence of lone-pair electrons, for hybridization changes which accompany bond length and bond angle deformations and for the effects of the higher terms in the dipole moment expansion. All of these factors together with related phenomena have been critically reviewed by Coulson.[9]

A clear example of how an apparent inconsistency can be understood, at least qualitatively, is in the case of benzene. Deformation of a CH

bond in a direction perpendicular to the plane of the ring can be expected to result in considerable delocalization of electronic charge about the C nucleus. The rehybridization will result in an increase of s character in the p_z orbital. A similar effect is not possible for CH deformation in the plane of the ring since the perpendicular p_z orbitals cannot be involved. The net effect is to make the CH dipole more positive in the out-of-plane (γ_{CH}) motion. Spedding and Whiffen[10] have deduced values for the dipole gradients associated with the two motions from infrared intensity studies using an L matrix from the Whiffen force field of benzene.[11,12] They show that the dipole gradient for out-of-plane motion is greater than that for the in-plane by an amount 0.3D. This is in accord with expectation provided that the H atom is at the positive end of the CH dipole as seems probable from the available evidence.

In the theory of Sverdlov[13] which extends the simple bond moment hypothesis to try and explain variations in the effective bond dipoles and bond dipole gradients it is assumed that the bond dipole vector departs from the bond direction as a result of the movement of atoms not associated with that particular bond. This necessitates the introduction of derivatives of the dipole perpendicular to the bond with respect to each type of bond distortion. The scheme is tedious and increases the number of parameters by a factor of three. Application of the Sverdlov theory to benzene has been claimed by Kovner and Snegirev.[14] They reject as physically meaningless the apparent inconsistency in the dipole gradients for the two types of motion and by introducing second order dipole derivatives such as $\frac{\partial^2 \mu}{\partial \beta^i \partial \beta^j}$ into the theory they obtain an

unequivocal value of 0.65D for the CH dipole produced by both motions. This value agrees well with the value for the out-of-plane motion as deduced by Spedding and Whiffen[10] (as indeed it must since no new parameters are introduced into $\frac{\partial \mu}{\partial S_{A2u}}$) and also with the value derived for ethylene by Sverdlov.[15] Thus, it appears that the apparent inconsistency in the value of the CH dipole for in-plane motion can be reconciled on the basis of two different theories.

It is the author's belief that the rehybridization phenomenon and the associated vibronic effects are of significance and that they are probably more physically meaningful than the second order dipole derivatives. Furthermore, it is suggested that they may be responsible for many of the discrepancies which exist between absolute intensity data for condensed and solution phases and the values predicted from vapour phase values using simple dielectric theories. Infrared intensities can offer several advantages over other spectroscopic techniques which are used to study environmental effects, specific interactions and 'weak complexes'. The concept of a rehybridization moment may also be significant in the interpretation of many of the intensity changes which are associated with π-π donor-acceptor interactions.

The work described in this thesis was undertaken with the primary aim of justifying the existence of a rehybridization moment and to attach some physical meaning to its potential importance. The phenomenon only involves the electron cloud associated with the carbon nuclei so that it is anticipated that the rehybridization moment should be insensitive to the substituent on the aromatic ring. For vapour phase intensity studies

in the infrared a volatile compound of high symmetry is essential. Apart from benzene itself, hexafluorobenzene is the only volatile aromatic of D_{6h} symmetry and its remarkable similarity to benzene makes it a natural choice for this project. The absolute intensities of hexafluorobenzene have been experimentally determined and interpreted in a similar manner to that used by Spedding and Whiffen for benzene.[10] The data for both molecules have been critically examined with particular emphasis on the choice of the signs of the dipole gradients and the reliability of the existing force fields.

CHAPTER TWO

The Force Fields of Benzene and Hexafluorobenzene

The work described in this thesis is essentially concerned with the absolute intensities of the fundamental vibrations of benzene and hexafluorobenzene. It is well appreciated that the interpretation of the absolute intensities of infrared absorption bands in terms of bond properties requires a detailed knowledge of the mode of vibration. The exact form of the normal coordinate associated with each vibrational frequency can only be determined from force constant calculations, since a knowledge of the normal coordinate implies a detailed knowledge of the force field, and therefore a close examination of the available force fields is important.

The symmetry of the molecules, benzene and hexafluorobenzene, is that of the point group D_{6h} which consists of the following symmetry operations.

$$E, 2C_6, 2C_3, C_2, 3C_2', 3C_2'', i, 2S_3, 2S_6, \sigma_h, 3\sigma_d, 3\sigma_v.$$

Table 2.1 contains the character table for the group D_{6h} and the analysis of the various coordinate representations into the irreducible representations. The representation is identical with that of a set of 3N cartesian displacement coordinates and when the contributions of the rotational and translational normal coordinates are subtracted the reduced form of the vibrational normal coordinates can be expressed:

$$2A_{1g} + A_{2g} + 2B_{2g} + E_{1g} + 4E_{2g} + A_{2u} + 2B_{1u} + 2B_{2u} + 3E_{1u} + 2E_{2u}$$

It is convenient to consider the in-plane and out-of-plane modes separately. The normal modes of species $2A_{1g} + A_{2g} + 4E_{2g} + 2B_{1u} + 2B_{2u} + 3E_{1u}$ constitute the in-plane modes, while those of species

Character Table for the Group D_{6h} and Analysis of the Various Coordinate Representations in Irreducible Representations

D_{6h}	E	$2C_6$	$2C_3$	C_2	$3C_2'$	$3C_2''$	i	$2S_3$	$2S_6$	σ_h	$3\sigma_d$	$3\sigma_v$	n_c	n_x	n_T	n_R	n_v
A_{1g}	1	1	1	1	1	1	1	1	1	1	1	1	1	1	0	0	2
A_{2g}	1	1	1	1	-1	-1	1	1	1	1	-1	-1	1	1	0	1	1
B_{1g}	1	-1	1	-1	1	-1	1	-1	1	-1	1	-1	0	0	0	0	0
B_{2g}	1	-1	1	-1	-1	1	1	-1	1	-1	-1	1	1	1	0	0	2
E_{1g}	2	1	-1	-2	0	0	2	1	-1	-2	0	0	1	1	0	1	1
E_{2g}	2	-1	-1	2	0	0	2	-1	-1	2	0	0	2	2	0	0	4
A_{1u}	1	1	1	1	1	1	-1	-1	-1	-1	-1	-1	0	0	0	0	0
A_{2u}	1	1	1	1	-1	-1	-1	-1	-1	-1	1	1	1	1	1	0	1
B_{1u}	1	-1	1	-1	1	-1	-1	1	-1	1	-1	1	1	1	0	0	2
B_{2u}	1	-1	1	-1	-1	1	-1	1	-1	1	1	-1	1	1	0	0	2
E_{1u}	2	1	-1	-2	0	0	-2	-1	1	2	0	0	2	2	1	0	3
E_{2u}	2	-1	-1	-2	0	0	-2	1	1	-2	0	0	1	1	0	0	2

Table 2.1

$$2B_{2g} + E_{1g} + A_{2u} + 2E_{2u}$$

are the out-of-plane modes. In-plane and out-of-plane modes are conveniently distinguished by reference to the character of $_h$ which is positive for in-plane modes and negative for out-of-plane.

The selection rules for fundamentals allow the

$$2A_{1g}(\text{polarized}),\ E_{1g} \text{ and } 4E_{2g}$$

frequencies to be Raman active and the

$$A_{2u}(\text{parallel}) \text{ and } 3E_{1u}(\text{perpendicular})$$

frequencies to be infrared active. The remaining nine frequencies are forbidden in both spectra.

Analysis of the vibrational spectrum of benzene has been the subject of some intensive work and the complete vibrational assignment of all fundamentals is now well accepted.[11,16,17,18]

The vibrational spectrum of hexafluorobenzene has been analysed by Delbouille[19] and also by Steele and Whiffen.[20] Agreement between the two analyses is good except that the assignments of ν_{20} and ν_{11} are reversed. In particular, Steele and Whiffen assigned the three bands at 1531, 1020-1002 and 315cm^{-1} to the three doubly degenerate E_{1u} fundamentals ν_{18}, ν_{19} and ν_{20} respectively and the band at 215cm^{-1} to the A_{2u} fundamental ν_{11}. Delbouille reversed the assignment of the two low frequency infrared active fundamentals. Clear-cut evidence in favour of the Steele and Whiffen assignment is afforded by the infrared band contour of the band at 215cm^{-1}. The observed PR separation is in good agreement with the separation calculated for a parallel band of a symmetric top molecule. A similar conclusion was reached by Person et al[21]. However,

these workers also note that the band at 315cm^{-1} showed no splitting in the crystal, while the bands at 1531 and 1020-1002 cm^{-1} both showed the characteristic splitting observed for the E_{1u} fundamentals in benzene.[22] Person et al tentatively suggest that the low intensity of the band at 315cm^{-1} is responsible for the failure to observe correlation field splitting in the crystal spectrum. It is concluded that the assignment by Steele and Whiffen is acceptable.

Table 2.2 contains the fundamental frequencies of benzene and hexafluorobenzene assigned to the various symmetry species. The data for benzene are based on the assignment of Mair and Hornig;[23] the final numerical values of the fundamental frequencies are taken from Brodersen and Langseth.[24] The data for hexafluorobenzene are based on and are taken from the assignment of Steele and Whiffen.[20] The frequency of the lowest lying fundamental of hexafluorobenzene has been tentatively re-assigned by Counsell et al[25] on the basis of thermodynamic data.

Fundamental Frequencies of C_6H_6, C_6D_6 and C_6F_6

Sym.Species	Freq.No.	C_6H_6 [24]	C_6D_6 [24]	C_6F_6 [20]
A_{1g}	1 2	993 3073	945 2303	559 1490
A_{2g}	3	1350	1059	691
B_{2g}	4 5	707 990	599 829	249 714
E_{2g}	6 7 8 9	606 3056 1599 1178	579 2274 1558 869	264 1655 1157 443
E_{1g}	10	846	660	370
A_{2u}	11	673	496	215
B_{1u}	12 13	1010 3057	970 2285	640 1323
B_{2u}	14 15	1309 1146	1282 824	1253 208
E_{2u}	16 17	398 967	345 787	125* 595
E_{1u}	18 19 20	1037 1482 3064	814 1333 2288	1530 1020-1002 315

* data of Counsell et al [25]

Table 2.2

In general we follow the notation, definition of axes and the systems of coordinates adopted by Whiffen.[11] Figure 2.1 indicates the numbering of atoms and the orientation of the molecule-fixed axes.

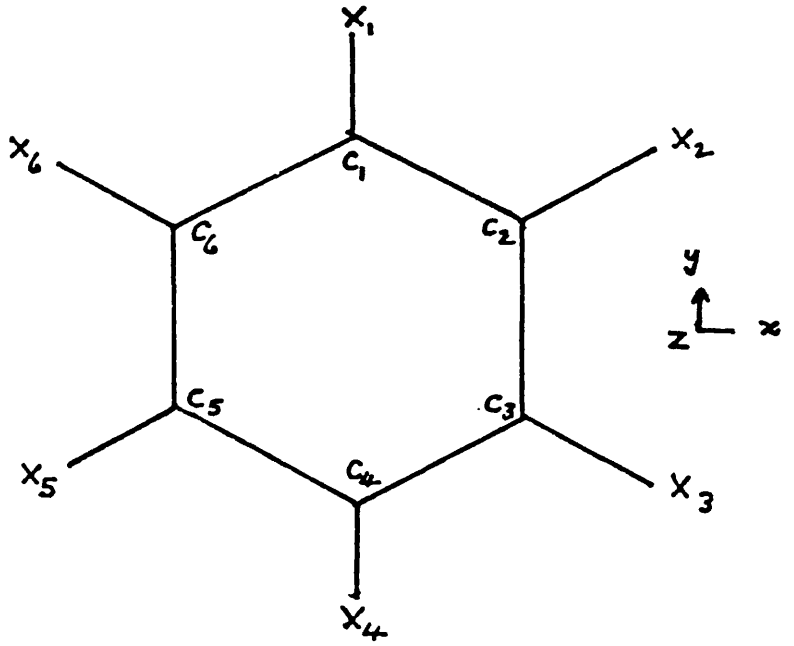

Fig.2.1.

The force fields of benzene and hexafluorobenzene have been referred to in terms of 24 planar internal displacement (valency) coordinates or in terms of 20 internal symmetry coordinates. Tables 2.3 and 2.4 indicate the coordinate systems. They are all identical to Whiffen's convention with the exception of the E_{1u} species where a complication arises due to a redundancy. The symmetry coordinates are constructed from complete sets of equivalent internal coordinates.

$$\Gamma_R\ (C\text{-}C) = A_{1g} + E_{2g} + B_{2u} + E_{1u}$$
$$\Gamma_r\ (C\text{-}H) = A_{1g} + E_{2g} + B_{1u} + E_{1u}$$
$$\Gamma_\alpha\ (C\text{-}C\text{-}C) = A_{1g} + E_{2g} + B_{1u} + E_{1u}$$
$$\Gamma_\beta\ (H\text{-}C\text{-}C) = A_{2g} + E_{2g} + B_{2u} + E_{1u}$$

The choice of internal coordinates is such that the symmetry coordinates

Planar Internal Displacement Coordinates in C_6X_6

R_o	is the C-C equilibrium distance.	
r_o	" " C-X " "	
ΔR_i	:	increase in length of C_i-C_{i+1} bond.
Δr_i	:	increase in length of C_i-X_i bond.
$R_o\Delta\alpha_i$	:	increase in angle C_{i-1}-$\hat{C}_i$-C_{i+1} scaled with R_o.
$r_o\Delta\beta_i$	:	increase in angle between C_iX_i and the external bisector of the C_{i-1}-$\hat{C}_i$-C_{i+1} angle (positive if X_i moves in anti clockwise direction) scaled with r_o.

Table 2.3

Planar Symmetry Coordinates for C_6X_6

(including E_{1u} redundancy)

Symmetry		Coefficients for i =						N	Internal
Species	Coord.	1	2	3	4	5	6	factor	Coordinate
A_{1g}	S_1	1	1	1	1	1	1	$6^{-\frac{1}{2}}$	ΔR_i
	S_2	1	1	1	1	1	1	$6^{-\frac{1}{2}}$	Δr_i
A_{2g}	S_3	1	1	1	1	1	1	$6^{-\frac{1}{2}}$	$r_o\Delta\beta_i$
E_{2g}	S_{6a}	-2	1	1	-2	1	1	$12^{-\frac{1}{2}}$	$R_o\Delta\alpha_i$
	S_{6b}	0	-1	1	0	-1	1	2^{-1}	$R_o\Delta\alpha_i$
	S_{7a}	-2	1	1	-2	1	1	$12^{-\frac{1}{2}}$	Δr_i
	S_{7b}	0	-1	1	0	-1	1	2^{-1}	Δr_i
	S_{8a}	-1	2	-1	-1	2	-1	$12^{-\frac{1}{2}}$	ΔR_i
	S_{8b}	-1	0	1	-1	0	1	2^{-1}	ΔR_i
	S_{9a}	0	-1	1	0	-1	1	2^{-1}	$r_o\Delta\beta_i$
	S_{9b}	2	-1	-1	2	-1	-1	$12^{-\frac{1}{2}}$	$r_o\Delta\beta_i$
B_{1u}	S_{12}	-1	1	-1	1	-1	1	$6^{-\frac{1}{2}}$	$R_o\Delta\alpha_i$
	S_{13}	-1	1	-1	1	-1	1	$6^{-\frac{1}{2}}$	Δr_i
B_{2u}	S_{14}	-1	1	-1	1	-1	1	$6^{-\frac{1}{2}}$	ΔR_i
	S_{15}	-1	1	-1	1	-1	1	$6^{-\frac{1}{2}}$	$r_o\Delta\beta_i$
E_{1u}	S_{18a}	0	1	1	0	-1	-1	2^{-1}	$r_o\Delta\beta_i$
	S_{18b}	2	1	-1	-2	-1	1	$12^{-\frac{1}{2}}$	$r_o\Delta\beta_i$
	S'_{19a}	-1	0	1	1	0	-1	2^{-1}	ΔR_i
	S'_{19b}	1	2	1	-1	-2	-1	$12^{-\frac{1}{2}}$	ΔR_i
	S_{20a}	-2	-1	1	2	1	-1	$12^{-\frac{1}{2}}$	Δr_i
	S_{20b}	0	1	1	0	-1	-1	2^{-1}	Δr_i
	S'_{21a}	-2	-1	1	2	1	-1	$12^{-\frac{1}{2}}$	$R_o\Delta\alpha_i$
	S'_{21b}	0	1	1	0	-1	-1	2^{-1}	$R_o\Delta\alpha_i$

Table 2.4

Planar Symmetry Coordinates for C_6X_6

(E_{1u} redundancy removed)

E_{1u}	S_{18a}	0	1	1	0	-1	-1	2^{-1}	$r_0\Delta\beta_i$
	S_{19a}	-1	0	1	1	0	-1	$2^{-\frac{1}{2}}$	ΔR_i
	S_{20a}	-2	-1	1	2	1	-1	$12^{-\frac{1}{2}}$	Δr_i

Table 2.4a

must obey redundancy conditions in A_{1g} and E_{1u} (24 internal coordinates to describe 2N-3 = 21 in-plane displacements). For the A_{1g} species the redundancy condition is simply a consequence of the fact that the ring must close.

$$\sum_{i=1}^{6} \alpha_i = 0 \quad \text{or} \quad S_{\alpha}^{A_{1g}} = 0$$

The four redundant symmetry coordinates in the E_{1u} species are denoted by S_{18}, S'_{19}, S_{20} and S'_{21}. From the definitions of S'_{19} and S'_{21}, it follows that the atomic displacements in the two coordinates are equal and opposite so that we can formulate a normalized redundancy condition

$$\frac{1}{\sqrt{2}} (S'_{19} + S'_{21}) = 0$$

The redundant coordinate, S_r, is eliminated if we choose the other coordinates orthogonal to S_r. With this condition, the G matrix elements belonging to S_r disappear and the orthogonal transformation applied to the original set of symmetry coordinates is

	S_{18}	S'_{19}	S_{20}	S'_{21}
S_{18}	1	0	0	0
S_{19}	0	$1/\sqrt{2}$	0	$-1/\sqrt{2}$
S_{20}	0	0	1	0
S_r	0	$1/\sqrt{2}$	0	$1/\sqrt{2}$

or simply

$$\begin{bmatrix} S_{19} \\ S_r \end{bmatrix} = \frac{1}{\sqrt{2}} \begin{bmatrix} 1 & -1 \\ 1 & 1 \end{bmatrix} \begin{bmatrix} S'_{19} \\ S'_{21} \end{bmatrix}$$

Table 2.5

The force fields of benzene and hexafluorobenzene can be represented in either internal coordinates or symmetry coordinates. Whiffen[10] used Latin symbols for the internal coordinate force constants and Greek symbols to denote symmetry force constants. It is perhaps more customary to denote symmetry force constants in the general form F_{ij}. The definition of the internal coordinate force constants is given in Table 2.6, and in Tables 2.7 and 2.8 the complete transformations from internal to symmetry and from symmetry to internal coordinate force constants are quoted.

Definition of Internal Coordinate Force Constants

	ΔR_i	Δr_i	$R_o\Delta\alpha_i$	$r_o\Delta\beta_i$
ΔR_i	D, d_o, d_m, d_p	h_o, h_m, h_p	i_o, i_m, i_p	j_o, j_m, j_p
Δr_i		E, e_o, e_m, e_p	k, k_o, k_m, k_p	l, l_o, l_m, l_p
$R_o\Delta\alpha_i$			F, f_o, f_m, f_p	n, n_o, n_m, n_p
$r_o\Delta\beta_i$				G, g_o, g_m, g_p

Table 2.6

Transformation from Internal to Symmetry Force Constants

$$\Lambda_1 = F_{11} = D+2d_o+2d_m+d_p$$
$$\xi_1 = F_{12} = 2h_o+2h_m+2h_p$$
$$\Omega_1 = F_{22} = E+2e_o+2e_m+e_p$$
$$\Gamma_1 = F_{33} = G+2g_o+2g_m+g_p$$
$$\Sigma_3 = F_{66} = F-f_o-f_m+f_p$$
$$\Psi_3 = F_{67} = K-k_o-k_m+k_p$$
$$\chi_3 = F_{68} = i_o-2i_m+i_p$$
$$\pi_3 = F_{69} = 3^{\frac{1}{2}}(-n_o+n_m)$$
$$\Omega_3 = F_{77} = E-e_o-e_m+e_p$$
$$\xi_3 = F_{78} = h-2h_m+h_p$$
$$\Upsilon_3 = F_{79} = 3^{\frac{1}{2}}(-l_o+l_m)$$
$$\Lambda_3 = F_{88} = D-d_o-d_m+d_p$$
$$\mu_3 = F_{89} = 3^{\frac{1}{2}}(-j_o+j_p)$$
$$\Gamma_3 = F_{99} = G-g_o-g_m+g_p$$
$$\Sigma_2 = F_{1212} = F-2f_o+2f_m-f_p$$
$$\Psi_2 = F_{1213} = K-2k_o+2k_m-k_p$$
$$\Omega_2 = F_{1313} = E-2e_o+2e_m-e_p$$
$$\Lambda_2 = F_{1414} = D-2d_o+2d_m-d_p$$
$$\mu_2 = F_{1415} = 2j_o-2j_m+2j_p$$
$$\Gamma_2 = F_{1515} = G-2g_o+2g_m-g_p$$
$$\Gamma_4 = F_{1818} = G+g_o-g_m+g_p$$
$$\mu_4 = F_{1819} = 2^{-\frac{1}{2}}(j_o+2j_m+j_p)-(3/2)^{\frac{1}{2}}(n_o+n_m)$$
$$\Upsilon_4 = F_{1820} = 3^{\frac{1}{2}}(l_o+l_m)$$
$$\Lambda_4 = F_{1919} = \tfrac{1}{2}(D+d_o-d_m-d_p)+\tfrac{1}{2}(F+f_o-f_m-f_p)-3^{\frac{1}{2}}(i_o-i_p)$$
$$\xi_4 = F_{1920} = (3/2)^{\frac{1}{2}}(h_o-h_p)-2^{-\frac{1}{2}}(k+k_o-k_m-k_p)$$
$$\Omega_4 = F_{2020} = E+e_o-e_m-e_p$$

Table 2.7

Transformation from Symmetry to Internal Force Constants

$$6D = \Lambda_1+\Lambda_2+2\Lambda_3+4\Lambda_4+4\Sigma_2-6\Sigma_3+4.3^{\frac{1}{2}}\chi_3$$
$$6d_o = \Lambda_1-\Lambda_2-\Lambda_3+2\Lambda_4+2\Sigma_2-3\Sigma_3+2.3^{\frac{1}{2}}\chi_3$$
$$6d_m = \Lambda_1+\Lambda_2-\Lambda_3-2\Lambda_4-2\Sigma_2+3\Sigma_3-2.3^{\frac{1}{2}}\chi_3$$
$$6d_p = \Lambda_1-\Lambda_2+2\Lambda_3-4\Lambda_4-4\Sigma_2+6\Sigma_3-4.3^{\frac{1}{2}}\chi_3$$

$$6E = \Omega_1+\Omega_2+2\Omega_3+2\Omega_4,\ 6G=\Gamma_1+\Gamma_2+2\Gamma_3+2\Gamma_4$$
$$6e_o = \Omega_1-\Omega_2-\Omega_3+\Omega_4,\ 6g_o=\Gamma_1-\Gamma_2-\Gamma_3+\Gamma_4$$
$$6e_m = \Omega_1+\Omega_2-\Omega_3-\Omega_4,\ 6g_m=\Gamma_1+\Gamma_2-\Gamma_3-\Gamma_4$$
$$6e_p = \Omega_1-\Omega_2+2\Omega_3-2\Omega_4,\ 6g_p=\Gamma_1-\Gamma_2+2\Gamma_3-2\Gamma_4$$

$$F = -\Sigma_2 + 2\Sigma_3,\ f_o = -\Sigma_2 + \Sigma_3$$

$$i_o = \chi_3$$

$$6h_o = \xi_1+\xi_3+6^{\frac{1}{2}}\xi_4-2.3^{\frac{1}{2}}\psi_2+3.3^{\frac{1}{2}}\psi_3$$
$$6h_m = \xi_1-2\xi_3$$
$$6h_p = \xi_1+\xi_3-6^{\frac{1}{2}}\xi_4+2.3^{\frac{1}{2}}\psi_2-3.3^{\frac{1}{2}}\psi_3$$

$$6j_o = \mu_2-3^{\frac{1}{2}}\mu_3+2^{\frac{1}{2}}\mu_4-\pi_3$$
$$6j_m = -\mu_2+2.2^{\frac{1}{2}}\mu_4-2\pi_3$$
$$6j_p = \mu_2+3^{\frac{1}{2}}\mu_3+2^{\frac{1}{2}}\mu_4-\pi_3$$

$$k = -\psi_2+2\psi_3,\ k_o = -\psi_2+\psi_3 \qquad n_o = -3^{-\frac{1}{2}}\pi_3$$
$$6l_o = -3^{\frac{1}{2}}\tau_3+3^{\frac{1}{2}}\tau_4,\ 6l_m=3^{\frac{1}{2}}\tau_3+3^{\frac{1}{2}}\tau_4$$

Table 2.8

Previous treatments of the force field for the planar vibrations of benzene have been critically assessed by Duinker[26] and by Duinker and Mills.[27] The most general harmonic force field is, of course, underdetermined by the frequency data available for benzene and its isotopic species and the number of different sets of force constants which reproduce the frequency data reflects this fact. Recently Duinker and Mills[27] have re-examined the problem in the light of additional data provided by the experimentally observed values for the Coriolis zeta constants of the E_{2g} species of C_6H_6 and C_6D_6 determined from electronic spectra.[28] In the force constant refinement procedure of (DM) the values of some interaction constants are chosen on the basis of the concept of orbital-following and rehybridization of the carbon atomic orbitals. The final set of (DM) force constants have been fitted to frequency data for C_6H_6, C_6D_6 and $C_6H_3D_3$ and agreement between the calculated and observed Coriolis zeta constants for the E_{2g} species of C_6H_6 and C_6D_6 is excellent. The force fields of Whiffen[10] and of Scherer[29] can be fitted satisfactorily to frequency data. However, both fields lead to incorrect calculated values for the Coriolis zeta constants for the E_{2g} species. In the case of the E_{1u} species there are at present no data available on the Coriolis zeta constants for any of the vibrations of this species. In principle it is possible to determine zeta constants from the infrared band contours of the unresolved fundamentals and indeed Duinker and Mills[27] have estimated a zeta value of -0.55 from the 1037cm^{-1} E_{1u} fundamental of benzene d_0. This value is in poor agreement with the calculated zeta values obtained from the available force fields and on this basis Duinker and Mills[27] conclude that "in the E_{1u} species of benzene the force field is seriously underdetermined

Internal (Latin) Force Constants mD/Å

	C_6H_6 & C_6D_6			C_6F_6
	Whiffen[10]	Scherer[29]	Duinker & Mills[27]	Steele & Whiffen[30]
E	5.093	5.120	5.125	7.405
e_o	0.025	0	0	0.087
e_m	0.008	0	0	-0.050
e_p	-0.040	0	0	0.032
G	0.866	0.866	0.881	0.821
g_o	0.016	0.002	0.024	0.072
g_m	0.013	0.002	-0.019	-0.093
g_p	-0.015	-0.003	-0.027	0.003
F	1.031	0.640	0.563	1.030
f_o	0.185	0	-0.050	0.141
i_o	-0.180	0.210	0.316	-0.180
h_o	0	0	0	0.708
h_m	0	0	0	0
h_p	0	0	0	-0.263
j_o	0.049	0.167	0.336	0.112
j_m	-0.050	0	0	-0.041
j_p	0.049	0	0	-0.033
K	0	0	-0.010	-0.076
k_o	0	0	0	0.344
n_o	-0.127	0	0.042	-0.127
l_o	0	0	0	0.170
l_m	0	0	0	-0.054
D	5.553	6.724	7.015	5.478
d_o	0.633	0.813	0.531	0.660
d_m	0.133	-0.469	-0.531	0.071
d_p	0.573	0.276	0.531	0.459

Table 2.9

Symmetry (Greek, F_{ij}) Force Constants mD/Å

	C_6H_6 & C_6D_6			C_6F_6	
	Whiffen[10]	Scherer[29]	Duinker & Mills[27]	Steele & Whiffen[30]	
$\Lambda_1 = F_{11}$	7.620	7.72	7.546	7.400	
$\xi_1 = F_{12}$	0	0	0	0.889	A_{1g}
$\Omega_1 = F_{22}$	5.120	5.12	5.125	7.512	
$\Gamma_1 = F_{33}$	0.857	0.87	0.863	0.780	A_{2g}
$\Sigma_3 = F_{66}$	0.846	0.64	0.614	0.889	
$\Psi_3 = F_{67}$	0	0	-0.010	-0.420	
$\chi_3 = F_{68}$	-0.180	0.21	0.316	-0.180	
$\pi_3 = F_{69}$	0.217	0	-0.073	0.178	
$\Omega_3 = F_{77}$	5.020	5.12	5.125	7.400	E_{2g}
$\xi_3 = F_{78}$	0	0	0	0.444	
$\tau_3 = F_{79}$	0	0	0	-0.390	
$\Lambda_3 = F_{88}$	5.380	6.64	7.546	5.205	
$\mu_3 = F_{89}$	0.000	-0.29	-0.582	-0.248	
$\Gamma_3 = F_{99}$	0.847	0.86	0.850	0.847	
$\Sigma_2 = F_{1212}$	0.661	0.64	0.664	0.748	
$\Psi_2 = F_{1213}$	0	0	-0.010	-0.764	B_{1u}
$\Omega_2 = F_{1313}$	5.100	5.12	5.125	7.100	
$\Lambda_2 = F_{1414}$	3.940	3.85	4.359	3.840	
$\mu_2 = F_{1415}$	0.300	0.33	0.672	0.235	B_{2u}
$\Gamma_2 = F_{1515}$	0.822	0.87	0.821	0.492	
$\Gamma_4 = F_{1818}$	0.910	0.87	0.952	0.991	
$\mu_4 = F_{1819}$	0.155	0.12	0.186	0.1216	
$\tau_4 = F_{1820}$	0	0	0	0.197	E_{1u}
$\Lambda_4 = F_{1919}$	3.670	3.83	3.483	3.701	
$\xi_4 = F_{1920}$	0	0	0.007	0.9984	
$\Omega_4 = F_{2020}$	5.15	5.12	5.125	7.509	

Table 2.10

by the presently available data".

The interpretation of the absolute infrared intensities for the fundamental absorption bands of benzene in terms of bond properties requires a detailed knowledge of the E_{1u} species force field so that a reinterpretation of the benzene intensities seems appropriate.

The force field governing displacements from the D_{6h} equilibrium configuration of the hexafluorobenzene molecule has been treated by Steele and Whiffen.[30] In the absence of further information from isotopic species, Coriolis zeta constants or centrifugal distortion constants, a choice between alternative solutions to the secular equation was necessary. The final set of force constants were chosen on the basis that in a simple valency force field treatment all interaction constants are approximately zero. Where this proved to be an insufficient criterion the symmetry force constants were taken to be approximately equal to those for benzene. Difficulties encountered with the larger E_{1u} and E_{2g} species were alleviated by means of an iterative procedure starting with a set of approximate constants. The final set of force constants reproduce the frequency data assigned by Steele and Whiffen[20] and some of the constants have been transferred satisfactorily to lower substituted fluorobenzenes.[31,32] The interpretation of the absolute infrared intensities for the fundamental vibrations of hexafluorobenzene in terms of bond properties requires a detailed knowledge of the E_{1u} species force field. We have calculated zeta constants for this species and in the case of the 315cm^{-1} E_{1u} band we have estimated a zeta value from the infrared band contour. The good agreement with the calculated value may indeed be fortuitous. However, it encouraged us to interpret the absolute intensities of hexafluorobenzene

using the Steele and Whiffen force field.[30] Fortunately we shall demonstrate that the derived effective bond dipoles are not very sensitive to the force field.

CHAPTER THREE

Experimental Determination of Vapour Phase Infrared Intensities

Experimental determination of accurate and reproducible values for the absolute intensities of infrared absorption bands has always proved an arduous task. Wilson and Wells[33] have reviewed the problems and introduced a method of overcoming some of the difficulties associated with absolute intensity measurements made on infrared spectrometers of limited resolving power. The major problem arises from the fact that, for finite slit widths, the beam is not monochromatic for a particular frequency ν', but rather a band of frequencies described by a slit function $g(\nu,\nu')$. Consequently, the measured intensity of radiation $T(\nu')$ at the frequency ν' differs from the true value $I(\nu)$ and is related to it by

$$T(\nu') = \int_0^\infty I(\nu)\, g(\nu',\nu)\, d\nu \qquad 3.1$$

Further, the apparent (measured) integrated intensity B is not equal to the exact theoretical quantity A.

$$\text{True intensity, } A = \frac{1}{pl}\int_{BAND} \log_e \frac{Io}{I}\, d\nu \qquad 3.2$$

$$\text{Apparent intensity, } B = \frac{1}{pl}\int_{BAND} \log_e \frac{To}{T}\, d\nu' \qquad 3.3$$

$$= \frac{1}{pl}\int_{BAND} \log_e \left\{\frac{\left(\int_0^\infty Io(\nu)g(\nu,\nu')d\nu\right)}{\left(\int_0^\infty I(\nu)g(\nu,\nu')d\nu\right)}\right\} d\nu' \qquad 3.4$$

Wilson and Wells[33] showed that

$$\lim_{pl\to 0} B = A \qquad 3.5$$

or for logarithmic integration

$$\lim_{pl \to 0} \Gamma_{APPARENT} = \Gamma_{TRUE} \qquad 3.6$$

The true absolute intensity is obtained by extrapolating the measured intensity to zero concentration. In practice, it is more usual to plot Bpl vs pl and A is then the slope of the tangent at the origin. Liquid and solution phase intensities are normally obtained in this manner. However, in the case of vapours the method is not entirely satisfactory because one relies heavily on data taken at low absorption.

An extension of the Wilson-Wells extrapolation is usually employed for accurate vapour phase intensities.[34] Experimental conditions are chosen so that I_0 and I are invariant over the range in which the slit function is finite. Under these conditions

$$B = \frac{1}{pl} \int_{BAND} \log_e \frac{I_0}{I} \, d\nu' = A \qquad 3.7$$

and the true integrated intensity is determined by direct summation.

Absolute intensity studies are usually made on spectra recorded on single beam spectrometers because atmospheric absorption, scattered light and irreproducibility can be readily detected. Therefore, with adequate evacuation, filtering and recording, rapid fluctuations in I_0 can be virtually eliminated. In the case of I values the same is true. However, individual rotational lines, which are resolved only for molecules of sufficiently small moment of inertia, give rise to rapid fluctuations in I and invalidate the approximation. Single rotational lines have a finite line width which increases with pressure.[35] However, at sufficiently high pressures the fine structure is completely smeared out to give a smooth

band contour. Consequently, by pressure broadening the sample, either by using sufficiently high pressures of the sample itself (self-broadening), or, by adding to the sample an infrared transparent and chemically inert (foreign) gas, it is possible to maintain I constant over the slit function. The pressure necessary for complete broadening depends on the rotational fine structure, the effectiveness of the broadening gas and on the performance of the spectrometer. It is usually considered sufficient when an increase of total pressure produces a linear Beer's Law plot.[36] Even when the individual rotational lines are sufficiently broadened, the smooth band contour may still have such steep gradients as to result in low measured I values. This difficulty is particularly the case with band contours having strong and sharp Q branches such as the out-of-plane, A_{2u}, deformation modes of benzene and hexafluorobenzene and care must be exercised.

Benzene and hexafluorobenzene have four infrared active fundamentals which have been assigned to three E_{1u} modes, ν_{18}, ν_{19} and ν_{20} and the A_{2u} mode, ν_{11}. The absorption frequencies are given in table 3.1.

	C_6H_6	C_6D_6	C_6F_6
		$\bar{\nu}_0$ cm^{-1}	
E_{1u}	3080	2289	1531
	1486	1331	1020-1002
	1038	808	315
A_{2u}	673	494	215

Table 3.1

The absolute infrared intensities of benzene have been reported previously[10] and the data has been analysed using the Whiffen force field for benzene.[10] In the case of hexafluorobenzene the absolute infrared intensities of only the two higher frequency fundamentals have been reported previously.[37] Absolute intensities of the two lower frequency modes are reported here and the data for all four modes is analysed and critically compared with the reported data for benzene.

Experimental

The sample of hexafluorobenzene used in this work was kindly given by Imperial Smelting Co. Ltd. Vapour phase chromatography and the infrared spectrum showed no trace of other components and the sample was used without further purification. B. pt. 80.1°C/760mm., m. pt. 5.5°C.

Spectra of the 315 and 215cm^{-1} infrared absorption bands were recorded on an evacuated single beam grating spectrometer previously described elsewhere.[38] Linearity of the amplifier and detector systems and the uniformity of illumination over the slits were verified by showing that the signal on the recorder was proportional to the square of the slit width as required for coupled entrance and exit slits to and from the monochromator.

For the 315cm^{-1} band a 625 lines/in. grating blazed at 25° was used together with 2 x NaF reststrahlen mirrors and for the 215cm^{-1} band a 312 lines/in. grating blazed at 25° was used together with 2 x NaCl reststrahlen mirrors and blackened polythene filter.

The sample was contained in a stainless steel cell (fig.3.1) of path length 11.51cm. with 1mm. thick convex high density polythene (Rigidex) windows. Partial pressures of hexafluorobenzene were measured with an

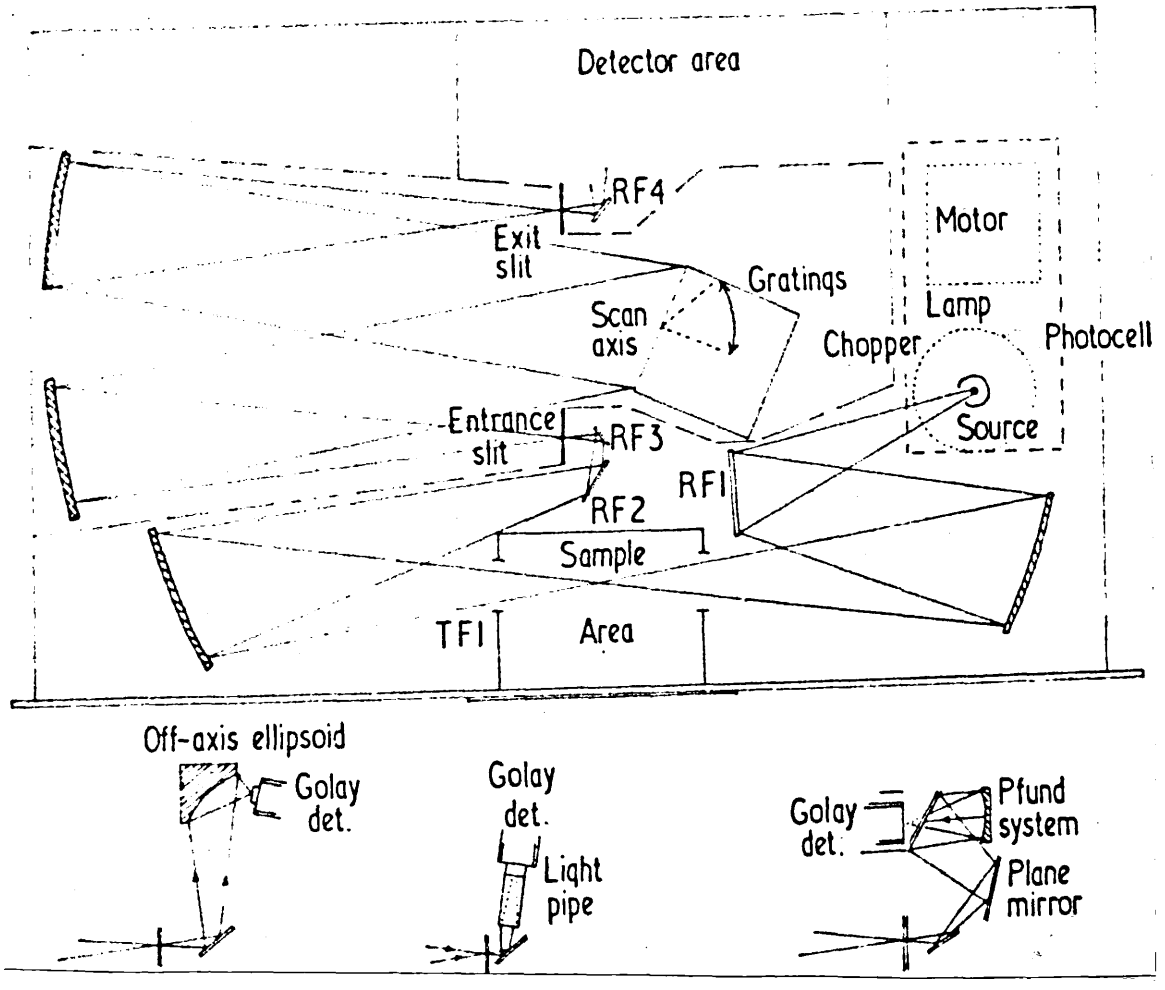

Plate 3.1 Optical System of the Far Infrared Spectrometer.
(reproduced by kind permission of the authors [38])

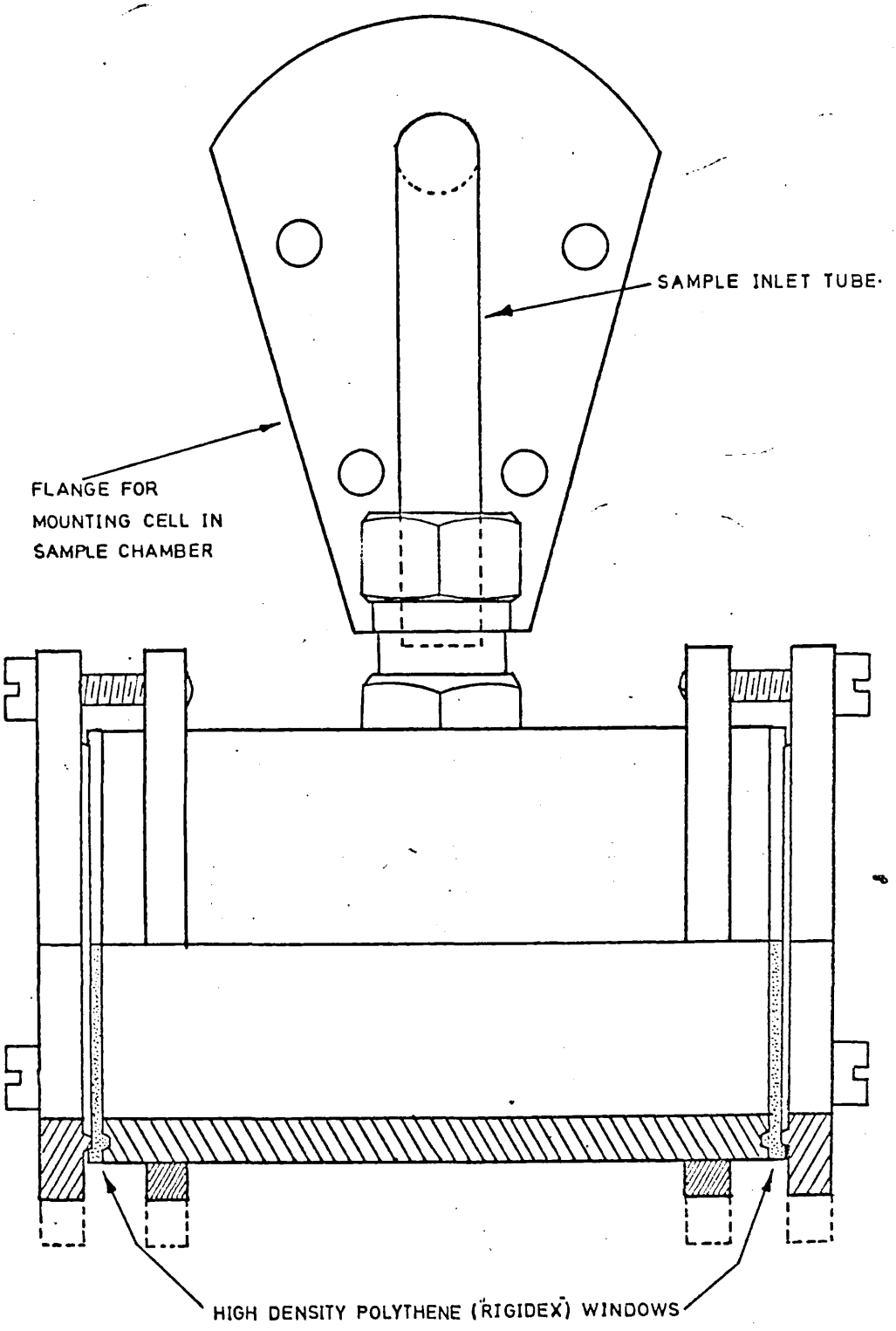

Fig. 3.1. Far Infrared Gas Cell.

ethylene glycol (d^{25} = 1.116 gm cm^{-3}) manometer and partial pressures of broadening gas (O_2 free N_2) were measured with a mercury manometer.

The procedure for sampling and recording spectra was as follows:

i) the spectrometer was calibrated by recording the water vapour spectrum from 400 - 150cm^{-1} and comparing with a reference spectrum.[39]

ii) the cell and the spectrometer were evacuated until no trace of water vapour remained. At least three backgrounds were recorded to check reproducibility and the absence of leaks.

iii) the sample of hexafluorobenzene was de-gassed by freezing to liquid nitrogen temperature, pumping on the frozen sample and then allowing to warm to room temperature. This was repeated at least twice.

iv) the sample of hexafluorobenzene vapour was introduced into the cell and its temperature and pressure were noted. Due to the possibility of absorption of the sample by glycol, the pressure was recorded as soon as possible after the tap was closed.

v) spectra of the two bands were recorded over a frequency range covering 60cm^{-1} either side of the band centres at a scan speed of about 4cm^{-1}/min.

vi) the broadening gas was introduced into the cell by quickly opening, then closing, the tap and after allowing sufficient time for equilibration the spectra were again recorded.

vii) the zero transmission reading was checked at regular intervals by blanking off the beam.

viii) at least two records of each spectra were obtained and the mechanical slit widths were noted.

A series of pressures of hexafluorobenzene was studied with a range

of partial pressures of broadening gas. The partial pressure of broadening gas was limited to 1 atm. There was no evidence for leaks or for absorption of the sample by the cell body or by the polythene windows.

From the transmission measurements spectral curves of $\log_{10} \frac{I_o}{I}$ against $\bar{\nu}$ were plotted. Following Crawford,[2] the curves were re-plotted on a $\log_{10} \frac{I_o}{I} / \bar{\nu}$ against $\bar{\nu}$ scale and the integrated area was obtained by counting the squares.

The absolute intensity is given, assuming ideal gas behaviour, by

$$\Gamma = \frac{22400 \times 760 \times T \times 2.303}{6.02252 \times 10^{23} \times p \times 273 \times l} \int_{BAND} \log_{10} \frac{I_o}{I} \, (d \log_{10} \bar{\nu})$$

where T is the absolute temperature, p is the pressure of the vapour in mms. of mercury, l is the path length of the cell and the integration is over the complete band.

The units of Γ are $mol^{-1}.cm^2.ln$. The error introduced by integrating the $\log_{10} \frac{I_o}{I}$ against $\bar{\nu}$ curve rather than the more accurate form is usually so negligible that many authors quote absolute intensities in terms of A values.

$$A = \frac{1}{pl} \int_{BAND} \log_e \frac{I_o}{I} \, d\bar{\nu} = \Gamma \bar{\nu}_o \qquad 3.8$$

The units of A are $mol^{-1}.cm.ln$. When the concentration is expressed as a molar quantity the unit "dark" is often used.

$$1 \text{ dark} = 10^3 \text{ mole}^{-1} \text{ cm.ln.}$$

Mills[40] has given a comprehensive review of the most commonly used intensity units.

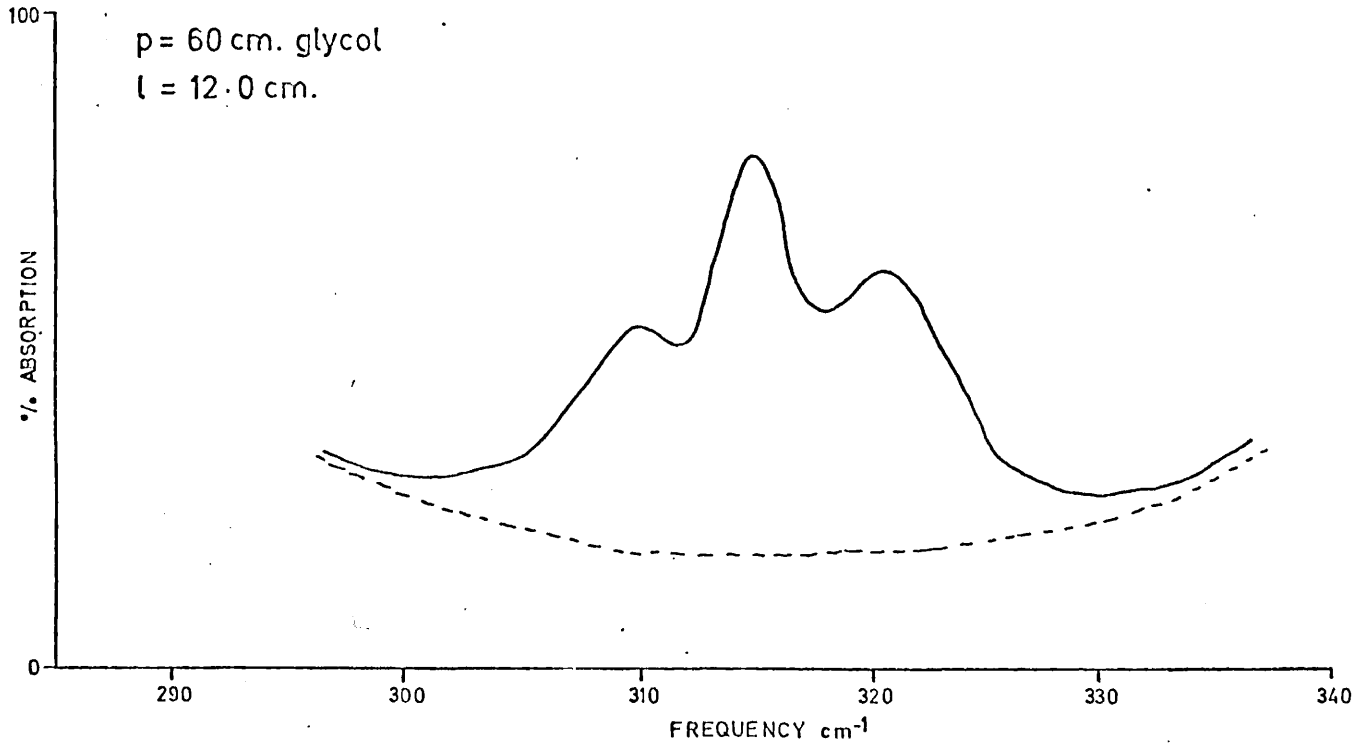

Fig.3.2. E_{1u} Band of HFB at 315 cm^{-1}

Discussion of E_{1u} Band of HFB at $315cm^{-1}$

A partial pressure of 50-80cm. glycol of hexafluorobenzene contained in a 12cm. gas cell was required to give reasonable values of $\log_{10} \frac{I_0}{I}$. The band contour and total area were insensitive to pressure broadening up to a total pressure of 1 atm. of oxygen-free nitrogen. Under these conditions it is reasonable to assume that Wilson-Wells conditions are met. The measurements at low partial pressure of hexafluorobenzene were of lower accuracy due to the weakness of absorption but tended to confirm the adequacy of the pressure broadening. It was most convenient to admit nitrogen to a total pressure of 1 atm. in every case. The spectra for a series of partial pressures of hexafluorobenzene were recorded and band areas were obtained from re-drawn spectra of $\log_{10} \frac{I_0}{I} / \bar{\nu}$ plotted against $\bar{\nu}$ by a counting of the squares procedure. A graph of total area against partial pressure of vapour gave a satisfactory straight line in accordance with Beer's Law. The final value for the integrated intensity of this band is the mean value obtained from four different partial pressures of vapour and from eight spectral recordings (two for each pressure).

It is instructive to divide the band envelope into three distinct sections corresponding to the P,Q and R-branches and to determine the separate areas of each. The experimental band shows a marked asymmetry with ~7% more intensity in the R-branch than in the P-branch.

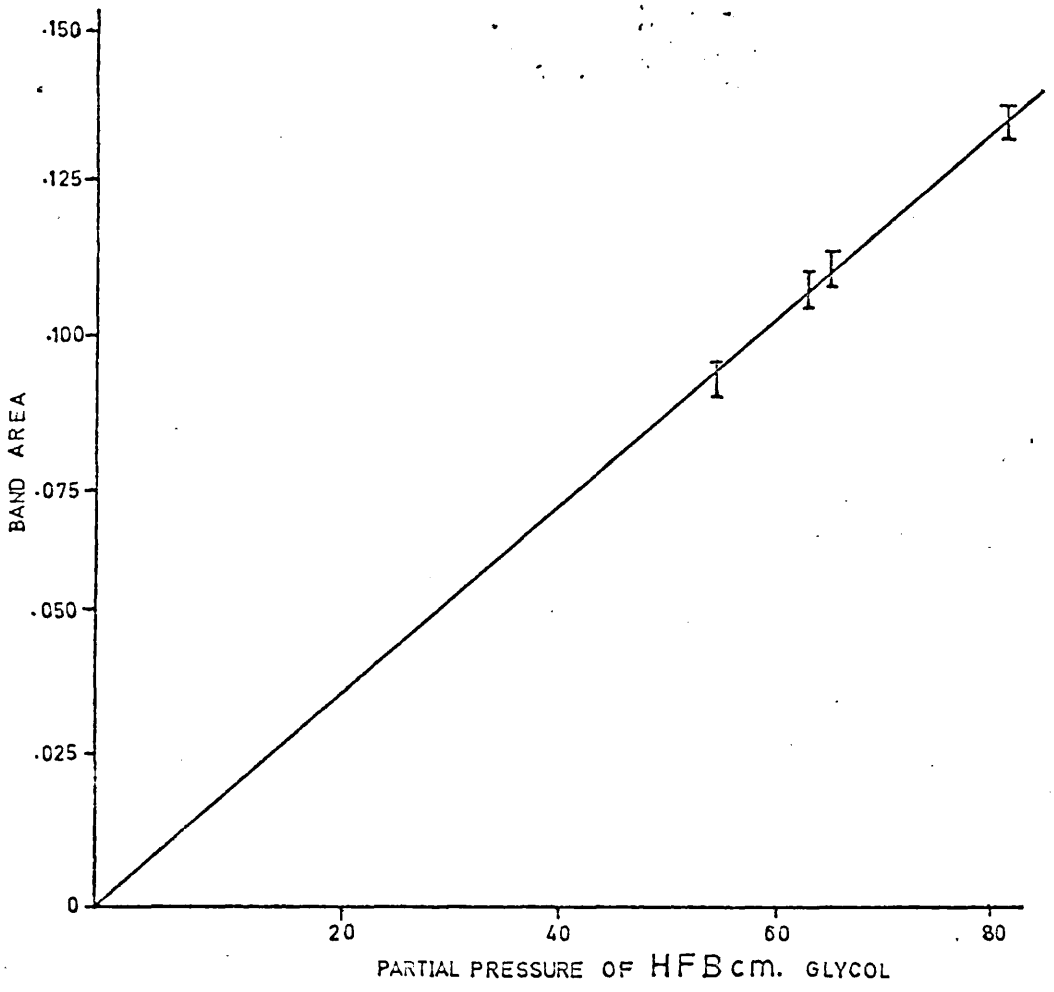

Fig.3.3. Beer's Law Plot for E_{1u} Band of HFB at 315 cm^{-1}

Experimental Data for 315cm^{-1} Band of HFB

Partial Pressure of HFB cm. glycol	Absolute Intensity x 10^{-21} cm.^{2} mol.$^{-1}$
55.6	1.31
62.5	1.35
63.7	1.37
78.6	1.30

Mean Absolute Intensity, Γ = 1.33 x 10^{-21} cm.^{2} mol.$^{-1}$

$A = \Gamma \bar{\nu} c$ = 1.25 x 10^{-8} cm.^{2} mol.$^{-1}$ sec.$^{-1}$

Table 3.2

	P-branch	Q-branch	R-branch
Fractional Intensity	0.26	0.41	0.33
Frequency max. $\bar{\nu}$ cm.$^{-1}$	320.4	315.0	309.7

Table 3.3

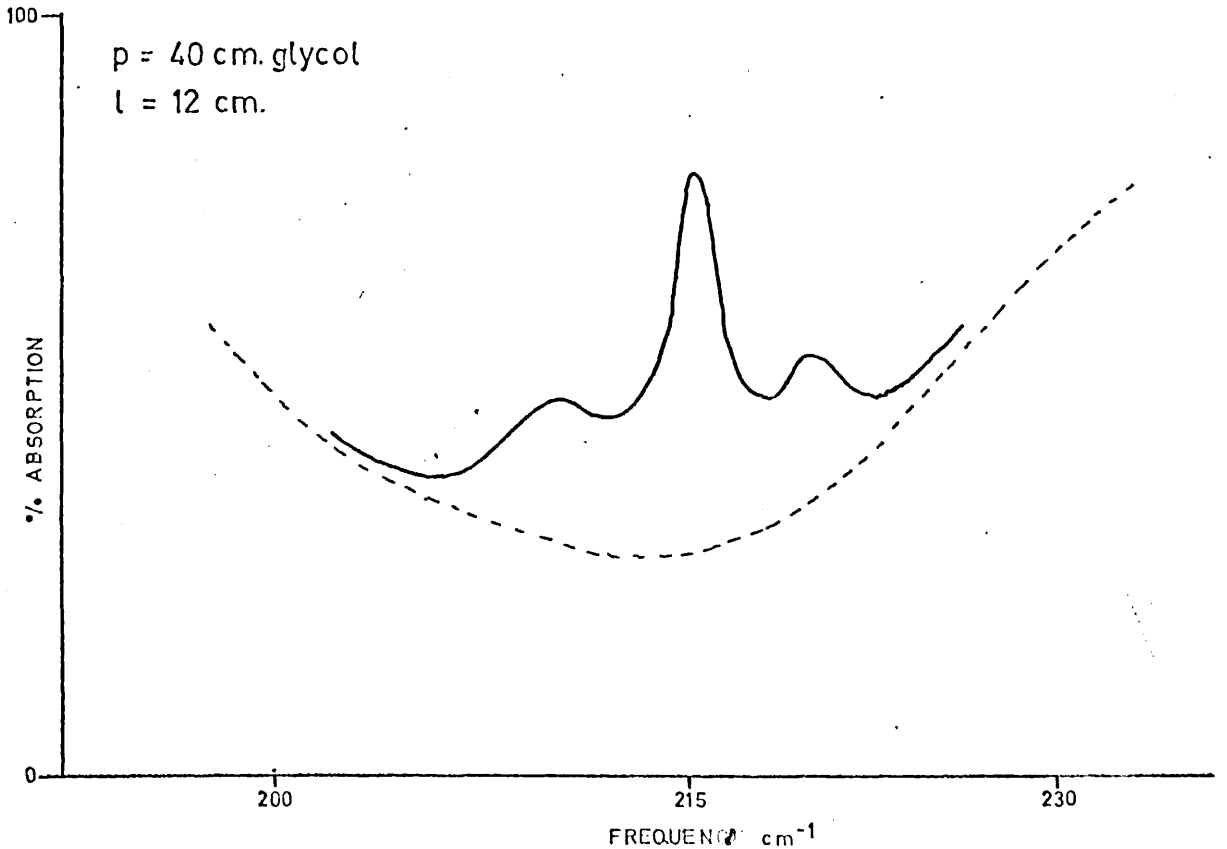

Fig. 3.4. A_{2u} Band of HFB at 215 cm^{-1}

Discussion of A_{2u} Band at 215cm^{-1}

A partial pressure of 50-80cm. glycol of hexafluorobenzene vapour contained in a 12cm. gas cell was required to give reasonable $\log_{10} \frac{I_0}{I}$ values. The band contour shows a regular PQR structure characteristic of a parallel type vibration with a PR separation of 12.0 ± 1cm.$^{-1}$ and a very intense Q-branch. The band was pressure broadened with up to 1 atm. of oxygen-free nitrogen and the intensity was determined by the Wilson-Wells method. The spectra for a series of partial pressures of hexafluorobenzene were recorded and band areas were obtained from re-drawn spectra of $\log_{10} \frac{I_0}{I} / \bar{\nu}$ plotted against $\bar{\nu}$ by a counting of the squares procedure. A graph of total area against partial pressure of vapour showed a slight curvature and therefore we followed exactly the same procedure used by Spedding and Whiffen[10] for their intensity measurement of the A_{2u} band of benzene. The band area was divided into three sections corresponding to the P,Q and R-branches and it was found that only the area of the Q-section showed curvature when plotted against pressure. The area of the Q-section was obtained by extrapolation to zero pressure. This process increases the total area by about 5%. It is well recognized that band contours with very steep gradients can result in low measured transmission values. The Q-branches are so narrow (width at half height about 4.5cm.$^{-1}$) that their widths are comparable with the effective slit width of the spectrometer.

The experimental band contour shows a marked asymmetry with ~ 5% more intensity in the R-branch than in the P-branch. The fraction of intensity in the Q-branch is in good agreement with the value calculated using the expressions of Gerhard and Dennison[41] and will be discussed further in Chapter 4 of this thesis.

Experimental Data for 215cm^{-1} Band of MFB

Partial Pressure of MFB cm. glycol	$\int \log_{10} \frac{I_o}{I} d\bar{\nu}$ cm.$^{-1}$
57.6	0.01562
49.7	0.01295
41.8	0.01078
29.7	0.00755

$$\Gamma = 2.01 \times 10^{-21} \text{ cm.}^2 \text{ mol.}^{-1}$$

$$A = \Gamma \bar{\nu}_o c = 1.28 \times 10^{-8} \text{ cm.}^2 \text{ mol.}^{-1} \text{ sec.}^{-1}$$

Table 3.4

	P-branch	Q-branch	R-branch
Fractional Intensity	0.25	0.43	0.32
Frequency max. $\bar{\nu}$ cm.$^{-1}$	206.5	212.5	218.5

Table 3.5.

CHAPTER FOUR

Band Shape Analysis

The moments of inertia of benzene and hexafluorobenzene are of such a magnitude that the fine structure of their vibrational-rotational spectra is impossible to resolve. Nevertheless, it is of great interest and of considerable value to determine the relationships between the dynamical parameters and the shapes of the envelopes of the unresolved bands.

Benzene and hexafluorobenzene are representative oblate symmetric top molecules and their infrared active absorption bands can be classified as the E_{1u} (perpendicular) vibrations and the A_{2u} (parallel) vibration.

Previous treatments[41,42,43] of the parallel bands of symmetric top molecules have employed the rigid-rotor harmonic-oscillator approximation in determining general relationships between band shape parameters and moment of inertia, temperature and transition probability. The general relationships are usually in good agreement with experimental band contours.

Perpendicular bands arising from transitions from a fully symmetric, non-degenerate ground state, to a doubly degenerate upper vibrational state have been treated in the same approximation.[42,44,45] The similar general relationships are usually in poor agreement with experimental band shapes as a result of a first order perturbation due to interaction of vibration and rotation (Coriolis effect). A recent paper[46,47] has quantitatively dealt with the effect of first order Coriolis coupling on the infrared band contours of spherical-top and symmetric-top molecules and Coriolis coupling constants obtained from infrared band contours with this theory have been confirmed in a few cases by high-resolution studies.[48,49]

The great value of Coriolis coupling constants lies in the fact that they are highly sensitive functions of especially the off-diagonal force constants so that they supplement frequency data in determining unique vibrational potential functions.[50,51] Integrated absorption coefficients and bond dipole gradients can also be determined with this theory. However, to the author's knowledge no literature exists on this subject.

The purpose of this chapter is to discuss the method of computing the infrared band contours for benzene and hexafluorobenzene. Comparison of computed and experimental band contours should lead to values for the transition moments, integrated intensities and the dipole gradients associated with the selected modes.

Symmetric top molecules are those having two identical moments of inertia, the third moment of inertia being different but not equal to zero. If the unique moment of inertia is greater (less) than the other two the molecule is termed an oblate (prolate) symmetric top. Benzene and hexafluorobenzene are representative oblate symmetric top molecules. The convention used for naming the axes is as shown.[52]

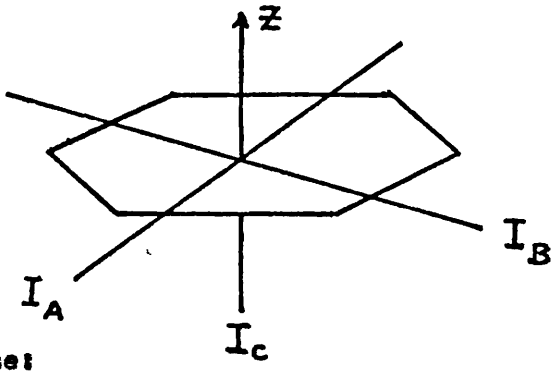

For the oblate case:

$$I_A = I_B < I_C \quad , \quad (A = B > C)$$

where A is the rotational constant $= \frac{h}{8\pi^2 c I_A}$ cm^{-1}

Rotational Constants

	C_6H_6	C_6D_6	C_6F_6
$I_A = I_B$ gm cm^2	148.129	179.112	807.187
$I_C \times 10^{-40}$	296.258	358.224	1614.374
$A = B$ cm^{-1}	0.18896	0.156275	0.034676
C	0.09448	0.0781375	0.017338

Table 4.1

PARALLEL TRANSITIONS

To a first approximation the energy levels of an oblate symmetric top molecule in a degenerate or a non-degenerate vibrational state are given by:[53,54]

$$T_{v,r} = G(v_1, v_2, \ldots\ldots) + F_{(\nu)}(J,K) \qquad 4.1$$

where $G(v_1, v_2, \ldots\ldots)$ is the vibrational term value given by a general expression for the vibrational levels of the molecule and $F_{(\nu)}(J,K)$ is the rotational term value associated with each vibrational state. $v_1, v_2, \ldots\ldots$ are the vibrational quantum numbers of the individual vibrational levels and J,K are the rotational quantum numbers.

The rotational term value for an oblate symmetric top molecule in a non-degenerate vibrational state is given by:[53,54]

$$F_{(\nu)}(J,K) = B_{(\nu)}J(J+1) + (C_{(\nu)} - B_{(\nu)})K^2 \qquad 4.2$$

Since $C - B < 0$, the lowest energy level in a given J is that for $K = J$. The energies of the various K levels decreases as K increases and each K level, except for $K = 0$, is doubly degenerate.

Allowed infrared transitions between two non-degenerate vibrational states give rise to parallel-type bands i.e. when the change in electric moment during a transition is parallel to the rotor axis. The symmetric rotor selection rules for parallel-type bands are:[53,54]

$$K \neq 0 \qquad \Delta J = 0, \pm 1 \qquad \Delta K = 0$$

$$K = 0 \qquad \Delta J = \pm 1 \qquad \Delta K = 0$$

For a particular K level, except for $K = 0$, ΔJ can take values of 0 and ± 1 so that there are three sub-bands corresponding to the P,Q and R branches (there is no Q branch for $K = 0$) with transition frequencies for

absorption from a lower state (ν'',J") to an upper state (ν',J') given by:[53,54]

$$\text{R branch } \nu_{J'',K}^{J''+1,K} = \nu_0^{SUB} + B'(J''+1)(J''+2) - B''J''(J''+1)$$
$$= \nu_0^{SUB} + 2B' + (3B'-B'')J'' + (B'-B'')J''^2$$

$$\text{P branch } \nu_{J''+1,K}^{J'',K} = \nu_0^{SUB} + B'(J''-1)J'' - B''J''(J''+1)$$
$$= \nu_0^{SUB} - (B'+B'')J'' + (B'-B'')J''^2$$

$$\text{Q branch } \nu_{J'',K}^{J'',K} = \nu_0^{SUB} + B'J'(J'+1) - B''J''(J''+1)$$

The complete parallel band is obtained by superposition of a number of such sub-bands corresponding to the various values of K that are populated at a given temperature. Due to differences of the rotational constants in the various vibrational levels, the origins of the sub-bands do not coincide exactly but vary according to the relation:

$$\nu_0^{SUB} = \nu_0 + \left[(C'-C'') - (B'-B'')\right] K^2 \qquad 4.4$$

with the result that the fine structure lines of the P and R-branches converge. To a good approximation B' = B" (= B) so that the expressions for the transition frequencies reduce to

$$\nu^R = \nu_0 + 2B(J''+1)$$
$$\nu^P = \nu_0 - 2BJ'' \qquad 4.5$$
$$\nu^Q = \nu_0$$

It is convenient to define a quantity[41]

$$\beta = \frac{C}{B} - 1 \qquad 4.6$$

For benzene and hexafluorobenzene (disk-shaped molecules) $\beta = -\frac{1}{2}$ and the frequency (cm^{-1}) separation of the P and R branch maxima is given by:[41]

$$\Delta\bar{\nu}_{PR} = S(\beta)\left[\frac{8kTB}{hc}\right]^{\frac{1}{2}} \qquad 4.7$$

where $S(\beta)$ is a separation function equal to 1.5 for disk-shaped molecules. Substitution in 4.7 gives $\Delta\bar{\nu}$ as a function of temperature

$$\Delta\bar{\nu}_{PR} = 1.5(2.358)(TB)^{\frac{1}{2}} \qquad 4.8$$

Table 4.2 contains calculated $\Delta\bar{\nu}_{PR}$ values at selected temperatures for benzene and hexafluorobenzene.

P-R Separations at Different Temperatures

	$\Delta\bar{\nu}_{PR}$ (calcd.) cm^{-1}		
T°K	C_6H_6	C_6D_6	C_6F_6
298.15	26.549	24.143	11.373
300	26.632	24.218	11.408
400	30.751	27.964	13.173
500	34.381	31.265	14.728

Table 4.2

The rigorous formulae for the line intensities have been derived on the basis of quantum mechanics.[55] For a given transition in absorption the intensity of rotational lines is given by:[53]

$$I(J,K) = C_{11}A_{J,K}\nu_{J,K}F_{J,K}\, e^{-F(J,K)hc/kT} \qquad 4.9$$

where C_{11} is a normalization constant independent of J and K but dependent

on the vibrational transition, $g_{J,K}$ is the statistical weight factor of the lower state, F(J,K) is the rotational term value of the lower state and $A_{J,K}$ is the line strength for the transition proportional to the square of the transition moment and summed over all orientations of J. The Hönl-London formulae for the quantities $A_{J,K}g_{J,K}$ are:[54]

$$J,/K/ \rightarrow J+1,/K/ \quad (2-\delta_{K,0})\frac{(J+K+1)(J-K+1)}{J+1}$$

$$J,/K/ \rightarrow J,/K/ \quad (2-\delta_{K,0})\frac{(2J+1)K^2}{J(J+1)}$$

$$J,/K/ \rightarrow J-1,/K/ \quad (2-\delta_{K,0})\frac{(J+K)(J-K)}{J}$$

in which J and K refer to the lower state and where $\delta_{K,0}$ is the Kronecker delta ($\delta_{K,0} = 1$ for $K = 0$ and $\delta_{K,0} = 0$ for $K \neq 0$). It is customary,[41,47] to split the normalization factor, $\bar{C}_{11}$, into two terms corresponding to the r and L terms in the paper of G and D[41] and to the γ and Q terms in the paper of E and M.[47] (N.B. $\gamma/Q = rL = \bar{C}_{11}$) The quantity r is the reciprocal of the approximate (classical) rotational partition function written in the form

$$r = \frac{1}{Q} = \left[\left(\frac{hcB}{kT}\right)^3 \frac{(1-C/B)}{\pi}\right]^{\frac{1}{2}} \qquad 4.10$$

and L, which can be shown to be equal to the sum of the intensities of all the fine structure lines can be written as

$$L = \gamma = \frac{8\pi^3}{3hc}(1-e^{-hc\bar{\nu}_0/kT})N_v\langle v/\mu/v'\rangle^2 \qquad 4.11$$

where N_v is the fraction of the molecules in the ground vibrational state and $\langle v/\mu/v'\rangle$ is the vibrational transition moment. The fraction of the total intensity contained in the Q-branch of parallel bands of molecules with $\beta < 0$ has been shown to be[41]

$$\frac{I_Q}{L} = \frac{\left\{ \left[-\frac{\beta}{1+\beta} \right]^{\frac{1}{2}} - \sin^{-1} (-\beta)^{\frac{1}{2}} \right\}}{-\beta \left[-\frac{\beta}{1+\beta} \right]^{\frac{1}{2}}} \qquad 4.12$$

For disk-shaped molecules $\beta = -\frac{1}{2}$ and the fraction is 0.43.

If only $0 \rightarrow 1$ vibrational transitions are considered the expression for L simplifies since

$$(1 - e^{-hc\bar{\nu}_o/kT}) \langle v/\mu/v' \rangle^2 = N_v \langle o/\mu/1 \rangle^2 \qquad 4.13$$

and with this approximation $\bar{C}_{11}$ can be written:

$$\bar{C}_{11} = \left\{ \frac{\frac{8\pi^3 N}{3hc}}{\left[\frac{\pi}{(\frac{hc\bar{B}}{kT})^{3} \frac{3}{B}} \right]^{\frac{1}{2}}} \right\} \langle o/\mu/1 \rangle^2 \qquad 4.14$$

The normalization constant, $\bar{C}_{11}$, is a function of $T^{-3/2}$ and is a constant for a particular molecule at a particular temperature. Table 4.3 contains calculated $\bar{C}_{11}$ values for benzene and hexafluorobenzene at a series of temperatures.

Normalization Constant $\bar{C}_{11} \times 10^{35}$ at

Series of Temperatures

T°K	C_6H_6	C_6D_6	C_6F_6
298.15	27.526	20.719	2.166
300	27.271	20.528	2.146
400	17.714	13.336	1.392
500	12.675	9.542	0.998

Table 4.3

A general computer program has been developed to calculate the quantity $\Sigma A_{J,K} g_{J,K} \nu_{J,K} e^{-F(J,K)hc/kT}$ for $J', J'' \; 0 \rightarrow 300$ and in frequency intervals of $0.2 cm^{-1}$. The computer program is written in CHLF3 Autocode and is presented in Appendix I. Table 4.4 contains a summary of the calculations for the A_{2u} (parallel) bands of benzene and hexafluorobenzene. The experimental and computed band shapes are shown in fig. 4.1.

$C_6H_6 \quad \nu_o = 673 cm^{-1}$

T°K	$\Sigma(Ag\nu)_{J,K} e^{-F(J,K)hc/kT}$	$\bar{C}_{11}\Sigma(\text{etc.})$	$\bar{C}_{11}\Sigma(\text{etc.})/\nu_o$
298.15	0.6055×10^8	16.667×10^{43}	2.477×10^{41}
300	0.6106	16.652	2.474
400	0.9403	16.656	2.475
500	1.3112	16.619	2.469

T°K	$\Delta\nu_{PR} cm^{-1}$	$\propto(\nu) \times 10^5$		
		P max.	Q max.	R max.
298.15	26.8	3.774	262.94	4.188
300	26.8	3.795	265.12	4.212
400	30.6	5.078	408.17	5.621
500	34.4	6.361	570.44	7.038

$$\text{Fraction of intensity in Q-branch} = \frac{\propto(\nu)_{Q\ max.}}{\Sigma(Ag\nu)_{J,K} e^{-F(J,K)hc/kT}}$$

$$= \underline{0.434}$$

Table 4.4

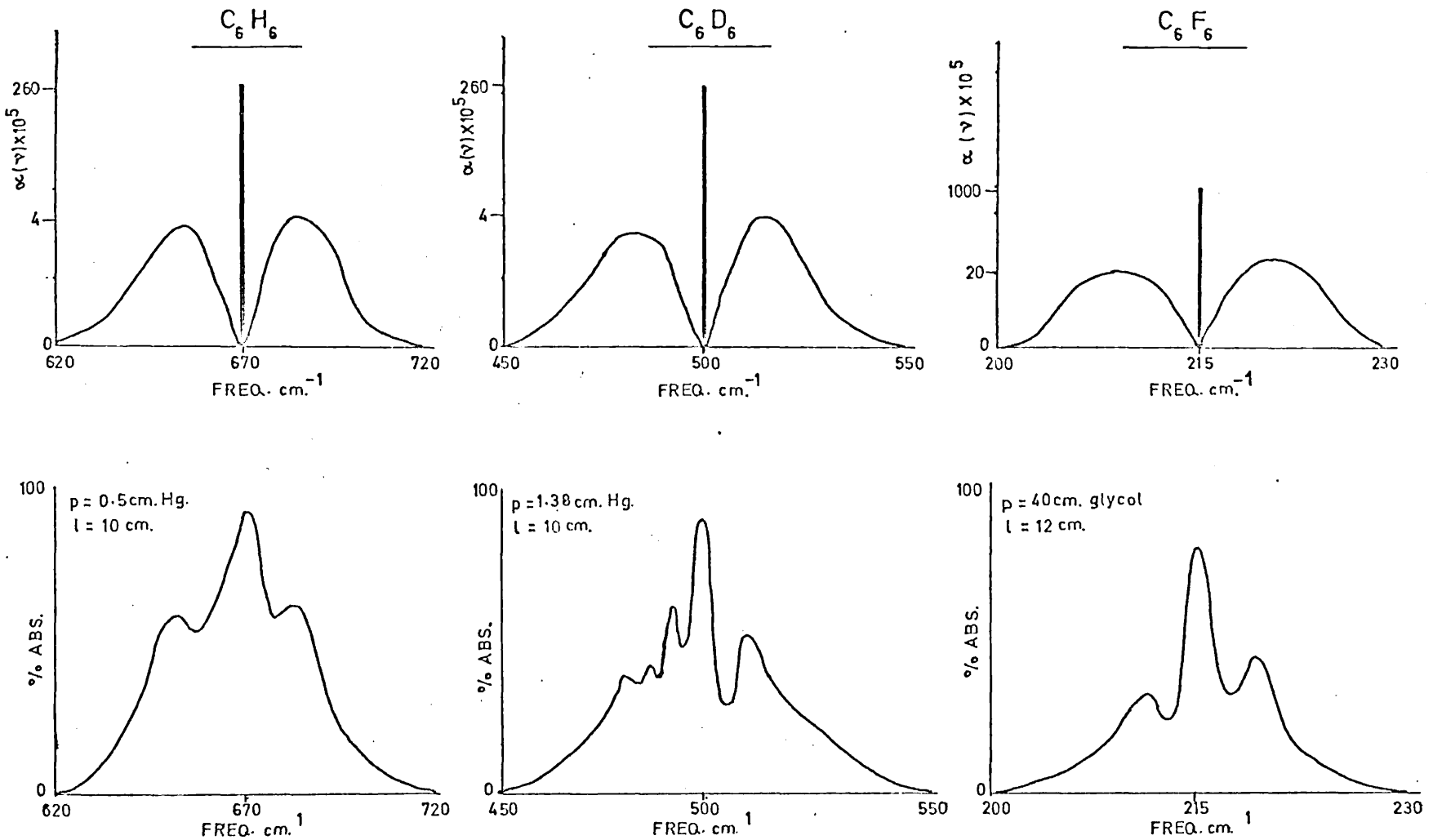

Fig.4. 1. Computed and Experimental Bands for A_{2u} Vibrations.

C_6D_6 $\nu_o = 496 cm^{-1}$

T°K	$\Sigma(Ag\nu)_{J,K}e^{-F(J,K)hc/kT}$	$\bar{C}_{11}\Sigma(etc.)$	$\bar{C}_{11}\Sigma(etc.)/\nu_o$
298.15	0.5942×10^8	12.311×10^{43}	2.482×10^{41}
300	0.5991	12.298	2.479
400	0.9233	12.313	2.482
500	1.2898	12.307	2.481

T°K	$\Delta\nu_{FR} cm^{-1}$	$\alpha(\nu) \times 10^5$		
		P max.	Q max.	R max.
298.15	24.0	3.362	257.66	3.746
300	24.2	3.381	259.80	3.765
400	28.2	4.519	399.98	5.032
500	31.6	5.654	558.99	6.304

Fraction of intensity in Q-branch = 0.433

C_6F_6 $\nu_o = 215 cm^{-1}$

T°K	$\Sigma(Ag\nu)_{J,K}e^{-F(J,K)hc/kT}$	$\bar{C}_{11}\Sigma(etc.)$	$\bar{C}_{11}\Sigma(etc.)/\nu_o$
298.15	2.4771×10^8	5.365×10^{43}	2.495×10^{41}
300	2.4977	5.360	2.493
400	3.8423	5.341	2.484
500	5.3490	5.338	2.483

T°K	$\Delta\nu_{FR} cm^{-1}$	$\alpha(\nu) \times 10^5$		
		P max.	Q max.	R max.
298.15	11.4	20.155	1068.1	21.846
300	11.4	20.264	1076.9	21.970
400	13.2	26.987	1653.3	29.382
500	14.6	33.672	2292.9	36.851

Fraction of intensity in Q-branch = 0.431

Table 4.4

Comparison of the computed and experimental bands shows that the frequency separations of the PR maxima are in quite good agreement and are also in good agreement with the values calculated from the expressions given by Gerhard and Dennison.[41] The computed and experimental band shapes differ for two reasons. No account has been taken of 'hot' bands which are likely to be of importance particularly at low frequency and also because the experimental bands were pressure broadened. 'Hot' bands are clearly evident in the experimental band of benzene d_6. Both factors lead almost solely to broadening of the Q-branches. The intensities in the P, Q and R branches of the experimental and computed curves have been separately estimated. Ratios of the Q-branch to the P- and R-branch intensities are in good agreement and also agree with those calculated from the expressions of Gerhard and Dennison.[41]

The possibility of estimating integrated absorption intensities from the computed band shapes by comparing the computed absorption coefficient at a given frequency in terms of the dipole moment derivative with respect to the associated normal coordinate, $\frac{\partial \mu}{\partial Q_i}$, with the experimental value has long been recognized. The average absorption coefficient within a frequency interval $\Delta\nu$ and at a particular frequency ν is related to the sum of the intensities due to transitions within that frequency range by[46,47]

$$\bar{\alpha}(\nu) = \sum_{\nu - \frac{\Delta\nu}{2}}^{\nu + \frac{\Delta\nu}{2}} \frac{\alpha(\nu)_j}{\Delta\nu} \qquad 4.15$$

where $\alpha(\nu)_j$ is the line intensity at the frequency ν. Two conditions are required for satisfactory usage of expression 4.15, i) the density of transitions within the interval $\Delta\nu$ must be sufficiently high for the edge

effects arising from finite band widths to be negligible and ii) that saturation of absorption over a given small frequency interval within the chosen interval does not occur. The former condition is certainly satisfied for heavy polyatomic molecules and the latter situation does not arise in infrared spectroscopy.

The absorption coefficient at a particular frequency ν is defined in terms of the intensity of the incident and transmitted beam of the same frequency by

$$\alpha(\nu) = \frac{1}{pl} \log_e \frac{I_0}{I} . \qquad 4.16$$

An infrared spectrometer measures $\alpha(\nu)$ values. Edgell and Moynihan[46] have shown that the measured absorption coefficient will equal the pressure independent average absorption coefficient provided that certain conditions are fulfilled, namely

$$\alpha(\nu) = \bar{\alpha}(\nu). \qquad 4.17$$

By comparing the average absorption coefficient obtained from the computed band with the experimental value, at the same frequency, we can estimate a value for the integrated absorption intensity. For convenience we choose to compare the absorption coefficients at the frequencies of the P- and R-branch maxima. The experimental band shapes of the A_{2u} vibrations of benzene and hexafluorobenzene show a marked asymmetry with $\sim 5\%$ difference in the intensities of the P- and R-branches. To explain the asymmetry it is necessary to consider differences between the rotational constants for the ground and excited states. Good agreement between the experimental and computed band shapes is obtained with $\frac{B' - B''}{B''} = 0.0005$.

The average absorption coefficient $\bar{\alpha}(\nu)$ at the frequency of the P-branch maximum can be written $\bar{\alpha}(\nu) = \dfrac{\bar{c}_{11}\,\alpha(\nu)_{P_{max.}}\,\langle o/\mu/1\rangle^2}{\Delta\nu}$ 4.18

The transition moment is related to the dipole moment derivative with respect to the associated normal coordinate by[3]

$$\left(\frac{\partial\mu}{\partial Q}\right)^2 = \frac{8\pi^2\nu_o}{h}\,\langle o/\mu/1\rangle^2 \qquad 4.19$$

Substitution for $\langle o/\mu/1\rangle^2$ in equation 4.18 yields

$$\bar{\alpha}(\nu) = \alpha(\nu)_{expt.} = \bar{c}_{11}\cdot\frac{\alpha(\nu)_{P_{max}}}{c}\cdot\frac{h}{8\pi^2\nu_o}\left(\frac{\partial\mu}{\partial Q}\right)^2 \qquad 4.20$$

Thus, if $\alpha(\nu)$ expt. is determined from the experimental band and $\alpha(\nu)_{P_{max.}}$ is determined from the computed band, then we obtain a value for $\frac{\partial\mu}{\partial Q}$ which should be in good agreement with the value of $\frac{\partial\mu}{\partial Q}$ obtained from integration of the complete experimental band. The great advantage of such a method for estimating $\frac{\partial\mu}{\partial Q}$ values lies in the fact that we need rely only on one experimental value of $\log_{10}\frac{I_o}{I}$ and this at a convenient part of the spectral band.

The quantity $\alpha(\nu)_{expt.}$ for the A_{2u} parallel vibrations of benzene and hexafluorobenzene is obtained from the equation

$$\alpha(\nu)_{expt.} = \frac{22400}{N}\cdot\frac{760}{p}\cdot\frac{273+t}{273}\cdot\frac{2.303}{l}\log_{10}\frac{I_o}{I} \qquad 4.21$$

where N is the Avagadro number, p is the pressure of vapour in mm. Hg, l is the path length of the cell and $\log_{10}\frac{I_o}{I}$ is the absorbance at a particular frequency ν. Table 4.5 shows the values of $\alpha(\nu)_{expt.}$ at the frequency of the P- and R-branch maxima for benzene and hexafluorobenzene.

$\alpha(\nu)_{expt.}$ Values

Molecule	$\alpha(\nu)_P \times 10^{-20}$	$\alpha(\nu)_R \times 10^{-20}$
C_6H_6, $\nu_o = 673 cm.^{-1}$	44.20	46.00
C_6D_6, $\nu_o = 494 cm.^{-1}$	16.60	18.80
C_6F_6, $\nu_o = 215 cm.^{-1}$	2.31	2.62

Table 4.5

Rearrangement of equation 4.20 leads to an expression for the calculated value of $\frac{\partial\mu}{\partial Q}$, calcd.

$$\left(\frac{\partial\mu}{\partial Q}\right)^2_{calcd.} = \frac{8\pi^2\nu_o c\,\Delta\nu}{h} \cdot \frac{\alpha(\nu)_{expt.}}{\bar{C}_{11}\alpha(\nu)_{P\ calcd.}} \quad . \qquad 4.22$$

The observed and the calculated values of $\frac{\partial\mu}{\partial Q}$ are shown in table 4.6. The units of $\frac{\partial\mu}{\partial Q}$ are $cm.^{3/2}\ sec.^{-1} \times 10^{-10}$.

Dipole Moment Derivatives

	$\left(\frac{\partial\mu}{\partial Q}\right)_{OBS.}$	$\left(\frac{\partial\mu}{\partial Q}\right)^P_{CALCD.}$	$\left(\frac{\partial\mu}{\partial Q}\right)^R_{CALCD.}$
C_6H_6	± 1.46	± 1.43	± 1.39
C_6D_6	± 1.09	± 0.92	± 0.93
C_6F_6	± 0.25	± 0.28	± 0.29

Table 4.6

Comparison of the observed and the calculated values for the dipole moment derivatives of the A_{2u} vibrations of benzene d_0, benzene d_6 and hexafluorobenzene indicates that absolute infrared intensities can be satisfactorily estimated using the method we have described.

PERPENDICULAR TRANSITIONS

The rotational term value of an oblate symmetric top molecule in which a degenerate vibrational state is singly excited is, to a first order of approximation,[53,54]

$$F_{(\nu)}(J,K) = B_{(\nu)}J(J+1) + (C_{(\nu)}-B_{(\nu)})K^2 \mp 2C_{(\nu)}\zeta_i K \qquad 4.23$$

where ζ_i is the Coriolis coupling constant for the i-th vibrational mode.

It was established by Teller[56] that the influence of vibration-rotation coupling (Coriolis interaction) was responsible for apparent discrepancies in the rovibrational spectra of the degenerate vibrational states of symmetric top molecules. The term $\mp 2C_{(\nu)}\zeta_i K$ is included in the rotational term value to account for the Coriolis interaction and is considered as a first order perturbation to the rigid-rotor harmonic oscillator problem in the case of degenerate vibrational states.

The system of coordinates used to describe the simultaneous vibration and rotation of a molecule are the three cartesian coordinates of the centre of mass of the molecule, the three Eulerian angles of a rotating cartesian coordinate system and 3N-6 internal coordinates which describe the relative positions of the atoms in the rotating axes. In such a coordinate system, the acceleration produced by the acting forces is supplemented by an additional acceleration due to the Coriolis force. The Coriolis force is due to the interaction of vibration and rotation and is directed at right

angles to the direction of motion of each atom and a right angles to the axis of rotation. The magnitude is proportional to the masses of the particles, their apparent velocities with respect to the rotating coordinate system and to the angular velocity of the rotating coordinate system with respect to the fixed coordinate system.

When one of the components of a doubly degenerate vibrational mode is excited the Coriolis forces produced act in the same direction as the displacement vectors of the other component of this perpendicular vibration. This has the effect of removing the degeneracy and the atoms concerned in the vibration acquire an additional, vibrational angular momentum, $\zeta_1 \, h/2\pi$, about the symmetry axis. The atoms move in ellipses, and not in straight lines, which are flatter the smaller the coupling between the two components of the degenerate modes. Each K rotational level is split into two sub-levels depending on the direction of the additional, vibrational angular momentum with respect to the rotational angular momentum. The splitting of each K rotational level is the same for a given K and increases with increasing K; it is zero for K = 0.

Allowed infrared transitions between lower non-degenerate vibrational states and upper degenerate vibrational states give rise to perpendicular-type bands i.e. the change in electric moment during a transition is perpendicular to the rotor axis. The symmetric rotor selection rules for perpendicular-type bands are

$$\Delta K = \pm 1 \; ; \; \Delta J = 0, \pm 1.$$

In the expression for the rotational term value the upper (–) sign of the term $\mp 2C_{(\nu)}\zeta_1 K$ applies when $\Delta K = +1$ i.e. when the vibrational angular momentum is in the same direction as the rotational angular

momentum and the lower (+) sign applies when $\Delta K = -1$ i.e. when the angular momenta are opposite in direction.

The selection rules allow more transitions than in the parallel case so that the structure of the overall band is much more complex. Corresponding to every K and ΔK value there is a sub-band consisting of a P,Q,R series arising from the transitions $\Delta J = 0, \pm 1$. The frequencies of the sub-band centres corresponding to the case when $J = 0$, are given by:

$$\nu_0^{sub} = \nu_0 + \left[C'(1-2\zeta) - B'\right] \pm 2\left[C'(1-\zeta) - B'\right]K'' + \left[(C'-B') - (C''-B'')\right]K''^2 \qquad 4.24$$

which reduces to:

$$\nu_0^{sub} = \nu_0 + C_{(\nu)}(1-2\zeta_1) - B_{(\nu)} \pm 2\left[C_{(\nu)}(1-\zeta_1) - B_{(\nu)}\right]K'' \qquad 4.25$$

if $B' = B''$ $(= B)$. K'' is the quantum number of the lower vibrational state and ν_0 is the fundamental vibrational frequency. The upper (+) sign refers to the R-branch sub-bands ($\Delta K = +1$) for which $K'' = 0,1,2,\ldots\ldots$ and the lower (−) sign refers to the P-branch sub-bands ($\Delta K = -1$) for which $K'' = 1,2,\ldots\ldots$ The separation of the various sub-bands is $2\left[C_{(\nu)}(1-\zeta) - B\right]$.

The frequencies of the Q-branch lines of the sub-bands are:

$$\nu^Q = \nu_0^{sub} + (B'-B'')J(J+1) \qquad 4.26$$

and the P- and R-branch transitions of the sub-bands are given by:

$$\nu^P = \nu_0^{sub} - (B'+B'')J + (B'-B'')J^2 \qquad 4.27$$

$$\text{and} \quad \nu^R = \nu_0^{sub} + (B'+B'')(J+1) + (B'-B'')(J+1)^2 \qquad 4.28$$

With the approximation $B' = B''$ $(= B)$ these expressions reduce to:

$$\nu^{Q} = \nu_{o}^{sub}$$

$$\nu^{P} = \nu_{o}^{sub} - 2BJ \qquad 4.29$$

$$\nu^{R} = \nu_{o}^{sub} + 2B'J+1).$$

The intensity of the rotational liner are given by

$$I(J,K) = \bar{C}_1 A_{J,K} \nu_{J,K} g_{J,K} e^{-F(J,K)hc/kT} .$$

For perpendicular-type bands the quantities $A_{JK} g_{JK}$ are[54]

$$J,/K/ \rightarrow J+1,/K/\pm 1 = \frac{(J\pm K+1)(J\pm K+2)}{J+1}$$

$$J,/K/ \rightarrow J,/K/\pm 1 = \frac{(2J+1)(J\mp K)(J\pm K+1)}{J(J+1)} \qquad 4.30$$

$$J,/K/ \rightarrow J-1,/K/\pm 1 = \frac{(J\mp K)(J\mp K-1)}{J}$$

in which J and K refer to the lower state. The normalization constant $\bar{C}_1$ is split into two terms corresponding to the r and L terms in the paper of G and D[41] and to the γ and Q terms in the paper of E and M.[47]

$$(\text{E.B. } \frac{rL}{2} = \frac{\gamma}{2Q} = \bar{C}_1 = \bar{C}_{11/2}).$$

r is the reciprocal of the approximate (classical) rotational partition function

$$r = \frac{1}{Q} = \left[\left(\frac{hcB}{kT}\right)^3 \frac{(1 - \frac{C}{B})}{\pi}\right]^{\frac{1}{2}} \qquad 4.31$$

and L, which can be shown to equal the sum of the intensities of all the fine structure lines, is

$$L = \gamma = \frac{8\pi^3}{3hc}(1-e^{-hc\bar{\nu}_o/kT}) N_v \langle v/\mu/v' \rangle^2 \qquad 4.32$$

If only $0 \rightarrow 1$ transitions are considered the intensity of the rotational lines can be expressed:

$$I(J,K) = \frac{8\pi^3 N}{3hc} \Bigg/ 2\left[\frac{\pi}{\left(\frac{hcB}{kT}\right)^3}\frac{C}{B}\right]^{\frac{1}{2}} \sum A_{J,K}\nu_{J,K}g_{J,K}e^{-F(J,K)\frac{hc}{kT}} \langle o/\mu/1 \rangle^2 \qquad 4.33$$

The normalization constant, $\bar{C}_1$, is a function of $T^{-3/2}$ and is a constant for a particular molecule at a particular temperature. Table 4.7 contains calculated $\bar{C}_1$ values at a series of temperatures for benzene and hexafluorobenzene.

Normalization Constant $\bar{C}_1 \times 10^{35}$ at Different Temperatures

T°K	C_6H_6	C_6D_6	C_6F_6
298.15	13.763	10.359	1.083
300	13.636	10.264	1.073
400	8.857	6.668	0.696
500	6.338	4.771	0.499

Table 4.7

A general computer program has been developed to determine the summation $\Sigma A_{J,K}g_{J,K}\nu_{J,K}e^{-F(J,K)hc/kT}$ for J',J" 0 → 250 and for a range of zeta values ($+1 \geq \zeta_1 \geq -1$) in the case of the degenerate vibrations of symmetric top molecules. The computer program is written in CHLF3 Autocode and processed on the Atlas (University of London) Computer. The program is presented in Appendix II. Computed band contours of selected E_{1u} bands of C_6H_6, C_6D_6 and C_6F_6 have been obtained from the values of the

summation at frequency intervals of $0.2cm^{-1}$. Table 4.8 contains a summary of the results for $J_{max.} = 250$. The computed band contour of the $315cm^{-1}$ E_{1u} band of hexafluorobenzene for a range of zeta values is shown in fig. 4.2. Best estimates of Coriolis zeta values can be obtained by comparing the computed band contour with the experimental band. The influence of Coriolis zeta value on the frequency separation of the P- and R-branch maxima and the fractional intensity contained in the separate P, Q and R-branches are carefully considered. In the case of the $315cm^{-1}$ E_{1u} band of hexafluorobenzene there is good agreement between the computed and experimental band contours for a zeta value of -0.6 ± 0.1. The results shown in Table 4.8 are for the best estimate of the zeta values for E_{1u} bands of C_6H_6, C_6D_6 and C_6F_6. It is only possible to estimate zeta values for bands which are approximately symmetric to the band centre and when other perturbations e.g. Fermi resonances are absent.

The asymmetry ($\sim 5\%$) in the experimental $315cm^{-1}$ band of hexafluorobenzene can be accounted for by allowing the rotational constants to vary between upper and lower states. A 5% asymmetry is introduced into the computed band contour with $\frac{B'' - B'}{B''} = 0.0005$. The influence of rotational constant variations between upper and lower states is shown in fig. 4.3.

Earlier in this chapter we discussed the determination of dipole moment derivatives from band shape calculations for parallel vibrations of symmetric top molecules. In principle, the method is exactly the same for perpendicular vibrations. However, in this case a degeneracy factor is introduced into the expression for the calculated value of $\frac{\partial\mu}{\partial Q}$,

$$\left(\frac{\partial\mu}{\partial Q}\right)^2_{CALC.} = \frac{8\pi^2 c\,\Delta\nu}{h} \cdot \frac{\alpha(\nu)_{expt.}}{g\alpha(\nu)_{CALC.}} \cdot \frac{\nu_0}{C1} \cdot \qquad 4.34$$

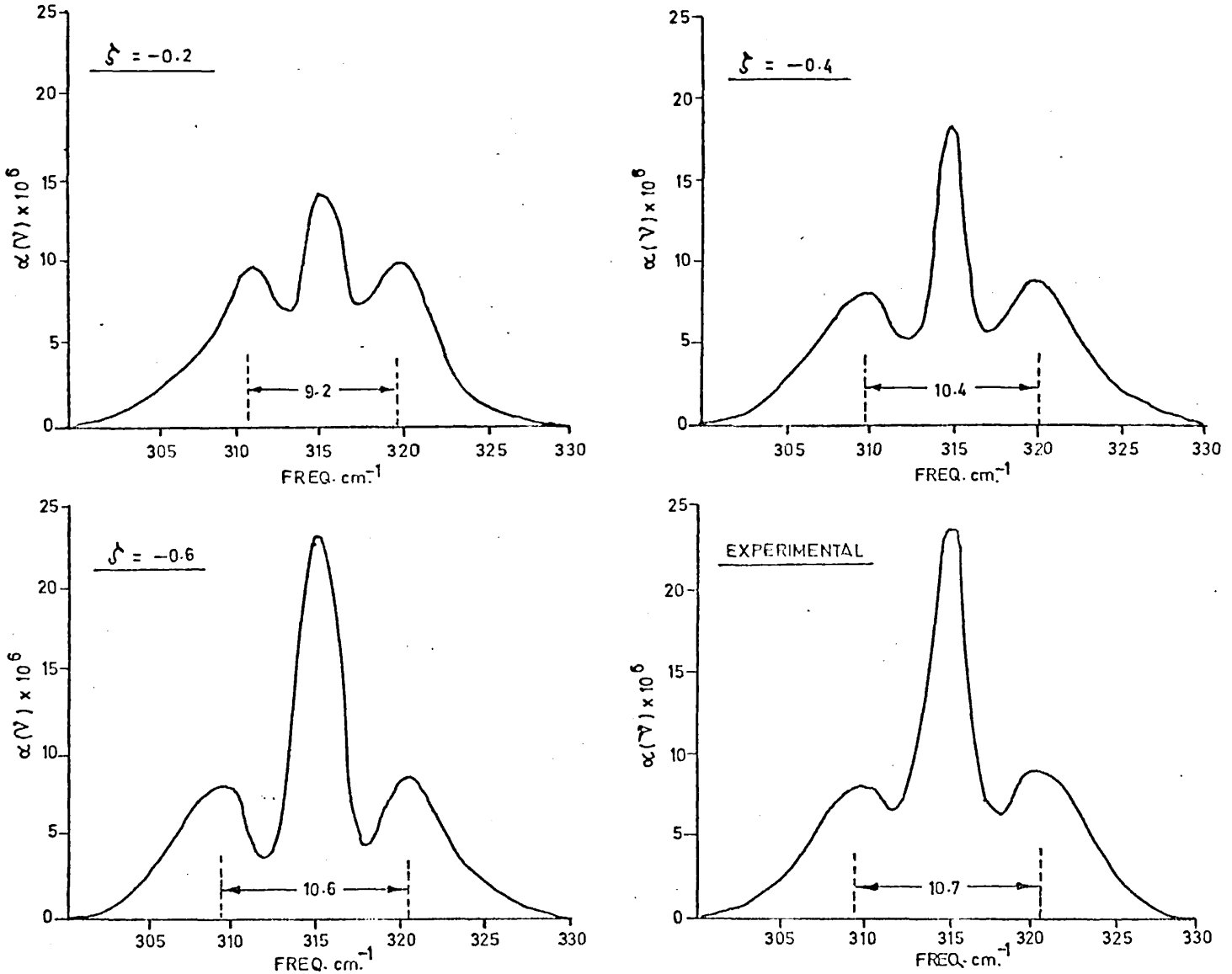

Fig. 4. 2. The Influence of Coriolis Coupling on the 315 cm^{-1} E_{1u} Band of HFB

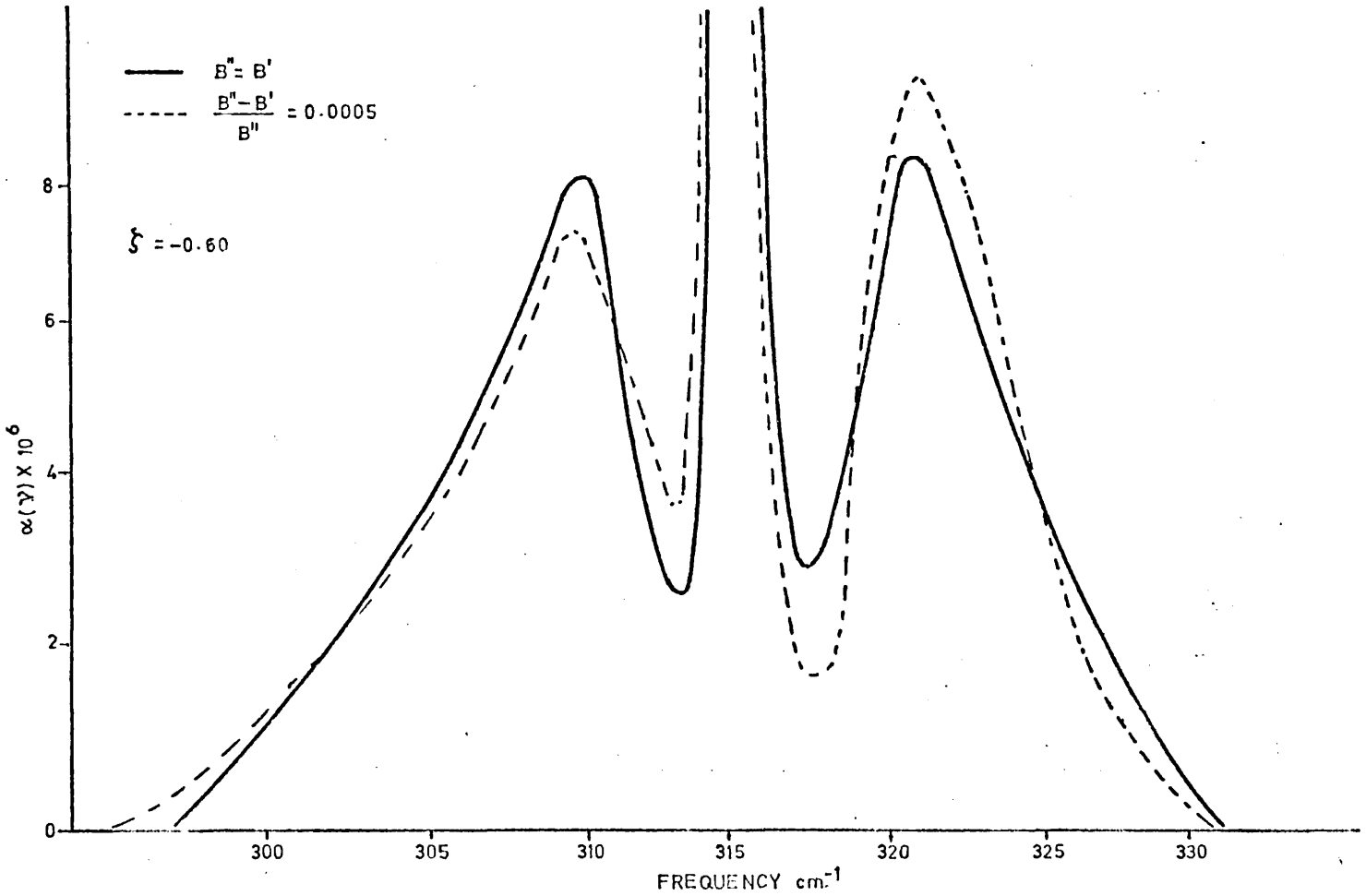

Fig. 4.3. The Influence of Changes in Rotational Constant for the 315 cm.$^{-1}$ Band of HFB.

C_6F_6 $\nu_0 = 315 cm^{-1}$ $\zeta = -0.60$

T°K	$(Ag\nu)_{J,K} e^{-F(J,K)hc/kT}$	$\bar{C}_1 \Sigma$ (etc.)	$\bar{C}_1 \Sigma$ (etc.)$/\nu_0$
298.15	7.240×10^8	7.841×10^{43}	2.489×10^{41}
300	7.289	7.821	2.312
400	11.144	7.756	2.462
500	15.304	7.637	2.424

T°K	$\Delta\nu_{PR} cm^{-1}$	$\alpha(\nu) \times 10^7$		
		P max.	Q max.	R max.
298.15	10.6	0.790	2.524	0.833
300	10.7	0.801	2.597	0.851
400	12.4	1.055	3.459	1.120
500	13.4	1.311	4.379	1.399

Table 4.8(i)

C_6H_6 $\nu_0 = 1038 cm^{-1}$ $\zeta = -0.55$

T°K	$(Ag\nu)_{J,K} e^{-F(J,K)hc/kT}$	$\bar{C}_1 \Sigma$ (etc.)	$\bar{C}_1 \Sigma$ (etc.)$/\nu_0$
298.15	1.866×10^8	25.681×10^{43}	2.474×10^{41}
300	1.882	25.662	2.472
400	2.899	25.676	2.474
500	4.048	25.656	2.472

T°K	$\Delta\nu_{PR} cm^{-1}$	$\alpha(\nu) \times 10^7$		
		P max.	Q max.	R max.
298.15	24.6	0.0906	0.2999	0.0955
300	24.6	0.0911	0.3018	0.0960
400	28.4	0.1159	0.3718	0.1310
500	31.8	0.1473	0.5104	0.1642

Table 4.8(ii)

C_6H_6 $\nu_o = 1483 cm^{-1}$ $\zeta = -0.45$

T°K	$(Ag\nu)_{J,K} e^{-F(J,K)hc/kT}$	$\bar{C}_1 \Sigma$ (etc.)	$\bar{C}_1 \Sigma$ (etc.)$/\nu_o$
298.15	2.663×10^8	36.720×10^{43}	2.476×10^{41}
300	2.690	36.681	2.473
400	4.147	36.730	2.477
500	5.793	36.716	2.476

T°K	$\Delta\nu_{FR} cm^{-1}$	$\alpha(\nu) \times 10^7$		
		P max.	Q max.	R max.
298.15	25.4	0.1321	0.3188	0.1413
300	25.4	0.1329	0.3206	0.1422
400	29.4	0.1749	0.4292	0.1893
500	32.0	0.2213	0.5380	0.2430

Table 4.8(iii)

C_6D_6 $\nu_o = 1335 cm^{-1}$ $\zeta = -0.40$

T°K	$(Ag\nu)_{J,K} e^{-F(J,K)hc/kT}$	$\bar{C}_1 \Sigma$ (etc.)	$\bar{C}_1 \Sigma$ (etc.) $/\nu_o$
298.15	3.197×10^8	33.117×10^{43}	2.481×10^{41}
300	3.224	33.091	2.479
400	4.970	33.140	2.482
500	6.949	33.154	2.483

T°K	$\Delta\nu_{FR} cm^{-1}$	$\alpha(\nu) \times 10^7$		
		P max.	Q max.	R max.
298.15	21.6	0.1878	0.5173	0.1994
300	21.6	0.1889	0.5202	0.2005
400	25.8	0.2503	0.6974	0.2644
500	28.4	0.3148	0.8748	0.3331

Table 4.8(iv)

C_6D_6 $\nu_o = 814 cm^{-1}$ $\zeta = -0.40$

T°K	$(Ag\nu)_{J,K} e^{-F(J,K)hc/kT}$	$\bar{c}_1 \Sigma$ (etc.)	$\bar{c}_1 \Sigma$ (etc.)$/\nu_o$
298.15	1.950×10^8	20.200×10^{43}	2.482×10^{41}
300	1.966	20.179	2.479
400	3.031	20.211	2.483
500	4.238	20.219	2.484

T°K	$\Delta\nu_{PR} cm^{-1}$	$\alpha(\nu) \times 10^7$		
		P max.	Q max.	R max.
298.15	21.6	0.1139	0.3154	0.1220
300	21.6	0.1146	0.3172	0.1229
400	25.0	0.1517	0.4252	0.1622
500	28.6	0.1906	0.5333	0.2045

Table 4.8(v)

The degeneracy factor $g = 2$ for the E_{1u} vibrations of C_6H_6, C_6D_6 and C_6F_6. Also the estimation of reliable $\alpha(\nu)_{calc.}$ values is dependent on the choice of zeta value. Table 4.9 shows the influence of zeta value on the value of $\alpha(\nu)_{calc.}$ at the frequency of the P, Q and R-branch maxima for the 315cm^{-1} E_{1u} band of hexafluorobenzene at 298.15°K.

Variation of $\alpha(\nu)_{calc.}$ with Zeta Value for the 315cm^{-1} E_{1u} Band of HFB at 298.15°K.

ζ_1 Value	$\alpha(\nu)_{calc.} \times 10^7$		
	P max.	Q max.	R max.
- 0.3	0.8672	1.4380	0.9153
- 0.4	0.8264	1.7755	0.8697
- 0.5	0.8199	2.0833	0.8569
- 0.6	0.7902	2.5240	0.8330
- 0.7	0.7365	3.2979	0.7768
- 0.8	0.7085	4.8403	0.7555

Table 4.9

We have obtained $\frac{\partial\mu}{\partial Q}_{calc.}$ values for the bands of C_6H_6, C_6D_6 and C_6F_6 for which we were able to make reasonable estimates for the zeta value. The $\alpha(\nu)_{calc.}$ values are taken from the P and R-branch maxima of the computed curves and the $\alpha(\nu)_{expt.}$ values are taken from the P and R-branch maxima of the experimental curves. Table 4.10 gives a summary of the results. The calculated values of $\frac{\partial\mu}{\partial Q}$ are in excellent agreement with the values obtained from integrating the complete experimental band. The great advantage of this method of estimating $\frac{\partial\mu}{\partial Q}$ values lies in the fact that we need to know only one $\log_{10}\frac{I_0}{I}$ value from the experimental curve for a

Calculated Values of $\frac{\partial \mu}{\partial Q}$

Molecule	Frequency cm^{-1}	ζ_i Value	$\alpha(\nu)_{expt.} \times 10^{-19}$		$\alpha(\nu)_{calc.} \times 10^{7}$		$\bar{c}_1$ $\times 10^{42}$	$\frac{\partial \mu}{\partial Q}$ calc.		$\frac{\partial \mu}{\partial Q}$ OBS. $\times 10^{-10} cm^{3/2} \cdot sec^{-1}$
			P max.	R max.	P max.	R max.		P max.	R max.	
C_6F_6	315	- 0.60	.2311	.2405	.7900	.8330	1.073	.1740	.1722	.1724
C_6H_6	1038	- 0.55	.3590	.3602	.0906	.0955	13.636	.3274	.3194	.3234
C_6H_6	1483	- 0.45	.5246	.5348	.1321	.1413	13.636	.3823	.3917	.3931
C_6D_6	814	- 0.40	.3569	.3165	.1169	.1220	10.264	.2971	.2701	.3087
C_6D_6	1335	- 0.40	.1179	.1095	.1878	.1994	10.264	.1708	.1597	.1856

Table 4.10

given pressure of vapour and path length. It is immediately clear that the method could be refined by determining the $\log_{10} \frac{I_0}{I}$ value at say the P and R-branch maxima for a series of pressures or path lengths and hence obtaining a mean value for $\alpha(\nu)_{expt.}$. For bands with very sharp Q-branches, the measured $\log_{10} \frac{I_0}{I}$ values in the Q-branch section are often in doubt because the half-width of the Q-branch may be comparable with the spectrometer slit-width. It is suggested that the method of determining intensities using the mean value of $\alpha(\nu)_{expt.}$ obtained only from the P and R-branch maxima may lead to more accurate values in these cases. The method is only applicable to symmetric and spherical top molecules and for band envelopes which are almost symmetric to the band centre and when other perturbations e.g. Fermi resonance are absent.

CHAPTER FIVE

Interpretation of Intensities in Terms of Bond Parameters

The absolute absorption intensities of the fundamental vibrations of benzene d_0 have been reported by Spedding and Whiffen.[10] A re-determination[57] of the intensities suggests that the data of Spedding and Whiffen are essentially correct. We have also determined the intensities of the benzene d_0 fundamentals under conditions of complete pressure broadening and the agreement is satisfactory. The results of our work are contained in Chapter 9. Spedding and Whiffen have interpreted the benzene d_0 intensity data in terms of bond properties on the basis of the simple bond-moment hypothesis. They obtain two different values for the effective CH bond moment, namely, 0.31D. for in-plane deformation and 0.61D. for out-of-plane deformation. We have discussed in Chapter 1 how this can be understood, at least qualitatively, by invoking the idea of a rehybridization moment. Spedding and Whiffen were able to calculate intensities of benzene d_6 which showed general agreement with the approximate intensities indicated by published spectra of benzene d_6.[16] Recently, Dows and Pratt[58] have reported absolute intensities of the benzene d_6 fundamentals which show satisfactory agreement with the calculated intensities. This suggests that any interpretation of the benzene d_6 data on the basis of the bond-moment hypothesis would lead to similar conclusions as those reached for benzene d_0. For the reasons discussed in Chapter 1, we expect closely similar conclusions from an interpretation of the absolute intensities of the hexafluorobenzene fundamentals.

The reported absolute intensities of the infrared absorption

fundamentals of benzene d_0 and d_6 and hexafluorobenzene in the vapour phase are presented in Table 5.1. For convenience we quote Γ values in units of $mol.^{-1}cm.^2$ and A values in units of $mol.^{-1}cm.^2sec.^{-1}$ (N.B. we use $A = \Gamma\bar{\nu}_0 c$).

Sym.	Sym.	Γ $mol.^{-1}cm.^2 \times 10^{-20}$			A $mol.^{-1}cm.^2sec.^{-1} \times 10^{-7}$		
Species	No.	C_6H_6	C_6D_6	C_6F_6	C_6H_6	C_6D_6	C_6F_6
A_{2u}	S_{11}	2.18[a] (2.08)[d]	1.67[c] (1.68)[b]	0.201[f] (0.348)[g]	4.39[a] (4.23)[d]	2.48[c] (2.50)[b]	0.128[f] (0.224)[g]
E_{1u}	S_{18}	0.324[a] (0.371)[d]	0.258[c] (0.230)[b]	5.93[e] (—)	2.99[a] (3.43)[d]	1.77[c] (1.58)[b]	27.2[e] (—)
	S_{19}	0.146[a] (0.180)[d]	0.038[c] (0.035)[b]	6.70[e] (6.83)[g]	0.65[a] (0.80)[d]	0.15[c] (0.14)[b]	20.3[e] (20.7)[g]
	S_{20}	0.141[a] (0.135)[d]	0.165[c] (0.173)[b]	0.132[f] (0.060)[g]	0.44[a] (0.42)[d]	0.40[c] (0.42)[b]	0.125[f] (0.057)[g]

Table 5.1

a experimental data of Spedding and Whiffen[10]
b calculated " " " " " [10]
c experimental " " Dows and Pratt[58]
d " " " Overend[57]
e " " " Steele and Whiffen[37]
f this work
g experimental data of Person et al[21]

values offer a direct comparison of the magnitudes of $\int_{BAND} \log_{10} \frac{I_0}{I} (d \log_{10}\bar{\nu})$ for the absorption bands of different samples at the

same pressure and path length. The choice of units means that values of the dipole moment gradients are calculated from expressions:

$$\Gamma = \frac{N\pi g}{3c^2\tilde{\nu}_0}\left(\frac{\partial\mu}{\partial Q_i}\right)^2 \text{ or } A = \frac{N\pi g}{3c}\left(\frac{\partial\mu}{\partial Q_i}\right)^2 \qquad 5.1$$

and the $\frac{\partial\mu}{\partial Q_i}$ values will have the units $cm.^{3/2}sec^{-1}$. The degeneracy factor, g, is 2 for an E_{1u} doubly degenerate mode and 1 for an A_{2u} non-degenerate mode. Values of the dipole moment gradients are presented in Table 5.2; the superscripts refer to those of Table 5.1. Since the absolute intensity of a vibrational fundamental is proportional

Sym. No.	Dipole Moment Gradients $\frac{\partial\mu}{\partial Q}$ $cm^{3/2}.sec^{-1}.$ x 10^{-10}		
	C_6H_6	C_6D_6	C_6F_6
S_{11}	$\pm 1.445^a$ $\pm 1.418^d$	$\pm 1.086^c$	$\pm 0.247^f$ $\pm 0.326^g$
S_{18}	$\pm 0.843^a$ $\pm 0.903^d$	$\pm 0.648^c$	$\pm 2.543^e$ $\pm 2.543^e$
S_{19}	$\pm 0.393^a$ $\pm 0.437^d$	$\pm 0.186^c$	$\pm 2.197^e$ ± 2.216
S_{20}	$\pm 0.323^a$ $\pm 0.317^d$	$\pm 0.309^c$	$\pm 0.172^f$ $\pm 0.116^g$

Table 5.2

to the square of the dipole moment derivative with respect to the normal coordinate associated with a particular vibration, it is clear that an error of 10% in the former will lead to a 5% error in the $\frac{\partial\mu}{\partial Q_i}$. However,

the sign of the square root will be undetermined.

To relate dipole moment gradients to quantities which are characteristic of individual chemical bonds we must express them as dipole derivatives with respect to internal symmetry coordinates. Normal coordinates are related to internal symmetry coordinates by means of the coordinate transformation:

$$S_j = \mathcal{L}_{ij} Q_i \qquad 5.2$$

$$\text{thus} \quad \frac{\partial \mu}{\partial Q_i} = \sum_j \frac{\partial \mu}{\partial S_j} \mathcal{L}_{ij} \qquad 5.3$$

The $\mathcal{L}$ matrices (eigenvectors) are obtained by solution of vibrational secular equation $GF\mathcal{L} = \mathcal{L}\Lambda$ for the particular symmetry class.

There is only one vibration S_{11} in the out-of-plane A_{2u} symmetry species so that the corresponding $_{11}$ vector is trivial.

$$\mathcal{L}_{11} \mathcal{L}_{11}^{+} = G_{11,11}, \therefore \mathcal{L}_{11} = G_{11,11}^{\frac{1}{2}} . \qquad 5.4$$

The complete G matrix elements for benzene (point group D_{6h}) have been tabulated in a simple reduced algebraic form by Crawford and Miller.[59]

$$G_{11,11} = \mu_c + \mu_x \qquad 5.5$$

where μ is the reciprocal mass of the atom in $(\text{a.m.u.})^{-1}$. Table 5.3 contains the numerical values of G_{11}, $\mathcal{L}_{11}$ and $\frac{\partial \mu}{\partial S_{11}}$. The units of $\mathcal{L}$ are $(\text{a.m.u.})^{-\frac{1}{2}}$ and the units of $\frac{\partial \mu}{\partial S_i}$ are Debyes/Å ($1D. = 10^{-18} g.^{\frac{1}{2}} cm.^{5/2} sec.^{-1}$).

	C_6H_6	C_6D_6	C_6F_6
$G_{11,11}$	1.075227	0.579648	0.135926
ℓ_{11}	1.03680	0.76135	0.36867
$\frac{\partial\mu}{\partial S_{11}}$	$\pm$ 1.394[a] $\pm$ 1.368[d]	$\pm$ 1.426[c]	$\pm$ 0.6699[f] $\pm$ 0.8843[g]

Table 5.3

The superscripts in Table 5.3 refer to those used in Tables 5.1 and 5.2.

In the case of the in-plane E_{1u} degenerate symmetry species there are three independent vibrations, namely, S_{13}, S_{19} and S_{20}. The matrix (3 x 3) vectors are obtained by solution of the vibrational secular (3 x 3) equation for this species. The planar force fields of benzene and hexafluorobenzene have been discussed in Chapter 2. It was seen that any of three different sets of reported force constants reproduce the observed frequencies of benzene d_0 and d_6 satisfactorily. Because of the paucity of data, only one set of force constants has been reported for hexafluorobenzene. Tables 5.4 and 5.5 contain the G and F elements for the E_{1u} species of benzene and hexafluorobenzene.

The G Matrix Elements for the E_{1u} Species

	Algebraic Form	C_6H_6	C_6D_6	C_6F_6
$G_{18,18}$	$\mu_x+\mu_c(1+\frac{7}{2}\rho+\frac{9}{8}\rho^2)$	1.227617	0.733033	0.331226
$G_{18,19}$	$-\frac{\sqrt{6}}{4}(2+3\rho)\mu_c$	-0.220784	-0.220784	-0.243350
$G_{18,20}$	$\frac{3}{4}\rho\mu_c$	0.0484812	0.0484812	0.057694
$G_{19,19}$	$3\mu_c$	0.249920	0.249920	0.249920
$G_{19,20}$	$-\frac{\sqrt{6}}{2}\mu_c$	-0.102029	-0.102029	-0.102029
$G_{20,20}$	$\mu_c+\mu_x$	1.075227	0.579648	0.135926

Table 5.4

The Force Constants for the E_{1u} Species

Force Constant		C_6H_6 and C_6D_6			C_6F_6
		Whiffen	Scherer	Duinker-Mills	Steele-Whiffen
$F_{18,18}$	Γ_4	0.910	0.87	0.952	0.991
$F_{18,19}$	μ_4	0.155	0.12	0.186	0.1216
$F_{18,20}$	Υ_4	0	0	0	0.197
$F_{19,19}$	Λ_4	3.670	3.83	3.483	3.701
$F_{19,20}$	ξ_4	0	0	0.007	0.9984
$F_{20,20}$	Ω_4	5.15	5.12	5.125	7.509

Table 5.5

For convenience a computer program was developed to calculate the eigenvalues and eigenvectors of a general (3 x 3) problem. The input data are the G matrix (3 x 3) elements and the F matrix (3 x 3) elements.

A computer program was also developed to calculate the $\frac{\partial\mu}{\partial S_i}$ values from the $\frac{\partial\mu}{\partial Q_i}$ values using the coordinate transformation $S_i = \mathcal{L} Q_i$. The input data are the $\mathcal{L}$ matrix (3 x 3) elements and the $\frac{\partial\mu}{\partial Q_i}$ values with appropriate signs. There are four possible solutions for $\frac{\partial\mu}{\partial S_i}$ values obtained from all sign permutations of $\frac{\partial\mu}{\partial Q_i}$. The computer programs are written in CHLF3 Autocode and are processed on the Atlas (University of London) Computer. They are shown in Appendix III.

We have obtained the $\mathcal{L}$ (eigenvector) matrices for the E_{1u} species of C_6H_6, C_6D_6 and C_6F_6 using the existing force fields which are available for these molecules. The eigenvector $\mathcal{L}$ matrices are tabulated in Table 5.6 and the possible solutions, with appropriate sign, for the dipole derivatives with respect to symmetry coordinates are shown in Table 5.7.

To relate the $\frac{\partial\mu}{\partial S_i}$ values to quantities which are directly related to bond properties the expressions derived by Spedding and Whiffen[10] are used. Calculated values of the dipole moment derivative with respect to CC stretching, CX stretching, CX deformation in the plane of the ring and CX deformation out of the plane of the ring are also given in Table 5.7. For convenience the expressions of Spedding and Whiffen[10] are shown below.

$$\frac{\partial\mu}{\partial\beta} = \frac{r_0}{\sqrt{3}}\frac{\partial\mu}{\partial S_{18}} \quad ; \quad \frac{\partial\mu}{\partial\gamma} = \frac{r_0}{\sqrt{6}}\cdot\frac{\partial\mu}{\partial S_{11}}$$

$$\frac{\partial\mu}{\partial\Delta r} = \frac{1}{\sqrt{3}}\cdot\frac{\partial\mu}{\partial S_{20}} \quad ; \quad \frac{\partial\mu}{\partial\Delta R} = \frac{\sqrt{2}}{\sqrt{3}}\cdot\frac{\partial\mu}{\partial S'_{19}} - \frac{1}{2}\frac{r_0}{R_0}\cdot\frac{\partial\mu}{\partial S_{18}}$$

It should be noted that the expression for $\frac{\partial \mu}{\partial \Delta R}$ differs slightly from that given by Spedding and Whiffen.[10] This is because the definition of S_{19} used in this work is $\sqrt{2}$ times greater than the S_{19} defined by Whiffen[11] (c.f.ch.2).

Eigenvector $\mathcal{L}$ Matrices

Force Field		S_{18}	S_{19}	S_{20}	Molecule
Whiffen	Q_{18}	.07493	1.01067	.44782	C_6H_6
	Q_{19}	-.11871	-.35600	.33029	
	Q_{20}	1.03598	-.03855	.02190	
Scherer	Q_{18}	.07555	.98199	.50755	
	Q_{19}	-.11975	-.37493	.30823	
	Q_{20}	1.03589	-.04129	.02121	
Duinker	Q_{18}	.07213	1.04125	.37177	
	Q_{19}	-.11687	-.33102	.35593	
	Q_{20}	1.03615	-.03329	.02261	
Steele -Whiffen	Q_{18}	.41759	.34223	.19930	C_6F_6
	Q_{19}	-.45913	-.18750	.06296	
	Q_{20}	.30618	-.20538	.00061	
Whiffen	Q_{18}	.13339	.68407	.49729	C_6D_6
	Q_{19}	-.19121	-.42199	.18781	
	Q_{20}	.75556	-.09142	.02058	
Scherer	Q_{18}	.13599	.66325	.52406	
	Q_{19}	-.19443	-.42780	.17059	
	Q_{20}	.75491	-.09691	.01927	
Duinker	Q_{18}	.12677	.70370	.47093	
	Q_{19}	-.18611	-.41674	.20399	
	Q_{20}	.75657	-.08221	.02213	

Table 5.6

C_6H_6 - Bond Dipoles Calculated from Exp. Data of Spedding and Whiffen[10]

Force Field	Sign Choice of $\frac{\partial\mu}{\partial q}$	$\frac{\partial\mu}{\partial s_{18}}$	$\frac{\partial\mu}{\partial s_{19}}$	$\frac{\partial\mu}{\partial s_{20}}$	$\frac{\partial\mu}{\partial\beta}$	$\frac{\partial\mu}{\partial\Delta r}$	$\frac{\partial\mu}{\partial\Delta R}$
Whiffen	± ± ±	± .5047	± .2415	± .8049	± .316	± .465	± .001
	± ± ∓	± .0367	∓ 1.0744	± .6879	± .023	± .397	∓ .892
	± ∓ ±	∓ .0206	± .9457	± .9236	∓ .013	± .533	± .780
	± ∓ ∓	∓ .4885	∓ .3702	± .8066	∓ .306	± .466	∓ .113
Scherer	± ± ±	± .5074	± .3268	± .8151	± .318	± .471	± .070
	± ± ∓	± .0727	∓ 1.0284	± .6925	± .045	± .400	∓ .863
	± ∓ ±	∓ .0564	± .9111	± .9204	∓ .036	± .531	± .767
	± ∓ ∓	∓ .4032	∓ .4441	± .7978	∓ .309	± .461	∓ .171
Duinker	± ± ±	± .4994	± .1719	± .7972	± .313	± .460	∓ .053
	± ± ∓	± .0064	∓ 1.1069	± .6853	± .004	± .396	∓ .906
	± ∓ ±	± .0092	± .9704	± .9252	± .006	± .534	± .789
	± ∓ ∓	∓ .4838	∓ .3084	± .8134	∓ .303	± .470	∓ .064

$$\frac{\partial\mu}{\partial q} = \pm 0.617 \text{ D.}$$

Table 5.7(i)

C_6D_6 - Bond Dipoles Calculated from Expm. Data of Dows and Pratt[58]

Force Field	Sign Choice of $\frac{\partial\mu}{\partial q}$	$\frac{\partial\mu}{\partial S_{18}}$	$\frac{\partial\mu}{\partial S_{19}}$	$\frac{\partial\mu}{\partial S_{20}}$	$\frac{\partial\mu}{\partial\beta}$	$\frac{\partial\mu}{\partial\Delta r}$	$\frac{\partial\mu}{\partial\Delta R}$
Wulffen	± ± ±	± .5087	± .2071	± .8198	± .318	± .437	∓ .008
	± ± ∓	∓ .2658	∓ 1.0111	± .6483	∓ .166	± .374	∓ .722
	± ∓ ±	± .3067	± .7235	± .9062	± .192	± .569	± .472
	± ∓ ∓	∓ .4677	∓ .4947	± .8146	∓ .293	± .470	∓ .223
Scherer	± ± ±	± .5053	± .1660	± .8097	± .316	± .468	∓ .061
	± ± ∓	∓ .2817	∓ 1.0172	± .6467	∓ .176	± .373	∓ .721
	± ∓ ±	± .3218	± .7102	± .9029	± .201	± .568	± .455
	± ∓ ∓	∓ .4952	∓ .4731	± .8199	∓ .291	± .473	∓ .206
Duinker	± ± ±	± .5085	± .2491	± .8321	± .318	± .480	± .006
	± ± ∓	∓ .2527	∓ 1.0008	± .6522	∓ .158	± .377	∓ .719
	± ∓ ±	± .2091	± .7386	± .9093	± .181	± .571	± .491
	± ∓ ∓	∓ .4721	∓ .5114	± .8094	∓ .295	± .467	∓ .234

$$\frac{\partial\mu}{\partial\gamma} = \pm 0.631 \text{ D.}$$

Table 5.7(ii)

C_6F_6 - Bond Dipoles Calculated from Expm. Data of Steele et al.[37]

Force Field	Sign Choice of $\frac{\partial\mu}{\partial Q}$	$\frac{\partial\mu}{\partial S_{18}}$	$\frac{\partial\mu}{\partial S_{19}}$	$\frac{\partial\mu}{\partial S_{20}}$	$\frac{\partial\mu}{\partial\beta}$	$\frac{\partial\mu}{\partial\Delta_r}$	$\frac{\partial\mu}{\partial\Delta R}$
Steele & Whiffen	$\pm\pm\pm$	$\pm$ 0.8659	$\pm$ 0.0876	$\mp$ 9.3408	$\pm$ 0.650	$\mp$ 5.393	$\mp$ 0.328
	$\pm\pm\mp$	$\mp$ 0.3726	$\mp$ 1.4663	$\mp$ 9.9844	$\mp$ 0.278	$\mp$ 5.768	$\mp$ 1.026
	$\pm\mp\pm$	$\mp$ 1.1653	$\pm$ 6.4099	$\pm$ 2.8980	$\mp$ 0.874	$\pm$ 1.673	$\pm$ 5.772
	$\pm\mp\mp$	$\mp$ 2.4038	$\pm$ 4.8555	$\pm$ 2.2545	$\mp$ 1.804	$\pm$ 1.302	$\pm$ 5.074

$$\frac{\partial\mu}{\partial\gamma} = \pm 0.351 \text{ D.}$$

Table 5.7(iii)

Examination of Tables 5.7(i) and 5.7(ii) shows that an interpretation of the absolute intensities of C_6H_6 and C_6D_6 using the simple bond moment hypothesis leads to values of $\frac{\partial\mu}{\partial S_i}$ and of the effective bond dipoles which are only slightly different for all three available force fields. We will discuss the sensitivity of the derived quantities to the force field later in this Chapter. The Tables also reveal that the values of the derived quantities are almost the same for both molecules which is in accord with the predictions of Spedding and Whiffen[10] and lends considerable support to the idea of a rehybridization phenomenon.

It is necessary to choose the most appropriate solution for $\frac{\partial\mu}{\partial S_i}$ values from the four possible solutions obtained from all sign permutations of the $\frac{\partial\mu}{\partial S_i}$ values. Spedding and Whiffen[10] have interpreted the absolute intensities of benzene using the Whiffen force field[11] and they present plausible arguments, based on the intensities of partially deuterated benzenes, for choosing the solution obtained from the sign choice for $\frac{\partial\mu}{\partial S_i}$ of $(\pm\pm\pm)$. Close inspection of the alternative solutions shows that the solution obtained from $(\pm\mp\mp)$ only differs significantly from the solution obtained from $(\pm\pm\pm)$ in the value of $\frac{\partial\mu}{\partial\Delta R}$ and in the signs of the derived quantities. Jones[60] and also Brown[61] have suggested that the value for $\frac{\partial\mu}{\partial\Delta R}$ obtained from solution $(\pm\mp\mp)$ is more realistic than the value obtained from the solution $(\pm\pm\pm)$ and Jones[60] has clearly chosen solution $(\pm\mp\mp)$ as the most appropriate solution for the benzene intensities. Brown[61] using a perturbation theory has reported a value for $\frac{\partial\mu}{\partial\Delta R}$ of

0.9 D/Å which far exceeds the values obtained from solutions ($\pm\pm\pm$) and ($\pm\mp\mp$). In fact, only solutions ($\pm\pm\mp$) and ($\pm\mp\pm$) produce reasonable agreement with Brown's estimate of $\frac{\partial\mu}{\partial\Delta R}$. However, these two solutions must be disregarded due to lack of credulity in the values of the other derived quantities and also because of the arguments discussed by Spedding and Whiffen.[10]

Whether or not a choice is made between solutions ($\pm\pm\pm$) or ($\pm\mp\mp$), the effective bond dipole obtained from out-of-plane deformation, described by γ, is greater than that obtained from in-plane deformation, described by the angle β, by an amount 0.3 D. This can be readily understood, at least qualitatively, as being a consequence of rehybridization changes which accompany bond angle deformations. Deformation of the CH bond in a direction perpendicular to the plane of the ring is expected to result in considerable delocalization of electronic charge about the carbon nucleus. The result of such a change in the rehybridization will increase the s-character in the p_z orbital of the C atom and allow the π electrons to congregate on the opposite side of the ring from the hydrogen atoms. A similar effect is not possible for a CH deformation in the plane of the ring since the perpendicular p_z orbitals cannot be involved. The net effect is to make the effective CH dipole more positive in the out-of-plane motion by an amount 0.3 D.

The values for the derived quantities of C_6D_6 are closely similar to those for C_6H_6 which is in accord with the predictions of Spedding and Whiffen.[10] Again solutions ($\pm\pm\mp$) and ($\pm\mp\pm$) are disregarded and the two more appropriate solutions ($\pm\pm\pm$) and ($\pm\mp\mp$) produce values for the effective β_{CD} bond moment which are less than the γ_{CD} motion by an amount

0.3 D. This lends tremendous support to the idea of a rehybridization moment.

Table 5.7(iii) shows the possible solutions obtained from an interpretation of the absolute infrared intensities of C_6F_6 using the force field of Steele and Whiffen.[20] Whilst the assumptions used in this force field are now known to be ill-chosen[27] there seems little point at present in deriving what must be an equally arbitrary force field. We shall try to demonstrate later in this chapter that the derived effective bond dipoles are not very sensitive to the force fields used in their determination.

Of the four possible solutions for the derived quantities of C_6F_6 only those obtained from a sign choice for $\frac{\partial\mu}{\partial Q}$ of $(\pm\pm\pm)$ and $(\pm\pm\mp)$ can be regarded as possible. The solutions obtained from $(\pm\mp\mp)$ and $(\pm\mp\pm)$ are disregarded because of the lack of credulity in the values obtained for the effective bond dipoles which bear no resemblance to the reported values for other CF bonds.[62] We must now decide between the two more appropriate sign choices, $(\overset{+++}{---})$ and $(\overset{++-}{--+})$, both of which give reasonable values for the effective bond dipoles.

The sign choice for $\frac{\partial\mu}{\partial Q}$ of $(\pm\pm\pm)$ yields a value for $\frac{\partial\mu}{\partial\beta}$ which is greater than $\frac{\partial\mu}{\partial\gamma}$ by an amount 0.3 D. whereas the sign choice $(\pm\pm\mp)$ shows $\frac{\partial\mu}{\partial\beta}$ to be almost equal to $\frac{\partial\mu}{\partial\gamma}$. Thus $(\pm\pm\pm)$ predicts a rehybridization moment of 0.3 D. in the opposite direction to that obtained for benzene d_0 and benzene d_6 and $(\pm\pm\mp)$ predicts an almost zero rehybridization moment. A rehybridization moment of the same order of magnitude as in the case of benzene is expected for hexafluorobenzene since such a moment will involve

only the π electrons associated with the carbon nucleus and will therefore be almost independent of an X-substituent on the benzene ring. It is known[63] that in benzene the hydrogen atom is at the positive end of a moving CH dipole and it seems most likely that in hexafluorobenzene the fluorine atom is at the negative end of a moving CF dipole. For out-of-plane deformation of a CH in benzene, rehybridization at the carbon atom takes place in the form of s-character being introduced into the p_z orbital. The effect is to make the hydrogen atom appear less negative i.e. more positive and thus the effective dipole will be greater for out-of-plane deformation than for in-plane motion. In the case of hexafluorobenzene the effect of rehybridization changes during out-of-plane deformation is also to make the fluorine atom appear less negative and thus we expect the effective dipole for out-of-plane deformation to be less than for the in-plane motion.

Our results show a rehybridization moment of 0.3 D. for the molecules C_6H_6, C_6D_6 and C_6F_6. The opposite direction of the moment in the case of C_6F_6 is due to the different direction of a CF dipole. On the basis of our results the reason for the failure of the simple bond moment hypothesis becomes quite clear. It fails because it assumes that the electronic charge distribution in a molecule does not change during a vibration. The movement of electrons during particular vibrations must contribute an appreciable rehybridization moment[61,64] and bond dipoles calculated from the experimental infrared intensities must be the resultant of a bond moment as expected from the bond moment hypothesis plus a rehybridization moment which will be different for each vibration. Table 5.8 gives the chosen sets of values for the effective bond dipoles of C_6H_6, C_6D_6 and C_6F_6.

Effective Bond Dipoles

Molecule	$\frac{\partial\mu}{\partial\beta}$ D.	$\frac{\partial\mu}{\partial\Delta r}$ D/Å	$\frac{\partial\mu}{\partial\Delta R}$ D/Å	$\frac{\partial\mu}{\partial\gamma}$ D.
C_6H_6	± 0.32	± 0.47	± 0.001	± 0.62
C_6D_6	± 0.32	± 0.47	∓ 0.03	± 0.63
C_6F_6	± 0.65	∓ 5.39	± 0.35	± 0.35

Table 5.8

Sensitivity of Bond Dipoles to Force Field

It is well appreciated that the vibrational frequencies of polyatomic molecules are, in general, not sufficient data from which to define the most general harmonic potential function. Coriolis (zeta) coupling coefficients appear to be highly sensitive functions of the off-diagonal force constants and whenever they can be determined from high-resolution spectra or from their influence on infrared band contours, they can provide additional data for use in force constant calculations. Conversely, zeta values can be calculated from existing and necessarily approximate force fields and comparison with the experimentally determined quantities provides a test of such approximations. The extreme importance of zeta values in force constant calculations has been stressed particularly by Mills and co-workers[50,51] and general methods for their calculation[65,66] and experimental determination[46,47] have also been discussed in several papers.

The purpose of this section is to calculate Coriolis coefficients for the vibrations of the E_{1u} species of C_6H_6, C_6D_6 and C_6F_6 using the existing force fields and subsequently to compare the calculated values with the

values estimated from the infrared band shape studies presented in Chapter 4.

A very useful relationship exists between the individual zeta values for the vibrations of a given degenerate species. In the harmonic approximation, the sum of the individual zeta values is a constant which is independent of the force field. The Coriolis sum rules[67] for the degenerate vibrations of symmetric top molecules have been generalized in tabular form and may be written down by inspection. For molecules of D_{6h} symmetry the zeta sum rules are: E_{1g}, E_{2g} and $E_{2u} = 0$; $E_{1u} = -1$.

The individual Coriolis coupling coefficients depend on the masses and the relative dimensions of the molecule as well as on the force constants. Neal and Polo[65,66] have given a general procedure for the calculation of zeta values between the components of a doubly degenerate vibration. The method can be applied to any normal coordinate calculation and is described below for the E_{1u} degenerate vibrations of C_6H_6, C_6D_6 and C_6F_6 on the basis of the existing force fields.

The total classical kinetic energy of a molecule undergoing simultaneous rotation and vibration is:

$$T = T_{VIB.} + T_{ROT.} + T_{COR.}$$

It is convenient to express the term due to Coriolis interaction in the form:

$$T_{COR.} = \Omega_x \omega_x + \Omega_y \omega_y + \Omega_z \omega_z$$

where Ω is the component of the vibrational angular momentum with respect to the cartesian axes and ω is the component of the angular velocity of the rotating system of axes with respect to the cartesian axes.

Since Ω is a vector quantity it may be defined by:

$$\Omega_a = \sum_a (q_a^x \times \dot{q}_a^x).e_a = \frac{\partial T}{\partial \omega_a}$$

where q_a^x ($= x_a m_a^{\frac{1}{2}}$) is a mass-weighted cartesian displacement coordinate, e_a is a unit vector, m_a is the mass of atom a and a = x,y or z.

The expression for Ω may be simplified by introducing three matrices $(M^x)_a$, $(M^y)_a$, $(M^z)_a$ for each atom a,

$$(M^x)_a \begin{vmatrix} 0 & 0 & 0 \\ 0 & 0 & 1 \\ 0 & -1 & 0 \end{vmatrix} \quad (M^y)_a \begin{vmatrix} 0 & 0 & -1 \\ 0 & 0 & 0 \\ 1 & 0 & 0 \end{vmatrix} \quad (M^z)_a \begin{vmatrix} 0 & 1 & 0 \\ -1 & 0 & 0 \\ 0 & 0 & 0 \end{vmatrix}$$

where $(M^z)_a$ are N identical (3 x 3) sub-matrices along the main diagonal of a matrix $M^z(3N \times 3N)$. With this simplification Ω may be written in the form $\Omega_z = q^+ M^z \dot{q}$.

The displacement coordinates, q, are due to displacements in the vibrational normal coordinates, Q, and are related by the orthogonal coordinate transformation:

$$Q = lq$$

where l is a transformation matrix and satisfies the relationship:

$$l\, l^+ = E$$

where E is a unit matrix.

In normal coordinates the expression for Ω becomes

$$\Omega^z = Q^+ l M^z l^+ \dot{Q}$$

which reduces to $\Omega^z = Q^+ \zeta^z \dot{Q}$

since the matrix of the Coriolis coupling coefficients is defined by

$$\zeta^z = l M^z l^+.$$

The zeta matrix may be transformed into a form which is more convenient

for numerical calculation. In normal coordinate calculations we solve a secular equation $GFL = L\Lambda$ for eigenvectors L and eigenvalues when the problem is set up in terms of internal coordinates.

Since $ll^{+} = E$ and $ll^{+} = DD^{+} = G$ it follows that $l = L^{-1}D = L^{+}(D^{-1})^{+}$ and therefore the definition of the zeta matrix becomes:

$$\zeta^{z} = L^{-1}\,\mathrm{EMD}^{+}(L^{+})^{-1}.$$

If the normal coordinate problem is set up in terms of symmetry coordinates then the zeta matrix becomes:

$$\zeta^{z} = \mathcal{L}^{-1}\,\mathrm{UEMD}^{+}\mathrm{U}^{+}(\mathcal{L}^{+})^{-1}.$$

It is often convenient to write

$$C^{z} = \mathrm{UEMD}^{+}\mathrm{U}^{+}$$

because many elements of the C^{z} matrix cancel due to symmetry. The C^{z} matrix for the E_{1u} symmetry species of molecules with D_{6h} symmetry has been given in algebraic form by Duinker.[26]

A computer program has been used to calculate the zeta matrix for the E_{1u} species of the molecules C_6H_6, C_6D_6 and C_6F_6. The input data is the $\mathcal{L}^{-1}$ and $(\mathcal{L}^{+})^{-1}$ matrices for the existing force fields of these molecules. The Coriolis sum rule $\sum\zeta(E_{1u}) = -1$ is used to check the numerical calculations. Table 5.8 shows the calculated zeta matrices for the E_{1u} species of C_6H_6, C_6D_6 and C_6F_6 using the available force fields.

Calculated Zeta Matrices

Force Field		ζ_{18}	ζ_{19}	ζ_{20}	Molecule
Whiffen		-.0372	-.8334	-.5522	C_6H_6
			-.2790	.4775	
				-.6838	
Scherer		-.0376	-.8001	-.5994	
			-.3351	.4979	
				-.6273	
Duinker		-.0333	-.8704	-.4921	
			-.2168	.4426	
				-.7500	
Steele -Whiffen		-.8384	-.4815	-.2555	C_6F_6
			.4345	.7612	
				-.5961	
Whiffen		-.1229	-.7073	-.6962	C_6D_6
			-.4297	.5614	
				-.4474	
Scherer		-.1272	-.6835	-.7191	
			-.4656	.5616	
				-.4097	
Duinker		-.1100	-.7285	-.6762	
			-.4038	.5535	
				-.4862	

Table 5.9

We can now compare some of the calculated zeta values with the values we estimated from the band shape studies (Chapter 4). From comparison of the experimental and computed band contours of C_6H_6 a zeta value of -0.50 ± 0.1 can be estimated for the $1038cm^{-1}$ ν_{20} band and a value of -0.45 ± 0.1 can be estimated for the $1482cm^{-1}$ ν_{19} band. A reliable estimate of the zeta value for the $3080cm^{-1}$ ν_{18} band cannot be obtained because of complications due to Fermi resonance. However, because of the zeta sum rule, the zeta value must be approximately zero. Comparing these estimated zeta values with the calculated values given in Table 5.8 shows that there is poor agreement for all three available force fields. It must be concluded that the force field for the E_{1u} species of C_6H_6 is seriously ill-defined. In the case of C_6D_6, we estimate zeta values of -0.45 ± 0.1 for the $1335cm^{-1}$ ν_{19} band and -0.45 ± 0.1 for the $814cm^{-1}$ ν_{20} band. These estimates are only in fair agreement with the calculated zeta values. For C_6F_6, a zeta value of -0.60 ± 0.1 is estimated from the band shape calculations of the $315cm^{-1}$ ν_{20} band and this estimate is in very good agreement with the value of -0.596 calculated on the basis of the Steele-Whiffen force field. The $1010cm^{-1}$ ν_{19} band of C_6F_6 is complicated by Fermi resonance (doublet) so that it is impossible to obtain a reliable estimate of the zeta value. The remaining E_{1u} fundamental of C_6F_6 at $1530cm^{-1}$ ν_{18} is so intense that a reliable zeta value cannot be obtained. However, the contour suggests that it is large (~ -0.7) and certainly negative.

The agreement between the calculated and estimated zeta values for C_6F_6 may well be fortuitous. The set of force constants derived by Steele and Whiffen are based on assumptions which were chosen to minimize inter-

action constants and to retain a field having the form of Whiffen's benzene field. Whilst these assumptions are now recognized to be ill-chosen there seems little point at present in deriving what must be an equally arbitrary force field for C_6F_6 based on a new set of assumptions. Fortunately it is possible to demonstrate that the derived bond dipoles are not too sensitive to the force field. The Jacobian of the zeta matrix with respect to the force constants is calculated using the expressions given by Mills.[68]

$$\frac{\partial \zeta_{ii}}{\partial F_{uu}} = 2\sum_{j \neq i} \zeta_{ij} \frac{L_{ui} L_{uj}}{\lambda_i - \lambda_j}$$

$$\frac{\partial \zeta_{ii}}{\partial F_{uv}} = 2\sum_{j \neq i} \zeta_{ij} \frac{L_{ui} L_{vj} + L_{vi} L_{uj}}{\lambda_i - \lambda_j}$$

Tables 5.10(i), (ii) and (iii) give the Jacobian elements of the zeta matrix with respect to the force constants for the existing force fields of C_6H_6, C_6D_6 and C_6F_6.

In the case of C_6F_6 the zeta value for the 315cm^{-1} ν_{20} band shows greatest dependence on the $F_{18,20}$ off-diagonal force constant, $\partial\zeta_{20,20}/\partial F_{18,20} = 0.139$. If we increase $F_{18,20}$ from 0.197 to 0.207 and solve the secular equation then the values of the derived quantities obtained with the new L matrix are only slightly changed. The values of the Jacobian elements of the zeta matrix with respect to the off-diagonal force constants are surprisingly small for all three molecules and for all of the available force fields. This would suggest that any small changes in the force fields would not seriously alter the values of the bond dipole parameters.

C_6H_6 - Jacobian Elements of $\partial\xi/\partial F$

∂F \ $\partial\xi$	Whiffen			Scherer			Duinker		
	18,18	19,19	20,20	18,18	19,19	20,20	18,18	19,19	20,20
18,18	-.037	.678	-.641	-.037	.773	-.736	-.036	.545	-.509
18,19	.063	.193	-.256	.064	.114	-.178	.063	.270	-.333
18,20	-.509	.413	.096	-.505	.379	.126	-.513	.452	.061
19,19	-.008	-.152	.160	-.008	-.156	.164	-.007	-.141	.148
19,20	.066	-.171	.105	.067	-.174	.107	.065	-.163	.098
20,20	.011	-.017	.006	.011	-.017	.006	.009	-.015	.006

Table 5.10(i)

C_6D_6 - Jacobian Elements of $\partial\xi/\partial F$

∂F \ $\partial\xi$	Whiffen			Scherer			Duinker		
	18,18	19,19	20,20	18,18	19,19	20,20	18,18	19,19	20,20
18,18	-.098	.643	-.545	-.099	.653	-.554	-.094	.620	-.526
18,19	.167	-.269	.102	.168	-.315	.147	.163	-.220	.057
18,20	-.547	.298	.249	-.541	.263	.278	-.555	.333	.222
19,19	-.038	-.079	.117	-.038	-.068	.106	-.037	-.087	.124
19,20	.139	-.254	.115	.138	-.247	.109	.140	-.259	.119
20,20	.040	-.051	.011	.042	-.052	.010	.036	-.048	.012

Table 5.10(ii)

C_6F_6 - Jacobian Elements of $\partial\xi/\partial F$

∂F \ $\partial\xi$	Steele-Whiffen		
	18,18	19,19	20,20
18,18	-.208	.369	-.161
18,19	.315	-.335	.020
18,20	-.047	-.092	.139
19,19	-.095	.073	.022
19,20	-.053	.009	.044
20,20	.078	-.078	.0

Table 5.10(iii)

The conclusion is that the difference between the dipole moment derivative for out-of-plane deformation of a CX bond and that for the in-plane motion is certainly real and contributes to a rehybridization moment of about 0.3 D. in the molecules C_6H_6, C_6D_6 and C_6F_6. It is probable that the moment may be significant in many of the $\pi - \pi$ interactions which have been reported and also in explaining some of the intensity changes which frequently occur in the condensed and solution phase of systems involving aromatic molecules.

CHAPTER SIX

Vibrational Intensities for the Fundamental Vibrations of Hexafluorobenzene in Solution

Introduction

It is well recognized that infrared absorption bands undergo several changes on passing from vapour to liquid or solution phase. The frequencies of the vibrational modes of a molecule may be shifted to higher or lower values, the absolute intensity of a particular band may either increase or decrease and the half width of the band may also be affected. The reasons for these modifications are the shortened lifetime of the excited vibrational state giving rise to a slightly imprecise value for the energy of the transition and, more important, the intermolecular interactions which are likely to occur in the condensed phase owing to the closer proximity of neighbouring molecules.

Numerous studies have been made of the influence of solvents on the infrared spectra of molecules and although a great deal of data have been accumulated, it is clear that the present state of the theory accounting for the changes is not entirely satisfactory. The work described in this chapter is concerned with the absolute intensities of the active fundamental vibrations of hexafluorobenzene in various solvents. The experimental data are interpreted on the basis of the existing theories and an attempt is made to account for any discrepancies by invoking the idea of a rehybridization moment associated with certain vibrations.

Theory of Solvent Effects on Infrared Intensities

In general, the interactions occurring in the liquid or solution phase can be divided into two types: a) a non-specific interaction due to

the influence of the solvent considered as a continuous dielectric medium and b) a specific interaction between the solute molecule and one, or more, solvent molecule (N.B. a pure liquid is an extreme case of a solution in which solute and solvent are identical). Previous treatments of the influence of solvents on infrared intensities have considered systems in which specific interactions are absent or at least extremely weak and several relationships have been deduced to account for the effect of the non-specific interaction.

Chako,[69] Polo and Wilson[70] and van Kranendonk[71] considered the calculation of the ratio of the absolute intensity of an infrared absorption band in the liquid state, A_L, to its value, A_V, in the vapour state using dielectric polarization theory. The calculation is based on the relationship

$$\frac{A_L}{A_V} = \frac{F^2}{E_o^2} \qquad 6.1$$

where F is the 'effective' field acting on the unperturbed absorbing molecule in the liquid and E_o is the field acting on it in a vacuum. Dielectric theories can be used to calculate F which is taken to be the internal field acting at the centre of a small spherical cavity of radius, a, in the dielectric medium. The Onsager[72] treatment of dielectrics expresses F as the sum of a 'cavity field' factor, G, and a 'reaction field' factor, R, which is due to the polarization of the dielectric by the total (permanent and induced) dipole moment of the molecule.

$$F = G + R = \frac{3\varepsilon}{2\varepsilon+1} E + \frac{2\varepsilon-2}{2\varepsilon+1} \cdot \frac{m}{a^3} \qquad 6.2$$

where ε is the dielectric constant of the liquid, E is the macroscopic

electric field inside the liquid and m is total electric moment of the molecule. Within the range of infrared frequencies it is permissible to replace by the square of the refractive index n.

The total dipole moment is given by

$$m = \mu u + \alpha F \qquad 6.3$$

where μ is the permanent dipole moment of the isolated molecule, u is a unit vector with the direction of the permanent moment and α is the isotropic polarizability of the isolated molecule. Only the induced moment term αF contributes to the vibrating electric field at the absorption frequency because the re-orientation time of the molecule is much longer than the vibration time of infrared radiation. The polarizability α is given by the Clausius and Mosotti equation which is based on the treatment of molecules as isotropic spheres

$$\alpha = \frac{n^2-1}{n^2+2} \cdot a^3 \quad , \qquad 6.4$$

so that expression 6.2 becomes

$$F = \frac{3n^2}{2n^2+1} E + \frac{2n^2-2}{2n^2+1} \cdot \frac{n^2-1}{n^2+2} F \, . \qquad 6.5$$

Due to the invariance of the Poynting vector

$$\frac{E^2}{E_0^2} = \frac{1}{n} \qquad 6.6$$

and substitution for F and E_0 in equation 6.1 leads to the Polo-Wilson relationship[70]

$$\frac{A_L}{A_V} = \frac{1}{n}\left(\frac{n^2+2}{3}\right)^2 \, . \qquad 6.7$$

A similar expression has been derived by Bullard and Straley[73] and by Person[74] for solutions in solvents of refractive index, n_s,

$$\frac{A_S}{A_V} = \frac{1}{n_s}\left[\frac{n^2+2}{\left(\frac{n}{n_s}\right)^2+2}\right]^2 \qquad 6.8$$

where, A_S, is the intensity of a band for a molecule of refractive index, n, in a solvent of refractive index, n_s. This reduces to the Polo-Wilson equation when $n_s = n$. Another formula which has been proposed is due to Hirota[75]

$$\frac{A_S}{A_V} = \left[\frac{(n^2+2)(2\varepsilon_s+1)}{3(2\varepsilon_s+n^2)}\right] \qquad 6.9$$

where ε_s is the dielectric constant of the solvent.

In general, the refractive index of a molecule decreases with wavelength and it has been the custom to use a value for n obtained by extrapolating the visible or ultra violet data or indeed simply using the NaD-line value. Orville-Thomas et al[76] have pointed out that such a procedure does not take into account the absorption of energy by the system as the wavelength changes through the region of a vibrational transition, so that whenever possible the refractive index at the frequency of the transition should be used. Substituting a value of n = 1.5 into the Polo-Wilson equation leads to the prediction that, in the absence of specific interactions, all infrared absorption bands should increase in intensity by 33% on passing from vapour to condensed phase.

Owing to experimental difficulties involved in obtaining accurate estimates of the necessary very small path lengths, few determinations of infrared band intensities for pure liquids have been reported.[79,80] Intensity data exist for the infrared active vibrations of benzene in the vapour[10] and liquid[77,78] phases. The results show that the intensity

changes due to change of phase are far greater than can be satisfactorily accounted for by use of the Polo-Wilson equation. Similar results have been reported for other liquids[79,80] and some of these have been confirmed[81,82] using the dispersion method which is based on the interferometric measurement of refractive index. In the case of solution studies, there are many examples of intensity changes on passing from vapour to solution phase which far exceed the predictions of the foregoing expressions.[83,84]

In general conclusion reached by workers in this field is that the Polo-Wilson and related expressions for intensity changes with changes of phase or solvent do not adequately represent the observed effects for any real system. This conclusion is not surprising when it is considered that such treatments neglect completely such factors as the type of vibration and the shape of the molecule even if intermolecular interactions are absent.

More recently Buckingham[85,86] has discussed the effects of solute-solvent interactions on the vibrational intensities of diatomic molecules by considering the interaction energy as a power series in the normal coordinates of the solute molecule and then treating the interaction energy and the anharmonic terms in the potential energy function of the free molecule as perturbations to the harmonic oscillator hamiltonian. Such a treatment for non-polar solute molecules leads to an expression for the solution to vapour intensity ratio which is of the form

$$\frac{A_S}{A_V} = \frac{1}{n}\left[\frac{a_1}{1-f_1\alpha_1}\right]^2 \qquad 6.10$$

where f_i is the reaction field factor which depends upon the shape of the

molecule, a_i is the cavity field factor also dependent upon the shape of the solute molecule, α_i is the polarisability of the solute molecule in the direction appropriate to the i-th vibration and n is the refractive index of the solute molecule.

Kalman and Decius[87] have shown that Buckingham's expression can also be derived from an extension of the Polo-Wilson treatment if, instead of replacing α by the Clausius-Mosotti expression, the effective field is expressed in terms of α_i. They further show that such a treatment can be extended to polyatomic molecules and also to pure liquids.

$$\frac{A_i}{A_V} = \frac{1}{n}\left[\frac{a_i}{1-f_i\alpha_i}\right]^2 \qquad 6.11$$

Böttcher[88] has treated the calculation of a_i and f_i for the general case when the molecule is ellipsoidal with principal axes 2a, 2b and 2c; the axis 2a having the direction of the external field. The cavity field inside the ellipsoid is shown to be:[89,88]

$$a_i = \frac{\varepsilon}{\varepsilon + (1-\varepsilon)A} \qquad 6.12$$

where the quantity A is a shape factor given by

$$A = \frac{abc}{2}\int_0^\infty \frac{ds}{(s+a^2)^{3/2}(s+b^2)^{\frac{1}{2}}(s+c^2)^{\frac{1}{2}}} \quad . \qquad 6.13$$

Stoner[90] has tabulated values of A as a function of a, b and c. For the special case of a sphere a = b = c; A = 1/3 and equation 6.12 reduces to

$$a_i = \frac{3\varepsilon}{2\varepsilon + 1} \qquad 6.14$$

or, replacing ε by n^2, to

$$a_i = \frac{3n^2}{2n^2 + 1} \qquad 6.15$$

The reaction field factor for a dipole in an ellipsoidal cavity has been calculated by Scholte[91,88]

$$f_i = \frac{3}{abc} \cdot \frac{A(1-A)(\varepsilon-1)}{\varepsilon+(1-\varepsilon)A} \qquad 6.16$$

where A is the shape factor given previously.

For the special case of a spherical cavity equation 6.16 reduces to

$$f_i = \frac{2\varepsilon-2}{2\varepsilon+1} \cdot \frac{1}{a^3} \qquad 6.17$$

or, replacing ε by n^2, to

$$f_i = \frac{2n^2-2}{2n^2+1} \cdot \frac{1}{a^3} \qquad 6.18$$

Substituting equations 6.15 and 6.18 for the quantities a_i and f_i in equation 6.11, followed by replacement of α_i by the Clausius-Mosotti expression shows that for the special case of a spherical molecule in a spherical cavity this treatment leads to an expression for A_I/A_V given by:

$$\frac{A_I}{A_V} = \frac{1}{n}\left(\frac{n^2+2}{3}\right)^2 . \qquad 6.19$$

This is, of course, the Polo-Wilson expression. Clearly for the general case of an ellipsoidal molecule in an ellipsoidal cavity the ratio is

$$\frac{A_I}{A_V} = \frac{1}{n}\left[\frac{\dfrac{\varepsilon}{\varepsilon+(1-\varepsilon)A}}{1-\dfrac{3}{abc}\cdot\dfrac{A(1-A)(\varepsilon-1)}{\varepsilon+(1-\varepsilon)A}\cdot\alpha_i}\right] \qquad 6.20$$

where α_i is the polarizability of the molecule in the direction of the vibration and ε is the dielectric constant of the molecule.

The more general treatment of solvent effects on infrared intensities will clearly predict different ratios of A_I/A_V for vibrations in different directions and the ratios will also depend on the shape of the absorbing

molecule. Consequently, in principle, we expect the intensity ratios calculated on the basis of such a theory to be more in line with experimental observation and must represent an improvement on the Polo-Wilson treatment.

We have determined the vibrational band intensities of hexafluorobenzene in solution in benzene, carbon disulphide and cyclohexane. The data are treated in the light of the foregoing discussion.

Experimental

Purification of Materials

Hexafluorobenzene - The sample was kindly provided by Imperial Smelting Co. Ltd. Vapour phase chromatography and the infrared spectrum showed the absence of other components and the sample was used without further purification. B.pt. 80.1°C/760mm., n^D_{25} = 1.3761.

Benzene - B.D.H. (Analar) grade was contacted with concentrated sulphuric acid at room temperature and the treatment was repeated several times until the acid layer did not discolour. The benzene was washed several times with distilled water and dried over phosphorus pentoxide. Finally it was distilled under an atmosphere of nitrogen from freshly-cut sodium and stored over sodium wire. B.pt. 80.1°C/760mm., n^D_{25} = 1.4979.

Carbon Disulphide - B.D.H. (Analar) grade was shaken several times with mercury and finally distilled from phosphorus pentoxide. B.pt. 46.3°C/760mm., n^D_{25} = 1.6296.

Cyclohexane - B.D.H. (Spectroscopic) grade was used without further purification. B.pt. 80.7°C/760mm., n^D_{25} = 1.4235.

Spectral Recording

Infrared intensities for the fundamental vibrations of hexafluorobenzene in solution in benzene, carbon disulphide and cyclohexane have been determined by the Wilson-Wells method.[33]

For the high frequency fundamentals at 1530 and 1010cm^{-1} the samples were contained in conventional liquid cells with KBr windows and the infrared spectra were recorded with a Unicam SP100 grating spectrometer operating on the single beam principle. For the low frequency E_{1u} fundamental at 315cm^{-1} the samples were contained in conventional liquid

cells with CsI windows and for the A_{2u} fundamental at $215cm^{-1}$ containment was in high-density polythene (Rigidex) liquid cells fabricated as described elsewhere.[92] The spectra of the low frequency bands were recorded on an evacuated single beam spectrometer previously described elsewhere.[38] Fig. 6.1 shows the spectra re-drawn from the recorder chart and indicates the background absorption and also the zero transmission line.

The absolute intensity A is given by[33]

$$A = \lim_{cl \to 0} B \qquad 6.21$$

$$\text{where } B = \frac{1}{cl}\int_{BAND} \log_e \frac{T_o}{T} \, d\nu \, .$$

T_o and T are the observed values of the true monochromatic incident and transmitted intensities I_o and I, the concentration c is in molecules cm^{-3} and l is the cell thickness cm. The units of A are $mol.^{-1}cm.^{2}sec.^{-1}$

Percentage transmission values were obtained from the spectral traces at intervals of $2cm^{-1}$ and integration was carried out over a frequency range of $60cm^{-1}$ both sides of the band maxima by a counting of the squares procedure. Cell thicknesses were measured from the interference fringe system obtained with empty cells except in the case of the polythene cells when thicknesses were measured with a micrometer.

The Beer-Lambert law plots are shown in fig. 6.2 and the absolute intensities, as determined from the slopes of the plots of fig. 6.2, are given in Table 6.1, together with the frequencies of the band maxima. Due to overlapping solvent absorption the intensity of the $1530cm^{-1}$ band in benzene and in carbon disulphide could not be determined and in the

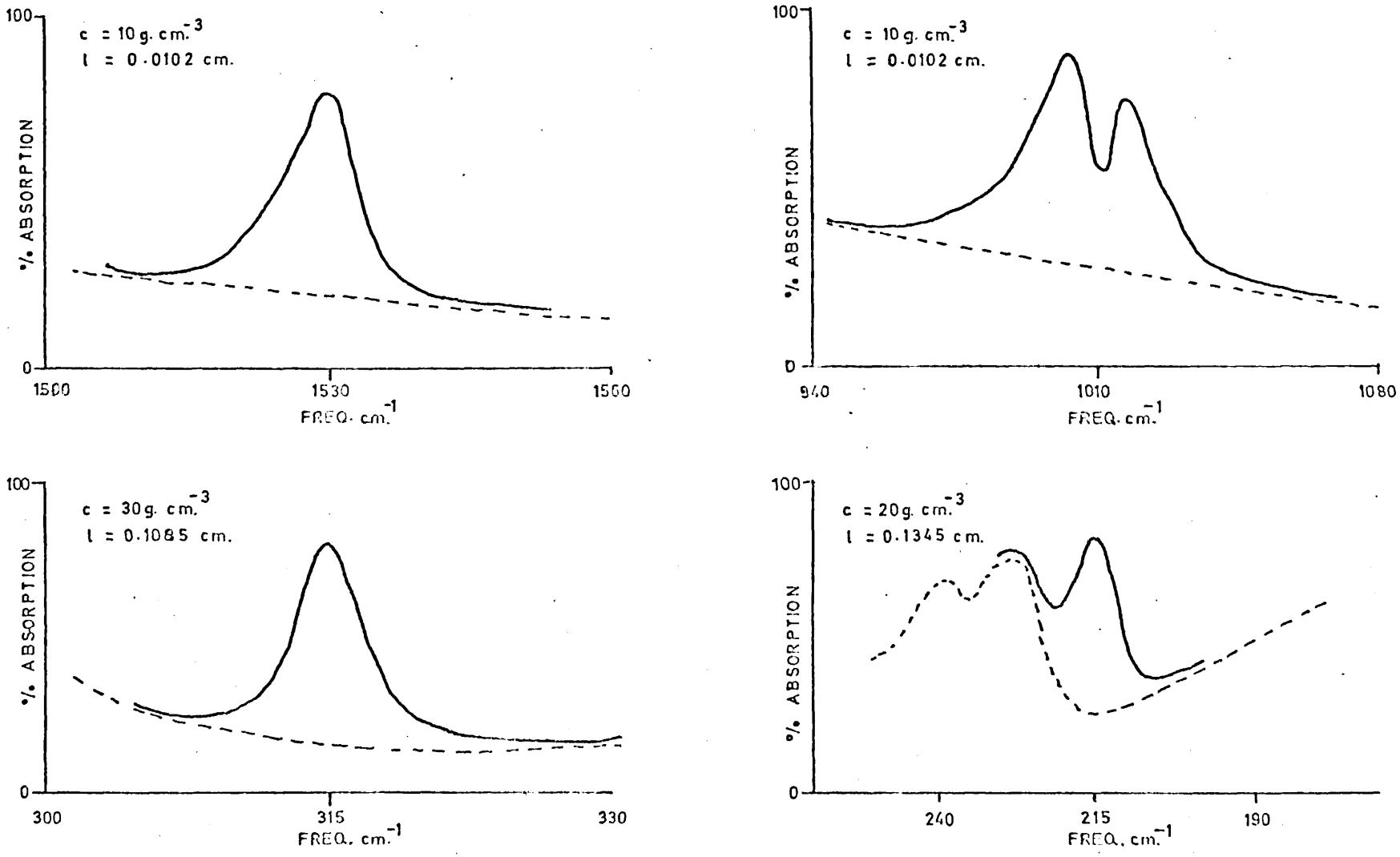

Fig. 6.1. Spectral Curves for the Fundamental Vibrations of Hexafluorobenzene in Solution.

case of the $1010cm^{-1}$ band the data for solution in benzene and in cyclohexane were obtained by subtracting the solvent absorption.

Intensity data for Hexafluorobenzene in Solution

Symmetry Class	Frequency No.	Frequency(obs.)cm^{-1}		Intensity A x $10^{-7}cm^2mol^{-1}sec^{-1}$			
		Vapour	Solution	Vapour	Benzene	CS_2	Cyclohexane
E_{1u}	18	1531	1530	27.2*	—[a]	—[a]	41.4
	19	1020-1002	1018-994	20.3*	30.1+	35.4	32.6+
	20	315	314	0.125	0.139	0.141	0.139
A_{2u}	11	215	215[b]	0.128	0.374	0.147	0.143

* data of Steele and Whiffen[37]

\+ by subtraction

a not measured due to overlapping bands

b refers to frequency in CS_2 and cyclohexane; observed frequency in benzene was $220cm^{-1}$ (cf ch.7.)

Table 6.1

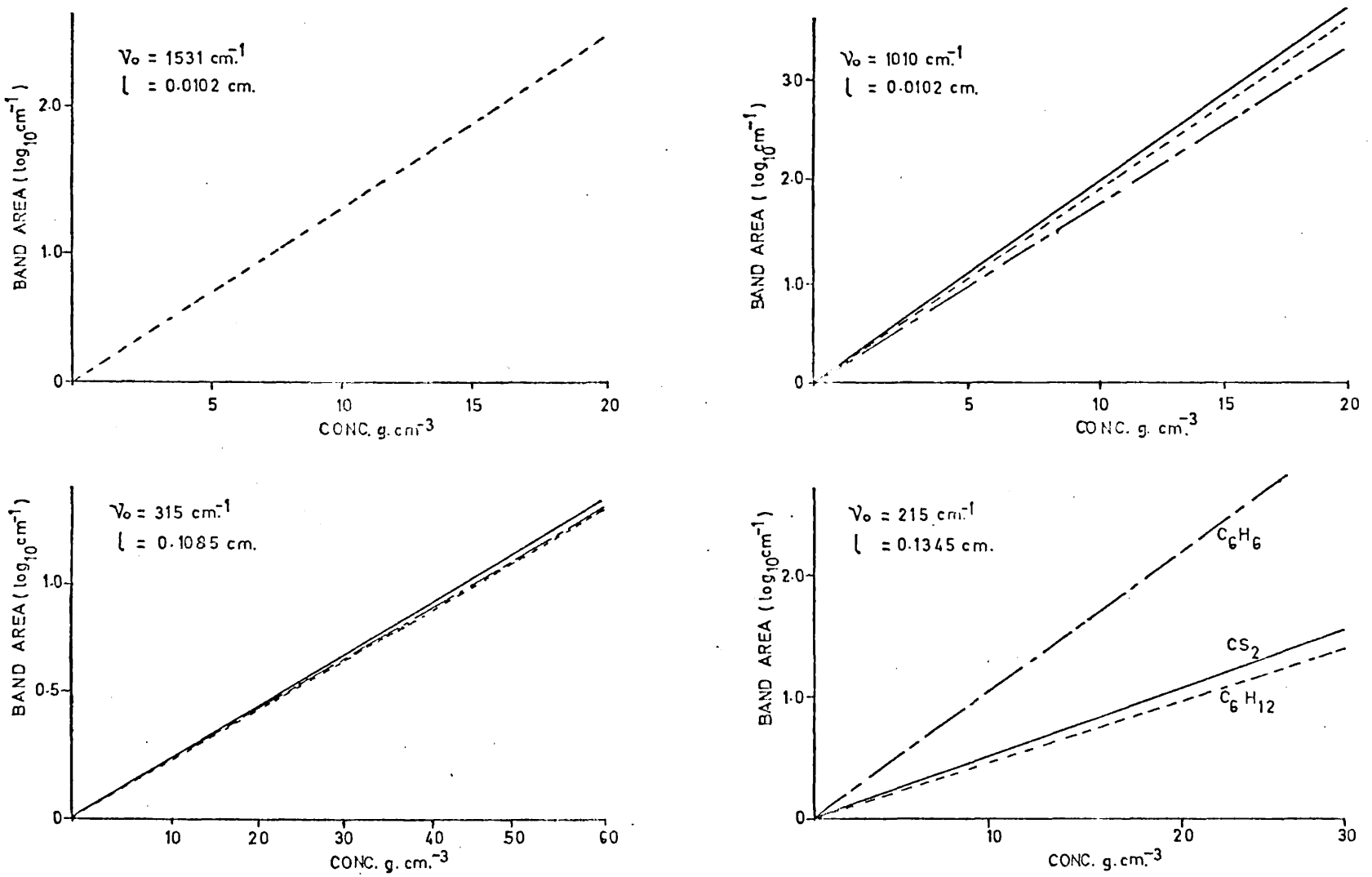

Fig. 6.2. Beer-Lambert Law Plots for the Fundamental Vibrations of Hexafluorobenzene in Solution.

Treatment of Data

We have seen that the ratio of liquid/vapour phase infrared intensities when a molecule is ellipsoidal is given by

$$\frac{A_L}{A_V} = \frac{1}{n}\left[\frac{a_i}{1 - f_i\alpha_i}\right]^2 \qquad 6.22$$

where a_i is a cavity field factor given by equation 6.12, f_i is a reaction field factor given by equation 6.16 and α_i is the anisotropic polarizability of the molecule in the direction of the i-th vibration.

It seems quite appropriate to treat hexafluorobenzene as an ellipsoidal molecule with equatorial semi-axis b = c and polar semi-axis a. The method used to obtain the dimensions a, b and c is shown in fig. 6.3.

The shape factors have been tabulated by Stoner;[90] $A_a = 0.5536$ and $A_b = A_c = 0.2232$. If hexafluorobenzene is considered to be a spherical molecule then the shape factors are $A_a = A_b = A_c = 0.3333$.

The isotropic polarizability of a molecule can be calculated from the Clausius-Mosotti equation

$$\alpha = \frac{n^2 - 1}{n^2 + 2} \cdot a^3 \qquad 6.23$$

where n is the refractive index and a is the radius of the molecule. The radius of a molecule is given by

$$a^3 = \frac{3}{4} \cdot \frac{M}{d} \cdot \frac{1}{N} \cdot 10^{24}\ \text{Å}^3 \qquad 6.24$$

where M is the molecular weight, d is the density of the molecule and N is the Avagadro number. For benzene $a^3 = 35.39\ \text{Å}^3$ and for hexafluorobenzene $a^3 = 45.70\ \text{Å}^3$. Substitution for a and n^D_{25} in the Clausius-Mosotti equation leads to a value of $10.37\ \text{Å}^3$ for the mean polarizability of benzene

DIMENSIONS OF HEXAFLUOROBENZENE AS ELLIPSOID

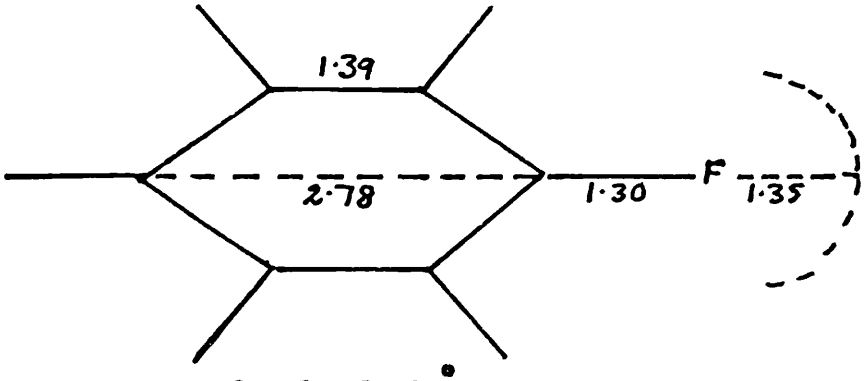

C - C 1.39 Å

C - F 1.30 Å

F (van der Waals) 1.35 Å

Thus equatorial axis 2b = 8.10 Å.

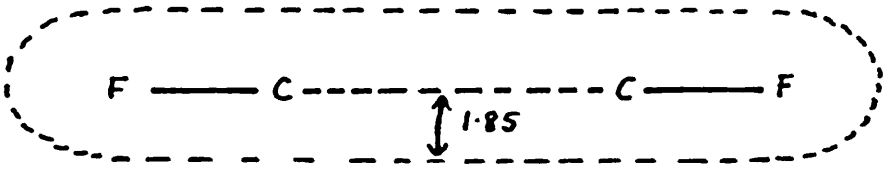

half-thickness of aromatic ring = 1.85 Å.[93]

Thus if a is polar semi-axis

and b is equatorial semi-axis (b = c)

then $m = \frac{a}{b} = \frac{3.70}{8.10} = 0.4568$

and $\mu = \frac{1}{m} = 2.1968$

From Stoner, D_a[90] = shape factor A_a = 0.5536.

Table 6.3

and a value of 14.11 $\mathring{A}^3$ for hexafluorobenzene. The anisotropy of the polarizability in benzene leads to experimental values for the principal polarizabilities in the a, b and c directions of 7.3, 11.1 and 11.1 $\mathring{A}^3$ respectively.[94] The mean of the experimental values is 9.833 $\mathring{A}^3$ which is a fractional discrepancy of 9.833/10.37 = 0.948 between the mean of the anisotropic polarizabilities and the mean isotropic polarizability. Experimental data is not yet available for the principal polarizabilities of hexafluorobenzene. However, we can estimate values for α_a, α_b and α_c by weighting the mean isotropic polarizability with the weighting factor obtained for benzene. From such a treatment the principal polarizabilities of hexafluorobenzene are estimated to be

$$\alpha_a = 10.85\ \mathring{A}^3, \alpha_b = \alpha_c = 14.65\ \mathring{A}^3.$$

The equation relating A_L/A_V (6.22) refers to pure liquid and vapour phases. Our data is for solutions of hexafluorobenzene in a series of solvents and therefore the dielectric constant in the expressions for a_i and f_i should refer to the dielectric constant of the mixture. Since we have used such dilute solutions for the intensity studies it is quite in order to use the dielectric constant of the pure solvent.

Calculated values of A_L/A_V for solutions of hexafluorobenzene in benzene, carbon disulphide and cyclohexane are shown in Table 6.2. The results indicate that the intensity of non-planar vibrations should be two to three times greater in solution than in the vapour phase whereas for planar vibrations the increase should be only 20-25%.

The A_L/A_V ratios predicted by the Polo-Wilson equation are the same for all vibrations. They show that the intensity in solution should be about 25% greater than in the vapour phase. Table 6.3 gives the predicted

Calculated Values of A_L/A_V for Hexafluorobenzene

in Solution - Ellipsoidal Cavity

	Solvent		
	C_6H_6	CS_2	C_6H_{12}
ε	2.280	2.640	2.023
a_a	1.451	1.524	1.389
$a_b = a_c$	1.143	1.161	1.127
f_a	0.0199	0.0231	0.0172
$f_b = f_c$	0.0110	0.0124	0.0098
α_a^{HFB}	10.85	10.85	10.85
$\alpha_b^{HFB} = \alpha_c^{HFB}$	14.65	14.65	14.65
n_{25}^{D}	1.5011	1.630	1.426
$(A_L/A_V)_a$	2.287	2.539	2.043
$(A_L/A_V)_{b,c}$	1.237	1.233	1.213

Table 6.2

A_L/A_V ratios for hexafluorobenzene in solution in benzene, carbon disulphide and cyclohexane using the Polo-Wilson equation for solutions (Mullard and Straley[73]).

Calculated Values of A_S/A_V for Hexafluorobenzene in Solution - Spherical Cavity (Mullard and Straley[73])

	Solvent		
	C_6H_6	CS_2	C_6H_{12}
A_S/A_V	1.251	1.264	1.237

Table 6.3

The observed ratios of solution to vapour phase intensities for the fundamental vibrations of hexafluorobenzene are given in table 6.4.

Experimental Values of A_S/A_V for Hexafluorobenzene in Solution

Frequency cm^{-1}	Solvent		
	C_6H_6	CS_2	C_6H_{12}
1531	—	—	1.52
1010	1.43	1.74	1.61
315	1.11	1.13	1.11
215	2.92	1.15	1.12

Table 6.4

Comparison of the experimental values of A_S/A_V with the values predicted on the basis of the ellipsoidal cavity theory or the Polo-Wilson (spherical cavity) equation shows poor agreement. The ellipsoidal cavity

theory appears to overestimate the intensity enhancement which occurs in solution phase whereas the Polo-Wilson equation predicts ratios which are ~20% too high for some vibrations and ~20% too low for others. It is probable that many of the discrepancies could be due to the large errors which are usually involved with infrared intensity measurements. Certainly a 20% difference between the calculated and experimental values of A_S/A_V is insufficient evidence for the failure of dielectric theories to explain the data.

There is one glaring discrepancy between the calculated and experimental values of A_S/A_V. This is for the $A_{2u}\gamma$ (CF) band of hexafluorobenzene in benzene solution where an intensity enhancement occurs which far exceeds the predictions of simple dielectric theories. The frequency of the band maximum is also increased, by $5cm^{-1}$, on passing from vapour phase to solution in benzene and the magnitude of the frequency change is much greater than is predicted using theories of solvent effects on infrared frequencies. From these observations we conclude that a specific interaction exists between hexafluorobenzene and benzene in solution. The benzene + hexafluorobenzene system is studied in greater detail in Chapter seven of this thesis.

CHAPTER SEVEN

THE BENZENE + HEXAFLUOROBENZENE COMPLEX

Introduction

Many workers have clearly demonstrated the existence of congruently melting compounds of equimolar composition in systems involving aromatic hydrocarbons + hexafluorobenzene.[94,95,96] Phase diagram studies for the system benzene + hexafluorobenzene indicate the formation of a 1:1 molecular complex with m.pt. 24.1°C.[97] Studies of excess thermodynamic functions show that the stability of the complex increases as the electron-donating power of the aromatic hydrocarbon is increased.[98,99]

It has been suggested that the complexes are of the charge transfer type with the aromatic hydrocarbon acting as the donor molecule and hexafluorobenzene as the acceptor.[94] The characteristic spectral band which is usually associated with charge transfer complexes (200-260 mμ) is not observed for this system. However, this may well be due to the fact that fluorocarbons absorb so strongly in this spectral range. Dipole moment measurements of hexafluorobenzene in solutions of aromatic hydrocarbons have been reported[98] and although the results are inconclusive they indicate that any complexing due to charge transfer interaction must be extremely weak.

In Chapter 6 of this thesis we have reported an intensity enhancement for the A_{2u} mode of hexafluorobenzene in solution in benzene which far exceeds the normal changes which can be predicted using theories of solvent effects on infrared intensities. Furthermore, the frequency of the band maximum is increased by $5cm^{-1}$ on passing from vapour phase to solution in benzene. The frequency change is greater than that predicted by theories

of solvent effects on infrared frequencies and also in the opposite direction. We conclude from this that a specific interaction exists between benzene and hexafluorobenzene in the liquid state.

Discussion

Studies of infrared absorption intensities offer a most sensitive and useful technique for establishing complexing. It was seen in Chapter 6 that the effect of solvents on infrared intensities can be reasonably accounted for using simple dielectric theories only when specific interactions are absent. Larger effects are usually assumed to be due to intermolecular interaction between the solute and solvent molecules. Horak and Pliva[100] have classified specific interactions into two groups according to the energy involved. A strong specific interaction between polar solutes and polar solvents results in the formation of stable donor + acceptor complexes. These systems involve large interaction energies and produce large changes in the infrared spectra which cannot be treated by dielectric theories. A weak specific interaction between non-polar or weakly polar solutes and solvents which involves small interaction energies. These systems produce only minor changes in the infrared spectra which, nevertheless, cannot be satisfactorily accounted for using dielectric theories. The nature of specific interactions is at present theoretically not well understood. However, it is clear from the work published so far in this field that there is no sharp borderline between the two types of interaction.

In the case of the hexafluorobenzene + benzene system the existence of a solid complex has been clearly demonstrated by a variety of physical techniques. However, as yet there is no clear-cut evidence to establish

complexing in the liquid phase. The purpose of this chapter is to make a detailed investigation of the effects of benzene on the A_{2u} band of hexafluorobenzene. If we measure the absolute intensity of this band for solutions containing a fixed concentration of hexafluorobenzene in a mixed solvent system extending from pure benzene to pure cyclohexane, then it should be possible to determine the equilibrium constant for the hexafluorobenzene + benzene complex from the intensity changes.

Experimental

The samples of hexafluorobenzene, benzene and cyclohexane were purified as in Chapter 6. Two stock solutions containing the same concentration, by weight, of hexafluorobenzene in cyclohexane and in benzene were made up. A series of solutions containing the same concentration of hexafluorobenzene in a mixed solvent solution containing varying amounts of benzene and cyclohexane were obtained by weighing small quantities of the stock solutions into sample tubes.

The infrared spectrum of each solution was recorded over the frequency range 240-180cm^{-1} with an evacuated single beam grating spectrometer previously described elsewhere.[38] The 2 x NaCl restatrahlen filters used in the earlier work were replaced by 2 x BaF_2 in order to give a flatter background absorption. Sample containment was in a high density polythene (Rigidex) liquid cell of path length 0.2cm. The same cell was used for all solutions and the path length was measured with a micrometer after each run. The possibility of the cell becoming deformed when under vacuum was reduced by firmly clamping the cell between the metal parts of a conventional liquid cell (R.I.I.C. F-01). There was no evidence for the sample 'leaking' from the cell after ten hours in the spectrometer. To

maintain a constant slit width for each solution, the cell was carefully placed in the same position on the sample platform for each run. Benzene and cyclohexane show no absorption in the spectral range concerned so that the background absorption was taken from the spectrum of the empty cell. At least three recordings of each solution were obtained and after careful fitting of the background absorption, values of $\log_{10} \frac{I_0}{I}$ were obtained across each band at frequency intervals of $1.4 cm^{-1}$ which is every 0.1 division of the arbitrary frequency scale. The frequency scale of the instrument was calibrated with a standard water vapour spectrum.[39]

Re-drawn spectra of $\log_{10} \frac{I_0}{I}$ plotted against the wavenumber frequency were obtained on large graph paper for each trace and the area of each band was determined by a counting of the squares procedure.

Results

The absolute intensity of an infrared absorption band for a molecule in solution is given by

$$\Gamma = \frac{M \times 1000 \times 2.303}{6.02252 \times 10^{23} \times c \times l} \log_{10} \frac{I_0}{I} \, d(\log \bar{\nu})$$

where M is the molecular weight of the molecule, c is the concentration in $g.l^{-1}$ and l is the path length in cm. The units of Γ are $cm^2 mol.^{-1}$ in. The absolute intensity of the A_{2u} band of hexafluorobenzene in the mixed, benzene and cyclohexane, solvent system is given in Table 7.1. Half-band widths and the frequency of the band maxima are also given in Table 7.1. The concentration of hexafluorobenzene in the benzene/cyclohexane solvent was $9.999 g.l^{-1}$ and the path length was 0.157cm.

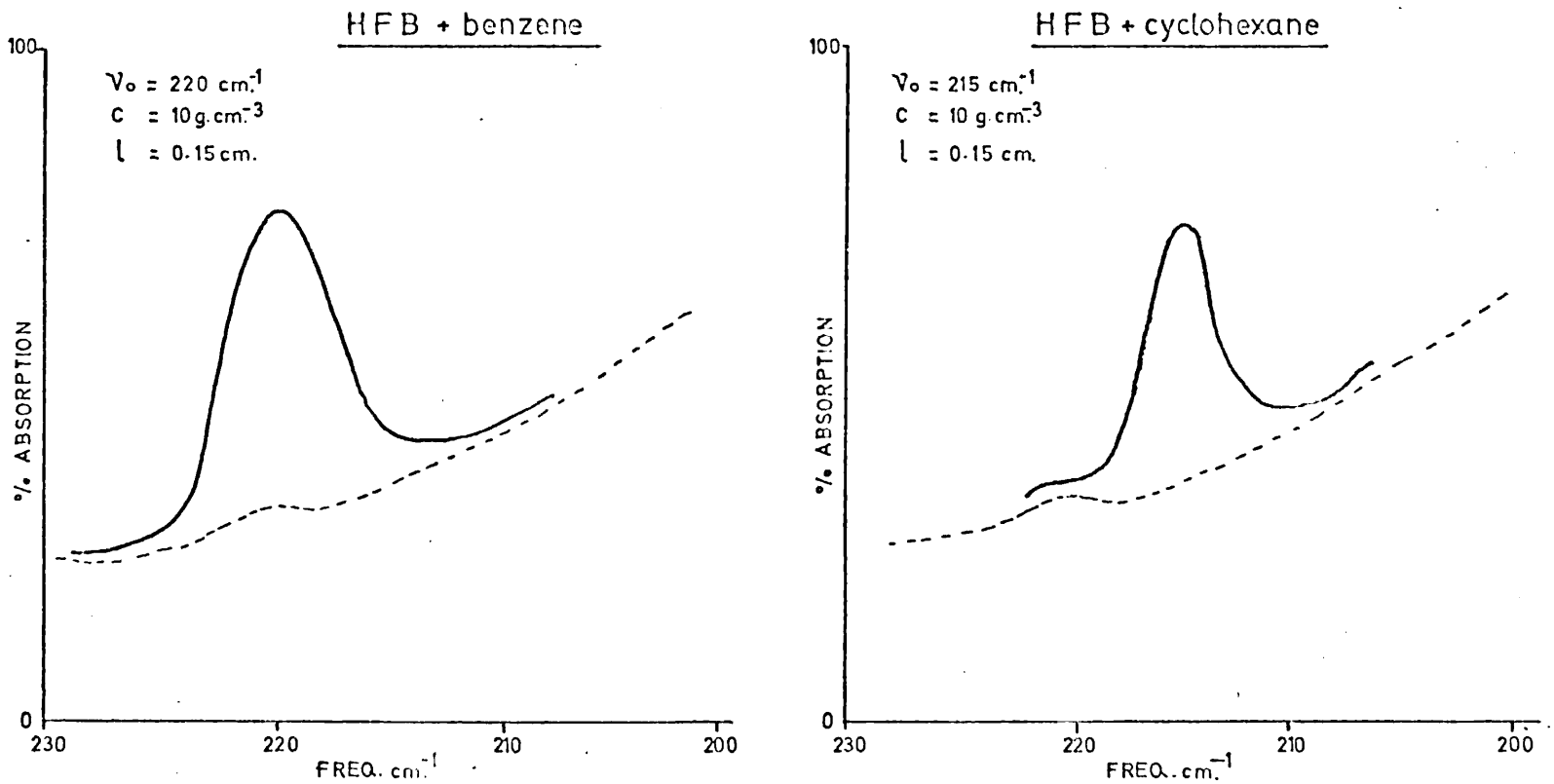

Fig.7.1. The A_{2u} Band of Hexafluorobenzene in Solution.

A_{2u} Band of HFB in Benzene/Cyclohexane Solution

% w/w benzene	$\tilde{\nu}_0$ cm^{-1}	$\Delta\nu_{\frac{1}{2}}$ cm^{-1}	A x 10^{-8} $cm.^2 mol.^{-1} sec.^{-1}$
0	217.0	5.0	1.53
22.20	217.6	9.3	3.12
40.02	219.7	10.0	3.34
53.12	220.2	10.1	3.42
73.22	220.7	10.0	3.36
88.49	220.9	10.2	3.50
92.80	221.3	10.0	3.41
95.77	221.4	10.1	3.56
100	221.8	10.1	3.42

Table 7.1

The absolute intensity of the A_{2u} band of hexafluorobenzene in pure cyclohexane is in very good agreement with the value obtained in Chapter 6. The intensity in benzene solution indicates that the value reported in Chapter 6 may be an over estimate, presumably due to difficulty with the sloping background absorption (2 x NaCl) which we mentioned at the time. Nevertheless, the intensity results of this section confirm the intensity enhancement in the A_{2u} band of hexafluorobenzene on passing from solution in cyclohexane to solution in benzene. We expected the intensity increase to occur gradually with increasing benzene concentration in the mixed benzene/cyclohexane solvent. Our results show, in fact, that the A_{2u} band of hexafluorobenzene undergoes a sharp increase in intensity and also a sharp increase in half-band width when the solvent is 80% cyclohexane and only 20% benzene. Time did not allow an investigation below 20% w/w benzene so that we were unable to find the composition of

mixed solvent which produces a gradual change in the intensity.

The frequency increase of the A_{2u} band on passing from solution in cyclohexane to solution in benzene is quite significant when it is considered that the value of $\Delta\nu/\nu$ is approximately 1/40. This would indicate that the interaction between hexafluorobenzene and benzene is not a localized electrostatic interaction[101] between the positively charged H atoms of the benzene and the negatively charged F atoms of the fluorocarbon.

It is likely that the π electron rehybridization phenomenon is a contributing factor to the bonding. Complexes between hexafluorobenzene and π-donors may then exist in solution, stabilized by forces due to overlap between the p_z orbitals of the donor and acceptor. It is probable that we would observe a similar intensity change in the A_{2u} mode of benzene in hexafluorobenzene solution.

CHAPTER EIGHT

THE BORON TRIBROMIDE + BENZENE COMPLEX

Introduction

The infrared inactive symmetric stretching vibration of boron trihalides appears as a weak absorption band in carbon disulphide solution whereas the intensity of absorption is greatly increased when benzene is the solvent.[102,103] It has been suggested that the intensity enhancement may be due to the formation of a weak donor + acceptor complex involving the π electrons of the benzene ring and the vacant p_z orbital on the boron atom. The planarity of the boron trihalide may be destroyed by such an interaction with the result that the symmetric stretching vibration would become infrared active.

A recent study[103] of the intensity change in the symmetric stretching vibration of boron tribromide in benzene solution has show the existence of a 1:1 species in solution with an equilibrium constant of 4.8 ± 0.8 l. mole^{-1}. Nuclear magnetic resonance studies[103] of ^{11}B chemical shifts for the boron tribromide + benzene system support the formation of a weak complex. A determination[104] of the dipole moment of boron tribromide in benzene gave a value of 0.194 e.s.u. and in view of the present evidence, it is possible that this value may represent a real deviation from zero. Phase diagrams for the boron tribromide + benzene system show no positive evidence for complex formation.[103]

The purpose of the present work is to confirm the existence of a weak complex between boron tribromide and benzene and to determine a value for the enthalpy change accompanying the complex formation. If the intensity of the symmetric stretching vibration of boron tribromide in benzene

solution show a negative temperature coefficient then this will confirm the presence of a complex between the two species in solution. By studying a series of concentrations of boron tribromide in benzene at a series of temperatures it should be possible to determine the equilibrium constant at each temperature and hence to obtain a value for the enthalpy change.

Molar enthalpy values for the formation of addition complexes in solution are of considerable importance when trying to compare the relative strengths of bonds between donor and acceptor molecules.[105] The reported ΔH values for a series of iodine complexes provide a good example. The molar enthalpy for the iodine complex in benzene is about 1 Kcal.,[106] the values in ethers range from 3.5 to 6 Kcals.[107] and larger values are found in the case of amines, ranging from 7 to 12 Kcal.[108] It will be of considerable interest to compare the enthalpy change for the boron tribromide + benzene system with these values.

Discussion

There are several examples of intensity changes in vibrational bands when the infrared spectrum of a donor + acceptor complex is compared with the spectra of the isolated molecules. In the boron tribromide + benzene system, the intensity enhancement in the infrared inactive symmetric stretching vibration of boron tribromide is the only change which occurs in the spectra of either molecule. A similar intensity increase also occurs in the stretching vibration of halogens in benzene solution.[109] However, in this case there are additional changes in the spectrum of the benzene molecule[110] and the frequency of the halogen stretching vibration is lower than the vapour phase value.[111] The intensity increase which

occurs in the stretching vibration of halogens in benzene was originally considered to be clear-cut evidence for complex formation with the halogen molecule in the complex situated in an unsymmetrical state. More recent work on the halogen + benzene system has indicated that the intensity increase in the halogen vibration does not necessarily mean that symmetrical nature of the halogen molecule is destroyed on complex formation. It has been suggested by Ferguson and Matsen[112] and by Friedrich and Person[113] that the intensity enhancement in the $\nu(X - X)$ vibration could occur through an 'electron vibration' mechanism even if the halogen molecule is in a symmetrical environment in the complex.

According to the electron vibration mechanism, the electron affinity of an acceptor molecule or the ionization potential of a donor molecule may change during a symmetric vibration. As a result the energy difference between the 'no bond' and the 'dative' states changes so that the mixing of these two wavefunctions will also change during the vibration. The electrons which are contributed by the donor molecule in forming the 'dative' structure with the acceptor molecule will therefore pulsate between the donor and acceptor with the frequency of the vibration. Such a process will result in a large change in the dipole moment derivative with respect to the stretching coordinate and hence an intensity enhancement will be observed in the symmetric vibration.

If we apply the electron vibration mechanism to the boron tribromide + benzene system it becomes clear that the intensity enhancement in the $\nu(B - Br)$ vibration is not due to non-planarity of boron tribromide in the complex. It is probable that in the complex the boron tribromide molecule remains in a symmetrical environment. At present, insufficient

information exists to enable a structure for the complex to be proposed.

Experimental

The sample of boron tribromide was purchased from B.D.H. and used without further purification. B.pt. 89.5°C/760mm., d_{25} = 2.62 g. cm^{-3}.

Analar grade benzene was treated as in Chapter 6. B.pt. 80.1°C/760mm., d_{25} = 0.875 g. cm^{-3}.

Solutions of boron tribromide in benzene of varying concentration were prepared by weighing the components into small, stoppered conical flasks. The stopper was fitted with a Teflon sleeve and considerable effort was made to keep the materials from the atmosphere. All transfer operations were carried out in a dry, oxygen-free atmosphere of nitrogen.

The infrared spectra were recorded on a far infrared grating spectrometer constructed in this department and previously described elsewhere.[38] Sample containment was in a conventional variable temperature liquid cell (R.I.I.C. FM-C1) fitted with KRS-5 windows. The cell spacer was a piece of high density polythene (Rigidex) and a cell path-length of about 3mm. was employed. The path length was measured with a micrometer.

The infrared inactive symmetric stretching vibration of boron tribromide has been assigned to band at 278cm^{-1} which appears weakly in the liquid phase spectrum. There can be no doubt about this assignment as confirmation is provided by a strong Raman active band at 279cm^{-1}. Benzene has a weak absorption band at 301cm^{-1} and boron tribromide also absorbs weakly at 301cm^{-1}. These bands are sufficiently well-separated from the 278cm^{-1} band that they do not overlap. We have recorded the spectrum of the 278cm^{-1} band of boron tribromide over the frequency range 350 to 220cm^{-1} for a series of concentrations of boron tribromide in

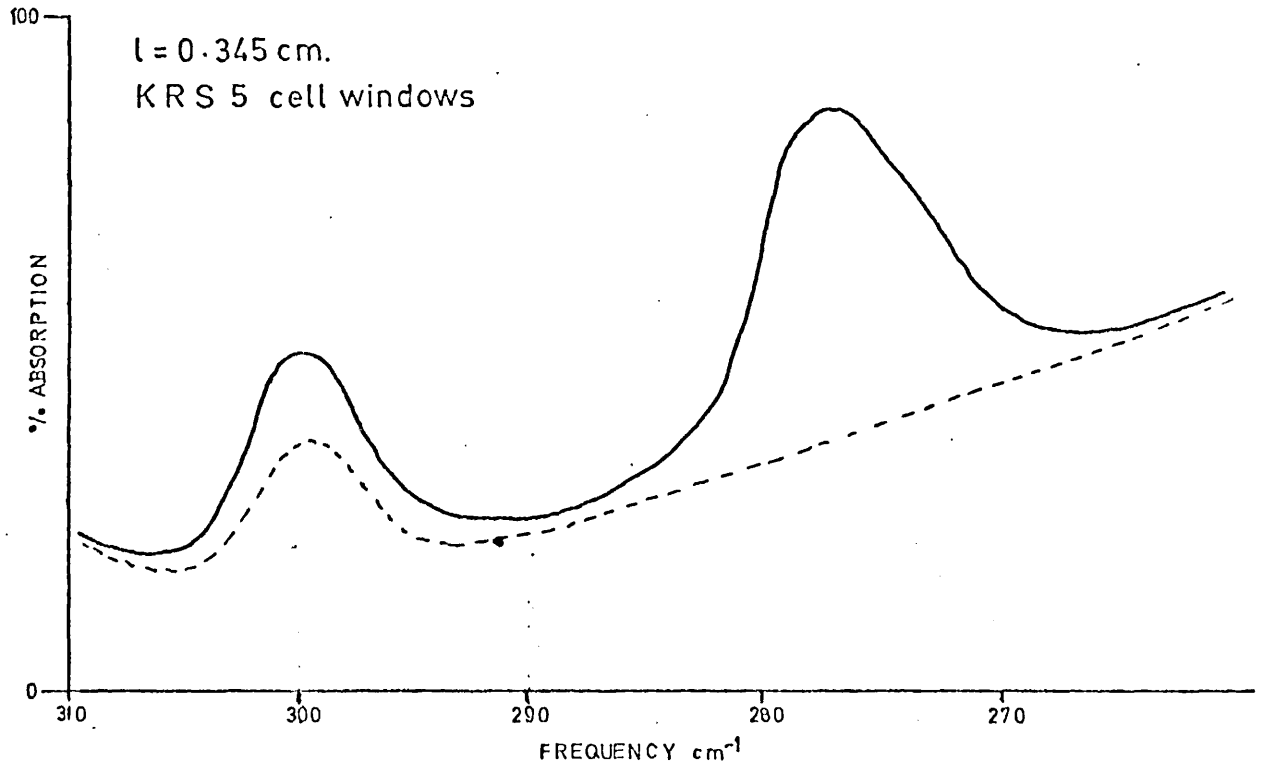

Fig. 8.1. Symmetric Stretching Vibrations of Boron Tribromide in Benzene Solution

benzene solution.

The temperature of the cell could be varied between 15°C and 65°C by circulating water from a Tempunit (Tecam TU.8.) through a stainless steel water jacket which surrounds the cell. Tempunits can control temperature to within ± 0.01°C under optimum conditions. After sufficient time allowance for thermostating the inlet and outlet temperatures of the circulating water only differed by ± 0.5°C. It is estimated that the temperature of the cell can be determined to an accuracy of ± 1°C.

The spectrum for a particular sample was recorded at least twice at each temperature setting, once while the sample was warming and again while cooling from the maximum temperature of 62°C. Background absorption was obtained with a cell filled with benzene and zero transmission was recorded at regular intervals. To maintain a constant slit setting we attempted to position the cell at the same point in the sample chamber for each run. Values of $\log_{10} \frac{I_0}{I}$ at the band maxima were measured from the spectral traces and were plotted against the composition of the mixture (percentage w/w boron tribromide in benzene) for five different temperatures between 15°C and 65°C. The results are shown in Table 6.1 and graphs of $\log \frac{I_0}{I}$ against % w/w concentration of boron tribromide in benzene are shown in fig. 8.2.

At low concentrations of boron tribromide in benzene solution satisfactory Beer's law plots are obtained. The shapes of the graphs at higher concentrations strongly suggests the existence of a complex. This is confirmed by the negative temperature coefficient of the $\log_{10} \frac{I_0}{I}$ values between 16°C and 62°C.

Average $\log_{10} \frac{I_0}{I}$ values for the ν(B-Br)

of BBr_3 in Benzene Solution at Different Temperatures

% w/w BBr_3 \ t°C	16.0	28.8	40.0	50.6	62.0
12.45	.0664	.0656	.0621	.0637	.0602
19.97	.105	.102	.0974	.0932	.0931
28.94	.145	.139	.128	.120	.118
32.61	.162	.159	.151	.143	.136
42.00	.269	.244	.221	.201	.188
42.68	.269	.244	.218	.196	.184
53.53	.256	.246	.237	.225	.215
56.39	.246	.239	.231	.222	.212
60.85	.241	.232	.226	.218	.211
73.47	.239	.228	.221	.215	.207
88.72	.222	.217	.212	.209	.202
100.00	.197	.193	.188	.186	.182

Table 6.1

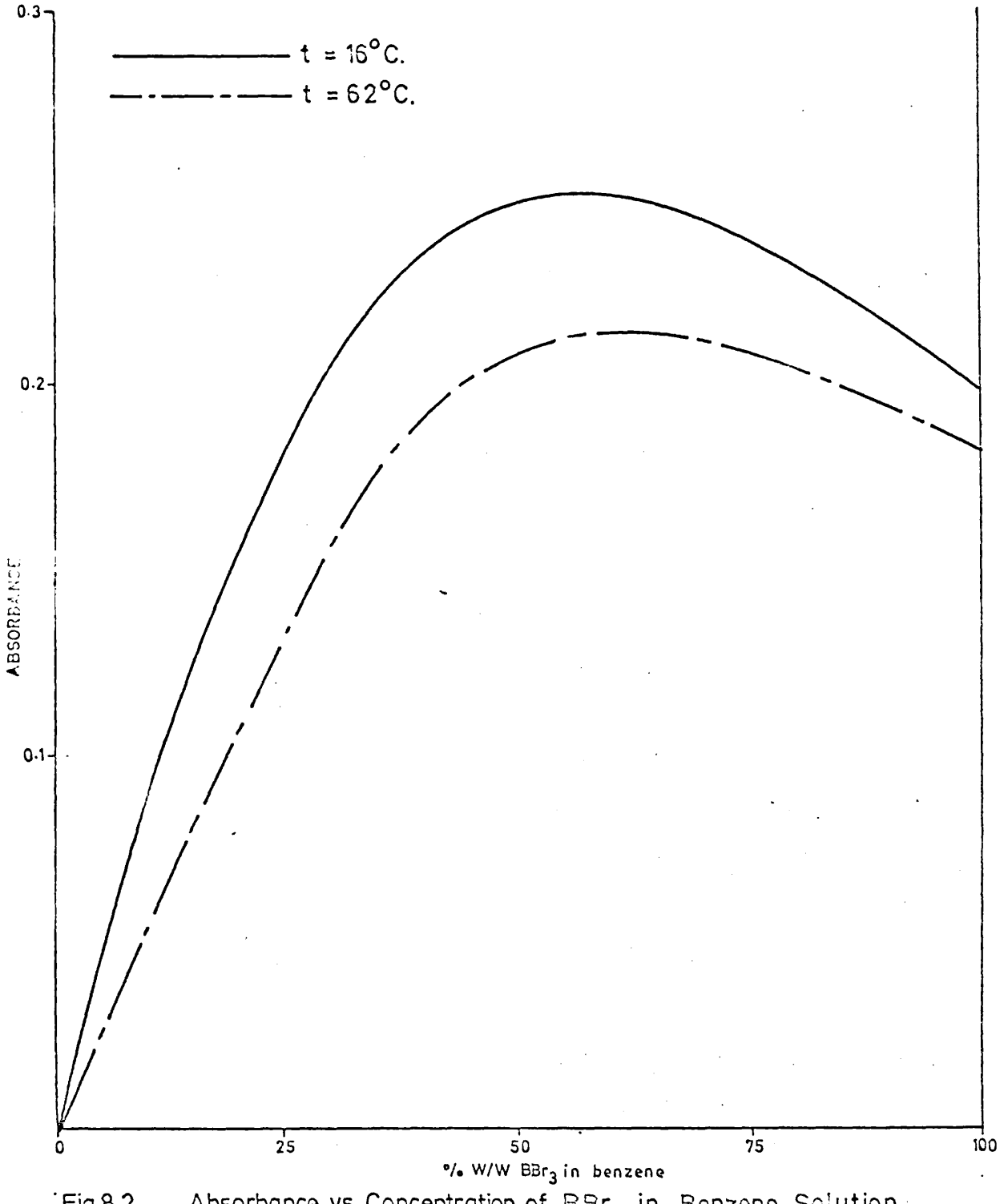

Fig.8.2. Absorbance vs Concentration of BBr_3 in Benzene Solution.

It is possible to join the experimental points of $\log_{10} \frac{I_o}{I}$ plotted against concentration of BBr_3 with a smooth curve. This gives one maximum value of $\log_{10} \frac{I_o}{I}$ for each temperature at a mole fraction of 0.5 and is in agreement with the findings of Finch, Gates and Steele.[103] Because of the scatter due to experimental uncertainty in the $\log_{10} \frac{I_o}{I}$ values, it may also be possible to join the experimental points in such a way as to obtain several maxima for $\log_{10} \frac{I_o}{I}$ values at mole fractions corresponding to the formation of 1:2 and 2:1 complexes in addition to a 1:1 species. The appearance of the $\nu(B - Br)$ in pure liquid BBr_3 is probably due to collisional interaction which is likely in the liquid state.

Treatment of Results

We can follow the procedure of Finch et al[103] and calculate the equilibrium constant for a 1:1 complex between boron tribromide and benzene at each temperature. From this treatment we should be able to obtain a value for the enthalpy change for the complex using the van't Hoff equation,

$$\frac{d \log_e K}{dT} = \frac{\Delta H}{RT^2} \quad .$$

Unfortunately if there are also 1:2 and 2:1 complexes present in mixtures of boron tribromide and benzene the plot of $\log_e K$ vs $\frac{1}{T}$ will not be a straight line of slope $\frac{\Delta H}{R}$. The existence of higher order complexes will produce a curvature in the plot and therefore it will not be possible to obtain a ΔH value.

If we assume the existence of only a 1:1 complex between boron

tribromide and benzene then the association can be written in the form

$$BBr_3 + C_6H_6 \rightleftharpoons C_6H_6 : BBr_3$$

and the equilibrium constant will be

$$K = \frac{ab}{(a_o - a_b)(b_o - a_b)}$$

where a_o is the total concentration of BBr_3, b_o is the total concentration of C_6H_6 and ab is the concentration of the complex. The observed value of the absorbance for a particular concentration of boron tribromide in benzene is due to the presence of free and associated BBr_3 so that we can write,

$$\log_{10}\frac{I_o}{I} = \varepsilon_a\, al + \varepsilon_{ab}\, abl$$

$$= \varepsilon_a\,(a_o - ab)\, l + \varepsilon_{ab}\, abl$$

$$= \varepsilon_a\, a_o\, l + (\varepsilon_{ab} - \varepsilon_a)\, abl$$

$$\text{hence} \quad ab = \frac{\log_{10}\frac{I_o}{I} - \varepsilon_a\, a_o l}{(\varepsilon_{ab} - \varepsilon_a)\, l}$$

where $\log_{10}\frac{I_o}{I}$ is the absorbance at a particular concentration a_o, l is the path length of the cell, ε_a is the molar extinction coefficient of pure liquid BBr_3 and ε_{ab} is the molar extinction coefficient of the species $C_6H_6 : BBr_3$ obtained from the initial Beer's law plot.

Values for the equilibrium constant of a 1:1 complex between BBr_3 and benzene have been determined at each temperature.

T°K	K l. mole^{-1}
289.15	4.75 ± 0.6
301.95	4.68 ± 0.6
313.15	4.60 ± 0.7
323.75	4.49 ± 0.5
335.15	4.41 ± 0.6

Table 8.2

The error in a particular equilibrium constant at a temperature t°C is greater than the change in equilibrium constant between t°C and t + 20°C. This implies that the ΔH value obtained from a plot of $\log_e K$ vs $\frac{1}{T}$ is very small and subject to a large error. The values of the equilibrium constant at the highest and lowest temperatures used indicate a negative temperature coefficient and this fact confirms the existence of a 1:1 complex. Our value of K at 28°C is in good agreement with the value of 4.8 ± 0.8 l. mole^{-1} for an unspecified temperature reported by Finch, Gates and Steele.[103] The greatest source of error in the value of the equilibrium constant is in the estimation of ε_{ab} from the initial Beer's law plot. This is due to the fact that a concentration of greater than 10% w/w boron tribromide in benzene solution is required to give reasonable $\log_{10} \frac{I_o}{I}$ values for a path length of 3mm. Greater accuracy would probably have been obtained if a longer path length cell had been used.

CHAPTER NINE

HIGH PRESSURE STUDIES ON THE FUNDAMENTAL VIBRATIONS OF BENZENE

Introduction

The literature values for the infrared absorption intensities of the fundamental vibrations of benzene in the condensed phase are in poor agreement with the values which can be predicted from the vapour phase data using the Polo-Wilson expression. The experimental data for both phases have been obtained by many workers and although agreement between the various sets of results is only fair, it is clear that the liquid phase intensities of benzene cannot be satisfactorily accounted for by simple dielectric changes or by the expected magnitude of intermolecular perturbations. An interesting problem is posed by this apparent discrepancy and one of the aims of this chapter is to describe an experiment which has been performed in an attempt to throw some light on a possible solution. For such purpose, we have designed a variable path length high pressure infrared gas cell which is capable of withstanding pressures up to 1500 p.s.i. and temperatures of 250°C. If we study the absolute intensities of the benzene fundamentals in the vapour phase at high pressures and temperatures and with small path lengths then it should be possible to observe any changes in the intensities due to intermolecular interactions. From such a study it should also be possible to test the theoretical prediction concerning the temperature independence of vibrational intensities for fundamental bands in the vapour phase.[4] Only a few investigations of temperature effects on infrared spectra appear in the literature[115] and it seems that no work of sufficient accuracy has yet been reported for any polyatomic molecule. It is well known that infrared

band contours of vapours undergo considerable changes with temperature and it may well prove informative to investigate the changes which occur in the contours of the fundamental absorption bands of benzene.

Description of Cell

The high pressure infrared absorption cell used in this work was designed in this laboratory by Mr. E. Smethurst and manufactured by Pendry and Son Ltd. (Thorpe, Surrey). It was constructed to withstand pressures of benzene vapour up to 1500 p.s.i. and temperatures up to 250°C. The cell body is made of stainless steel and has a stainless steel inlet tube screw threaded and welded to it. A high pressure bonnet type shut-off valve with PTFE gland packing (British Ermeto Co. Ltd., Maidenhead) is screwed on to the inlet tube. Polished potassium bromide windows (Technation Ltd.) are firmly held in stainless steel window mounts by screwing down on four screws through a stainless steel plate. Retaining rings of stainless steel are firmly screwed on to the ends of the cell to complete the design. The cell has a fixed increment variable path length facility by using window mounts of different lengths or by using potassium bromide windows of different lengths. We have used three sizes of window mount and various lengths of potassium bromide to produce path lengths ranging from 5cm. to 0.1cm. The increased length of potassium bromide does not appreciably reduce the transmission properties of the cell. In early work, great difficulty was experienced in obtaining effective sealing of the cell and also due to adsorption of benzene by the 'O' ring seals. We have had most success with three copper 'O' ring seals manufactured to specification by J. Walker and Co. Ltd. (Woking, Surrey) and two Viton 'O' ring seals purchased from Edwards (Crawley, Sussex). The copper 'O' rings

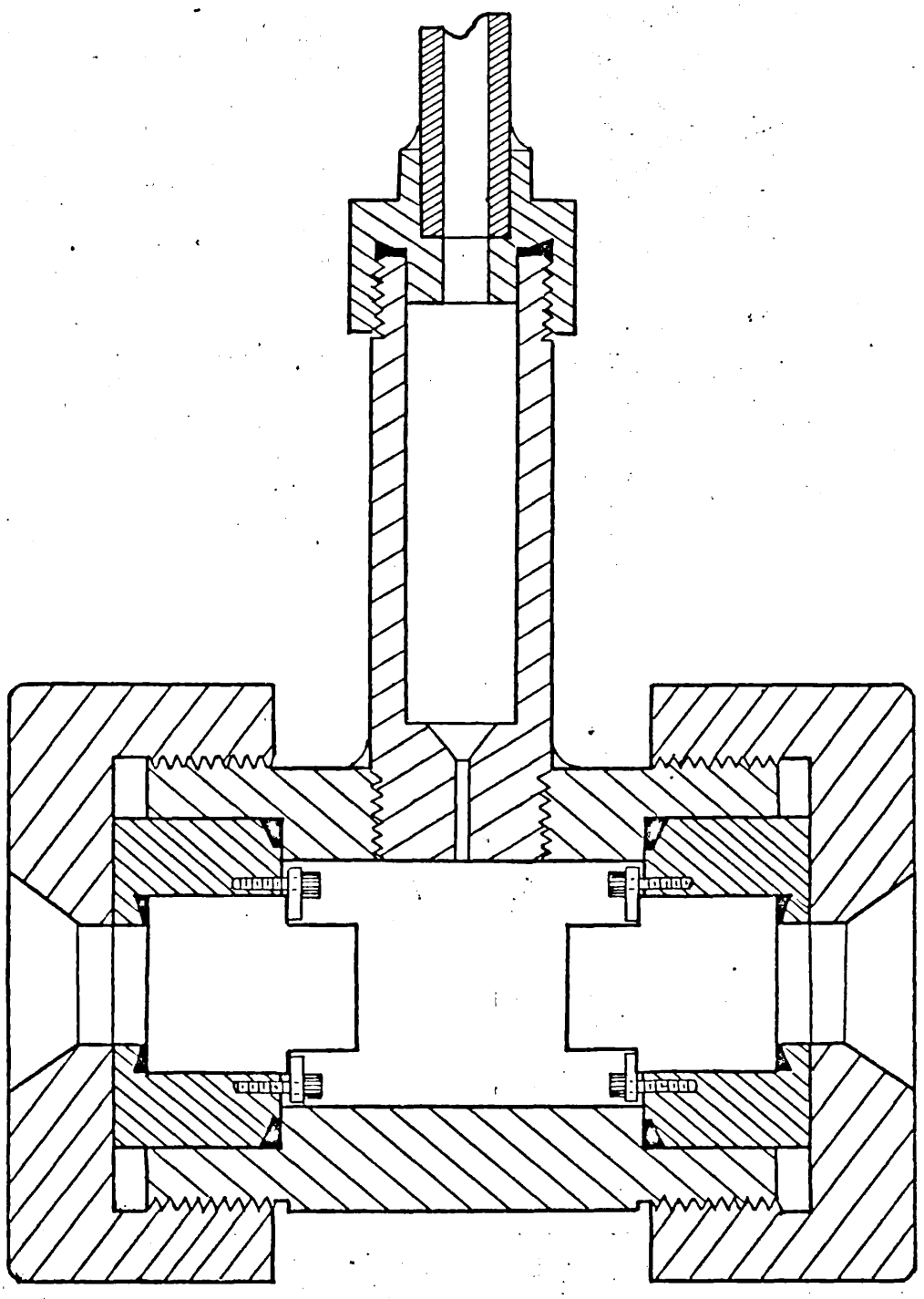

Fig.9.1. High Pressure Infrared Cell.

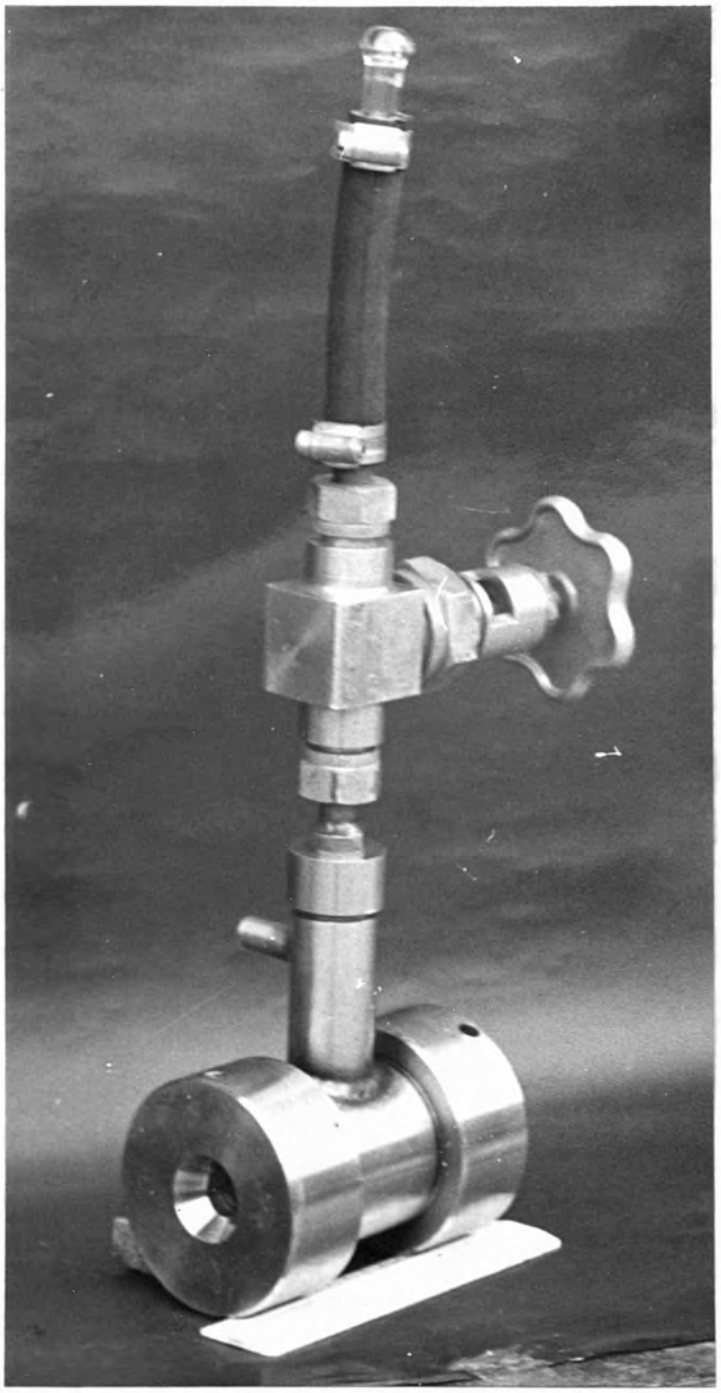

Plate 9.1. High Pressure Infrared Cell.

seal the metal-metal parts of the cell and the Viton 'O' rings seal the metal-potassium bromide parts. The cell can be completely assembled in about one hour. A good test for leaks is to evacuate the cell through the shut-off valve and monitor with a glycol manometer or to connect the cell to a pressurized cylinder of O_2 free N_2 through a short length of reinforced hose and monitor with the pressure gauge.

Description of Furnace

An electrically heated furnace was used to heat the cell for the variable temperature studies. It was designed and manufactured in this laboratory. The furnace is of cuboid construction (8 x 6 x 5.5 in.) manufactured from 0.25 in. asbestos sheeting and lined with aluminium foil of high reflectivity to reduce heat loss. The interior has partitions of asbestos sheeting which are partly cutaway to take up the shape of the cell body. There are two holes (diam. 0.7 in.) drilled in the furnace to allow the infrared beam to pass and a hole to allow the shut-off valve to lie outside the furnace. The furnace was designed in two identical halves which fit together to give a box-like appearance. Electrical heating of the furnace is via a Variac and is provided by Nichrome wire differentially wound through the partitioned asbestos supports. The heating is so arranged that the potassium bromide windows and retaining wings are preferentially heated as a precaution against condensation of hot vapours on cooler parts of the cell. The temperature of the furnace is monitored with the output current using an avometer and the temperature of the cell body is measured with a copper-constantan thermocouple calibrated between 0°C and 250°C. The shut-off valve is independently heated with Electrosil heating tapes with Simmerstat control. Tests showed that the temperature

of the cell could be maintained constant to ± 3°C and further tests showed that after allowing sufficient time for equilibration the temperature of the vapour is within 2°C of the temperature of the cell body.

Description of Optical System

The infrared spectra have been recorded with a Unicam SP100 (Mark 2) infrared spectrometer operating on a single beam principle. Due to the physical size of the furnace and the cell and also because of the dangers associated with high pressures of vapours it was necessary to devise an optical system which allowed the spectral recording of samples not placed in the sample cell-well of the conventional instrument. We have devised an optical system which allows spectral recording of samples when the cell is positioned on the top of an SP100 spectrometer. Fig. 9.2 shows the optical diagram of the single beam system which we have used. The source of infrared radiation is a Nernst filament (l = 2cm.) supplied by Unicam Ltd. (Cambridge) and held vertically in a source holder. It is 'struck' by heating with a burner and maintained by connecting to the A.C. supply to the source of the conventional instrument. The radiation passes through the cell and is reflected from a concave mirror (f = 40cm.) into the cell-well and onto a 45° plane mirror positioned at the bottom of the cell-well. For convenience we have used a 45° silvered prism as the intercepting mirror which rests on rails and is capable of adjustment in a horizontal plane. A plano-concave potassium bromide lens transmits a diverging beam into the monochromator so that the system operates as the conventional instrument in the single beam mode when the reference cell-well is blanked off.

Test runs have been performed to compare the performance of the

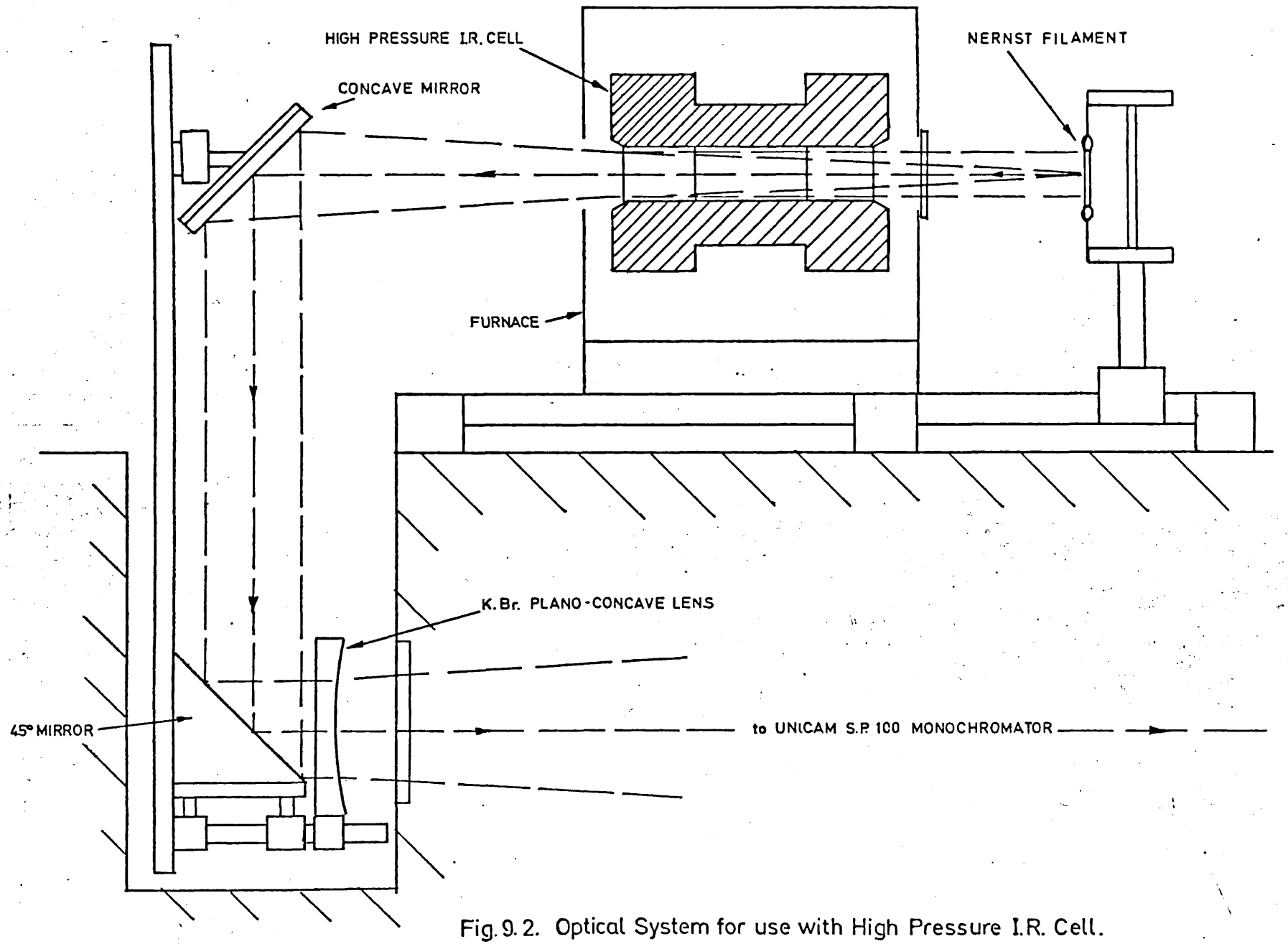

Fig. 9.2. Optical System for use with High Pressure I.R. Cell.

modified spectrometer with that obtained with the spectrometer operating in the normal single beam mode. These tests show that when the relative positions of the components in our optical system are optimized the incident energy is reduced by as little as 5%. The reproducibility of spectral traces is satisfactory and stray radiation is estimated at less than 1% by monitoring on a 100% absorbing sample of benzene. An infrared spectrum of water vapour shows that the resolving power of the instrument is not reduced by the modified optical system.

Sample Handling

The sample of benzene used in this work was B.D.H. reagent grade specially purified for molecular weight determinations. Vapour phase chromatography showed no detectable amounts of impurities and it was used without further treatment.

The method of introducing benzene vapour into the cell depends upon the required concentration and on the path length of the cell in use. For low concentrations and longer path lengths benzene was introduced directly as a vapour into a previously evacuated cell. The pressure of benzene vapour was measured on an ethylene glycol manometer to an accuracy equivalent to 0.005cm.Hg. Benzene is slightly adsorbed by glycol so that the pressure was always read as the shut-off valve was closed. For concentrations of benzene vapour above the vapour pressure at room temperature the sample of benzene was introduced into the cell as a liquid. A carefully weighed amount of benzene was sealed into a small glass ampule which was drawn out in a burner to a very fine point. The ampule was carefully placed into the inlet tube of the cell and the cell was re-assembled. After evacuating the cell the shut-off valve was closed and

the tip of the ampule was broken by vigorously shaking the cell. To prevent broken glass falling into the cell body a small piece of wire gauze was placed between the base of the inlet tube and the cell body.

Spectral Recording

The infrared absorption spectra for the fundamental vibrations of benzene vapour at a series of concentrations have been investigated over a range of temperatures. It was necessary to record spectra almost continuously during a particular run and over a considerable time in order to detect any leakage of the sample from the cell. Each fundamental absorption band was recorded in turn at a particular temperature setting and traces were often repeated to check the reproducibility. A further precaution was to record a spectrum, at a particular temperature setting, during the heating and again during the cooling of the sample. Recordings of zero transmission were made at the beginning and end of each trace. Background traces were obtained by recording the spectrum of the evacuated cell over the required frequency range.

In spite of the precautions taken, it is still found necessary to carefully examine the spectral traces for evidence of the sample having leaked from the cell or for adsorption of the sample by the cell components. Both factors were clearly indicated by the non-reproducibility of traces recorded at different times and on this account many of the early runs were invalidated. The criterion for acceptable spectra was that, providing sufficient time had been allowed for equilibration at a particular temperature setting, reproducible spectra could be obtained over a period of twenty four hours.

Measurement of Spectra

Background traces were fitted to the spectral traces for the fundamental vibrations of benzene and the spectra were re-drawn on large graph paper by plotting $\log_{10} \frac{Io}{I}$ against wavenumber frequency. The readings of $\log_{10} \frac{Io}{I}$ were taken from the spectral traces at frequency intervals of $5cm^{-1}$ and also at the positions of band maxima and minima. The integrated band areas were obtained by a counting of the squares procedure. Positions of band maxima and the frequency separation of the P- and R-branch maxima were determined from the re-drawn spectra.

Measurement of Path Length

In the determination of accurate values for the integrated intensities of infrared absorption bands we require an accurate measurement of the path length of the cell. We have used path lengths ranging from approximately 5cm. to 0.1cm. and difficulties arise in estimating the path length with sufficient accuracy because of the cell design. An additional difficulty is the possibility of the path length increasing as the temperature of the cell and the pressure inside the cell are increased.

For path lengths greater than a few millimetres we have determined the distance between the inner faces of the cell windows from measurements on the cell at room temperature taken with vernier callipers, a micrometer and a depth-gauge micrometer. Path lengths of less than a few millimetres were also determined in this manner. However, because of the large errors associated with measuring such small distances, an alternative method was also used as a check. A Beer's law plot for a band of carbon tetrachloride in the liquid phase was obtained from $(\log_{10} \frac{Io}{I})_{MAX.}$ values

in several conventional liquid cells of known path length. The small path lengths used in the high pressure cell were then obtained from this Beer's law plot by recording the $(\log_{10}\frac{I_0}{I})_{MAX.}$ for the band of carbon tetrachloride contained in the high pressure cell. It is estimated that path lengths can be estimated to an accuracy of better than 5%.

Results

The absolute intensities for the fundamental vibrations of benzene vapour have been determined at a series of temperatures between 27°C and 250°C. The fundamental vibration at 1485cm^{-1} has not been studied due to difficulties with the removal of water vapour bands. The absolute intensities for the remaining fundamental vibrations of benzene vapour at 27°C are in excellent agreement with the values reported by Spedding and Whiffen.[10] Furthermore, the absolute intensities appear to be temperature independent over the temperature range 27°C to 250°C. Mills and Whiffen[4] have shown that the absolute intensity for the fundamental vibration of a diatomic molecule should be temperature independent. Our findings for the fundamental vibrations of benzene suggests that this may also be true for polyatomic molecules particularly when temperature dependent intermolecular interactions are absent. The frequency separation of the P and R-branch maxima for the A_{2u} fundamental at 678cm^{-1} increases as the temperature is increased. The observed P-R frequency separations at a series of temperatures are in good agreement with the values calculated from the expression of Gerhard and Dennison.[41]

As the path length of the cell was gradually decreased the amount of liquid benzene added to the cell was increased so that the pressure of benzene vapour also increased. For the minimum path length used, 0.12cm.,

- -

Absolute Intensities for the Fundamental Vibrations of Benzene in the Vapour Phase

Frequency cm^{-1}	Spedding & Whiffen[10]	This Work
673	4.39	4.34
1037	0.44	0.42
1485	0.69	—
3082	3.19	3.10

The intensity unit is $10^{-7} cm.^2 mol.^{-1} sec.^{-1}$

Table 9.1

Observed and Calculated Values of $\Delta\nu_{FR}$ for the A_{2u} Fundamental at 673cm.$^{-1}$

T°K	$\Delta\nu_{FR}$ obs.cm.$^{-1}$	$\Delta\nu_{FR}$ calc.cm^{-1}
300.15	27.0	26.64
353.15	29.0	28.89
373.15	30.1	29.71
423.15	31.9	31.63
473.15	34.0	33.44
523.15	35.5	35.17

Table 9.2

the maximum amount of liquid benzene used was 1.2gms. which when vaporized in the cell (volume ~ 25cm.^{3}) is equivalent to a pressure of benzene vapour of approximately 20 atmospheres. There was no evidence for any departure from Beer's law over the concentration range studied. This suggests that specific interaction between benzene molecules is absent up to a pressure of 20 atmos. of vapour. The design of the high pressure cell used in this work did not allow investigation at higher pressures because of difficulties in obtaining shorter path lengths and in introducing larger amounts of benzene liquid.

The high pressure/variable temperature infrared gas cell developed in this work clearly has many important uses. It is envisaged that in the future it may be used to study temperature effects on complexes formed in the vapour phase and also for measuring absolute intensities of vapours of materials with low vapour pressure.

APPENDIX 1

Program to Calculate the Theoretical Band Contours for the Parallel Vibrations of Symmetric Top Molecules.

```
CHAPTERO
A>451
READ(G)                 >> frequency of band maximum
READ(B)                 >> rotational constant B
READ(A)                 >> rotational constant A
READ(D)                 >> frequency interval
READ(J)                 >> maximum J value

M=0(1)450
AM=0
REPEAT
K'=1(1)J
J'=K'(1)J

>>Delta K=0 Delta J=0
P=J'+K'
P'=J'-K'
R=P+1
R'=P'+1
Q=2J'+1
L'=J'J'+J'
J''=J'+1
X=0
V=X+G
F=L'B+K'X'A-K'K'B
F'=-0.00482575F
U=ØEXP(F')
W=2QK'K'/L'
Y=UVW
M=ØINTPT(200.5+X/D)
AM=AM+Y

>> Delta K=0 Delta J=+1
X'=2J''B
V'=X'+G
W=2RR'/J''
Y=UV'W
M=ØINTPT(X'/D+200.5)
AM=AM+Y
```

```
>> Delta K=0 Delta J=-1
X'=-2J'B
V'=X'-G
W=2P'P/J'
Y=UV'W
M=ØINTPT(X'/D+200.5)
AM=AM+Y

REPEAT
REPEAT
CAPTION
COMPUTED PARELLEL BAND SHAPES
MPRINT(ØNAME(AO),1,451,0,4,5)
NEWLINE
D''=0
I'''=0(1)450
D''=D''+AI'''
REPEAT
NEWLINE
CAPTION
SUM=
PRINT(D'')0,6
NEWLINE
END
CLOSE
```

Parallel Bands - Q Branch Spreading

```
CHAPTERO
A→451
READ(B'')                >>rotational constant B
READ(D)                  >>frequency interval
READ(J)                  >>maximum J value
M'=1(1)300
AM'=0
REPEAT
X=B''D
K'=1(1)J
K''=K'K'
J'=K'(1)J
J''=J'+1
L=J'J''
J'''=J'+J''
F=J'J''B''-0.5K''B''
F'=-0.0048257F
F'''=ØEXP(F')
F'=215F'''
A=2J'''K''/L
G=F'A
E=J'J''X
V=100E
M=ØINTPT(V)
AM=G+AM
REPEAT
REPEAT
CAPTION
COMPUTED Q BRANCH
NPRINT(ØNAME(AO),1,300,0,4,5)
NEWLINE
END
CLOSE
```

APPENDIX 2

Program to Calculate the Theoretical Band Contours for the Perpendicular Vibrations of Symmetric Top Molecules.

```
CHAPTERO
A>451
READ(G)                 >> frequency of band maximum
READ(B)                 >> rotational constant B
READ(A)                 >> rotational constant A
READ(C)                 >> zeta value
READ(E)                 >> increment in zeta value
READ(N)                 >> number of different zeta values
READ(D)                 >> frequency interval
READ(J)                 >> maximum J value
READ(D')                >> rotational constant change

N'=0(1)N
C'=C+N'E
M=0(1)450
AM=0
REPEAT
K'=1(1)J
J'=K'(1)J

>> Delta K=+1  Delta J=0
P=J'+K'
P'=J'-K'
R=P+1
R'=P'+1
Q=2J'+1
J''=J'+1
K''=K'+1
X'=K'A-K'B-K'C'A
X''=2K''C'D'A-K''K''D'A-J'J''D'B+K''K''D'B
X=A-B+2X'-2C'A+X''
V=X+G
L'=J'J'+J'
F=L'B+K'K'A-K'K'B
F'=-0.00482575F
U=ØEXP(F')
W=QP'Ø(P+1)/L'
Y=UVW
M=ØINTPT(200.5+X/D)
AM=AM+Y

>> Delta K=+1  Delta J=+1
V'=V+2J'B+2B-2J''D'B
W=RO/(P+2)/J''
Y=UV'W
X'=V'-G
X=X'/D
M=ØINTPT(X+200.5)
AM=AM+Y

>> Delta K=+1  Delta J=-1
V'=V-2J'B+2J'D'B
W=P'Ø(P'-1)/J'
```

```
Y=UV'W
X'=V'-G
X=X'/D
M=ØINTPT(X+200.5)
AM=AM+Y

>> Delta K=-1  Delta J=0
K'''=K'-1
X''=-K'''K'''D'A-2K'''C'D'A-J'J''D'B+K'''K'''D'B
V=A-2C'A+G-B-2K'A+2K'C'A+2K'B+X''
W=QPR'/L'
F=L'D+K'K'A-K'K'B
F'=-0.00482575F
U=ØEXP(F')
Y=UVW
X'=V-G
X=X'/D
M=ØINTPT(X+200.5)
AM=AM+Y

>> Delta K=-1   Delta J=+1
V'=V+2J'B-2J'D'B
W=J'R'Ø(P'+2)/L'
Y=UV'W
X'=V'-G
X=X'/D
M=ØINTPT(X+200.5)
AM=AM+Y

>> Delta K=-1   Delta J=-1
V'=V-2J'B+2J'D'B
W=PO/(P-1)/J'
Y=UV'W
X'=V'-G
X=X'/D
M=ØINTPT(X+200.5)
AM=AM+Y

REPEAT
REPEAT
CAPTION
COMPUTED BAND SHAPE ZETA =
PRINT(C')0,5
NEWLINE
NEWLINE
MPRINT(ØNAME(AO),1,451,0,4,5)
NEWLINE
D''=0
I'''=0(1)450
D''=D''+AI'''
REPEAT
NEWLINE
CAPTION
SUM =
PRINT(D'')0,6
NEWLINE
REPEAT
END
CLOSE
```

Perpendicular Bands for K=0

```
CHAPTER 0
A→451
READ(G)                 >> frequency of band maximum
READ(B)                 >> rotational constant B
READ(A)                 >> rotational constant A
READ(C)                 >> zeta value
READ(E)                 >> increase in zeta value
READ(N)                 >> number of different zeta values
READ(D)                 >> frequency interval
READ(J)                 >> maximum J value
READ(D')                >> rotational constant change
N'=0(1)N
C'=C+N'E
M=0(1)450
AM=0
REPEAT

K'=0
J'=1(1)J

>>DELTA K=+1 DELTA J=0
P=J'+K'
P'=J'-K'
R=P+1
R'=P'+1
Q=2J'+1
J''=J'+1
K''=K'+1
X'=K'A-K'B-K'C'A
X''=K''C'D'A-0.5K''K''D'A-J'J''D'B+K''K''D'B
X=A-B+2X'-C'A+X''
V=X+G
L'=J'J'+J'
F=L'B+K'K'A-K'K'B
F'=-0.00482575F
U=ØEXP(F')
W=QP'Ø(P+1)/L'
Y=0.5UVW
M=ØINTPT(200.5+X/D)
AM=AM+Y

>>DELTA K=+1 DELTA J=+1
V'=V+2J'B+2B-2J'J''D'B
W=RO/(P+2)/J''
Y=0.5UV'W
X'=V'-G
X=X'/D
M=ØINTPT(X+200.5)
AM=AM+Y
```

```
>>DELTA K=+1 DELTA J=-1
V'=V-2J'B-J'J'D'B+J'D'B
W=P'Ø(P'-1)/J'
Y=0.5UV'W
X'=V'-G
X=X'/D
M=ØINTPT(X+200.5)
AM=AM+Y
REPEAT
CAPTION
COMPUTED BAND SHAPE ZETA =
PRINT(C')0,5
NEWLINE
NEWLINE
MPRINT(ØNAME(A0),1,451,0,4,5)
NEWLINE
D''=0
I'''=0(1)450
D''=D''+AI'''
REPEAT
NEWLINE
CAPTION
SUM=
PRINT(D'')0,6
NEWLINE
REPEAT
END
CLOSE
```

APPENDIX 3

General 3 by 3 Eigenvalue Eigenvector Problem

```
CHAPTER0
>> THIS PROGRAM EVALUATES THE EIGENVALUES AND EIGENVECTORS
>> OF ANY GENERAL 3X3 MATRIX. THE MATRIX IS EITHER READ IN
>> (Z''=0) OR FORMED BY MULTIPLICATION OF F AND G (Z''=1).
>> IN EITHER CASE THE MATRIX IS STORED ROW BY ROW AS :
>> A1 A2 A3 A4 A5 A6 A7 A8 A9.
A->30
B->10
C->20
D->20
E->20
F->20
G->20
H->30
U->20
V->30
W->10
X->10
Y->10
Z->10
>> THE PROGRAM ALSO DETERMINES THE FACTORS E3 E4 E5 WHICH ARE
>> NECESSARY TO CONVERT THE NORMALISED L MATRIX INTO THE ACTUAL
>> L MATRIX.
S=1
1)READ(Z'')                >> test parameter
JUMP2,0.5>Z''
I=1(1)9
READ(GI)                   >> the G matrix
REPEAT
I=1(1)9
READ(FI)                   >> the F matrix
REPEAT
A1=G1F1+G2F4+G3F7
A2=G1F2+G2F5+G3F8
A3=G1F3+G2F6+G3F9
A4=G4F1+G5F4+G6F7
A5=G4F2+G5F5+G6F8
A6=G4F3+G5F6+G6F9
A7=G7F1+G8F4+G9F7
A8=G7F2+G8F5+G9F8
A9=G7F3+G8F6+G9F9
NEWLINE
CAPTION
THE GF MATRIX
NEWLINE
I=1(1)3
PRINT(AI)0,6
REPEAT
NEWLINE
I=4(1)6
PRINT(AI)0,6
REPEAT
NEWLINE
```

```
I=7(1)9
PRINT(AI)0,6
REPEAT
NEWLINE
JUMP3
2)I=1(1)9
READ(AI)                    >> the CF matrix
REPEAT
3)X=-A1-A5-A9
Y=A1A5+A1A9+A5A9-A6A8-A2A4-A3A7
Z=-A1A5A9+A1A6A8+A2A4A9-A2A6A7-A3A4A8+A3A5A7
>>USE SUBSTITUTION LAMBDA=W-X/3
>>THEN EQUATION IS OF THE FORM WWW+BW+C=0
B=Y-XX/3
C=2XXX-9XY+27Z
C=C/27
H1=-BBB/27
H2=ØSQRT(H1)
H3=2H2
H3=-C/H3
H4=1-H3H3
H5=ØSQRT(H4)
H6=ØARCTAN(H3,H5)
H7=-B/3
H8=ØSQRT(H7)
H9=H6/3
H10=ØCOS(H9)
W1=2H8H10
H11=2;/3
H12=H9+H11
H13=H9+2H11
H14=ØCOS(H12)
H15=ØCOS(H13)
W2=2H8H14
W3=2H8H15
I=1(1)3
BI=WI-X/3
REPEAT
NEWLINE
CAPTION
EIGENVALUES
NEWLINE
I=1(1)3
PRINT(BI)0,6
REPEAT
V10=A2A6+B1A3-A5A3
V7=B1B1+A1A5-B1A1-A5B1-A2A4
V7=V7/V10
V4=B1-A1-A3V7
V4=V4/A2
V11=1+V4V4+V7V7
V12=ØSQRT(V11)
V1=1/V12
V4=V4/V12
V7=V7/V12
V13=A2A6+B2A3-A3A5
```

```
V8=B2B2-B2A1+A1A5-A5B2-A4A2
V8=V8/V13
V5=B2-A1-A3V8
V5=V5/A2
V14=1+V5V5+V8V8
V15=ØSQRT(V14)
V2=1/V15
V5=V5/V15
V8=V8/V15
V16=A2A6+B3A3-A3A5
V9=B3B3-B3A1+A1A5-A5B3-A2A4
V9=V9/V16
V6=B3-A3V9-A1
V6=V6/A2
V17=1+V6V6+V9V9
V18=ØSQRT(V17)
V3=1/V18
V6=V6/V18
V9=V9/V18
NEWLINE
CAPTION
THE L MATRIX (EIGENVECTORS)
NEWLINE
I=1(1)3
PRINT(VI)0,6
REPEAT
NEWLINE
I=4(1)6
PRINT(VI)0,6
REPEAT
NEWLINE
I=7(1)9
PRINT(VI)0,6
REPEAT
U1=V1F1+V4F4+V7F7
U2=V1F2+V4F5+V7F8
U3=V1F3+V4F6+V7F9
E1=U1V1+U2V4+U3V7
E2=E1/B1
E3=ØSQRT(E2)
U1=V2F1+V5F4+V8F7
U2=V2F2+V5F5+V8F8
U3=V2F3+V5F6+V8F9
E1=U1V2+U2V5+U3V8
E2=E1/B2
E4=0/SQRT(E2)
U1=V3F1+V6F4+V9F7
U2=V3F2+V6F5+V9F8
U3=V3F3+V6F6+V9F9
E1=U1V3+U2V6+U3V9
E2=E1/B3
E5=ØSQRT(E2)
NEWLINE
CAPTION
NOMALIZATION FACTORS
I=3(1)5
```

```
PRINT(EI)0,6
REPEAT
I=1(3)7
V1=V1/E3
REPEAT
I=2(3)8
V1=V1/E4
REPEAT
I=3(3)9
V1=V1/E5
REPEAT
NEWLINE
CAPTION
ACTUAL L MATRIX
NEWLINE
I=1(1)3
PRINT(VI)0,6
REPEAT
NEWLINE
I=4(1)6
PRINT(V1)0,6
REPEAT
NEWLINE
I=7(1)9
PRINT(VI)0,6
REPEAT
D1=V1V1+V2V2+V3V3
D2=V1V4+V2V5+V3V6
D3=V1V7+V2V8+V3V9
D4=V4V1+V5V2+V6V3
D5=V4V4+V5V5+V6V6
D6=V4V7+V5V8+V6V9
D7=V7V1+V8V2+V9V3
D8=V7V4+V8V5+V9V6
D9=V7V7+V8V8+V9V9
NEWLINE
CAPTION
THE G MATRIX
NEWLINE
I=1(1)3
PRINT(DI)0,6
REPEAT
NEWLINE
I=4(1)6
PRINT(DI)0,6
REPEAT
NEWLINE
I=7(1)9
PRINT(DI)0,6
REPEAT
NEWLINE
S=S+1
READ(K)                    >> cycle parameter
JUMP1,K>_S
END
CLOSE
```

APPENDIX 4

Program to Calculate the Zeta Matrix for any Symmetry Species.

```
CHAPTER 0
A>100
B>1000
C>100
D>1000
E>1000
F>1000
U>10
V>1000
X>1000
Y>1000
Z>100
READ(P)                 >> number of columns in B matrix
READ(R)                 >> number of rows in B matrix
L=RP
L''=1(1)L
READ(BL'')              >> the B matrix
REPEAT
I=1(1)P
READ(CI)                >> the atomic masses
REPEAT
J'=1(1)P
CJ'=ØSQRT(CJ')
CJ'=1/CJ'
REPEAT
I''=1(1)R
J''=1(1)P
M'=I''P-P+J''
M''=J''
DM'=BM'CM''
REPEAT
REPEAT
MPRT(ØNAME(V(1)),ØNAME(D(1)),ØNAME(D(1)),6,6,24)
NEWLINE
CAPTION
THE G MATRIX
NEWLINE
T''=RR
S''=ØINTPT(0.333T''+1.05)
I=0
I'=1(1)S''
J''=1(1)3
PRINT(VI)0,6
I=I+1
REPEAT
NEWLINE
REPEAT
NEWLINE
NEWLINE
U=0.5P
P'=ØINTPT(U+0.2)
J=1(1)R
J'=JP-P
```

```
I=1(1)P'
I'=2I
K=J'+I'
K'=K-1
EK'=-DK
EK=DK'
REPEAT
REPEAT
I''=1(1)R
K''=1(1)R
M=I''R-R+K''
FM=0
J''=1(1)P
M'=I''P-P+J''
M''=K''P-P+J''
FM=FM+EM'DM''
REPEAT
REPEAT
REPEAT
N=RR
I=1(1)N
READ(AI)                    >> the L to tho minus one matrix
REPEAT
I''=1(1)R
K''=1(1)R
M=I''R-R+K''
XM=0
J''=1(1)R
M'=I''R-R+J''
M''=J''R-R+K''
XM=XM+AM'FM''
REPEAT
REPEAT
REPEAT
NEWLINE
CAPTION
THE ZETA MATRIX
NEWLINE
I=1(1)N
READ(ZI)                    >> the L transpose to the minus one matrix
REPEAT
I''=1(1)R
K''=1(1)R
M=I''R-R+K''
YM=0
J''=1(1)R
M'=I''R-R+J''
M''=J''R-R+K''
YM=YM+XM'ZM''
REPEAT
PRINT(YM)0,6
REPEAT
NEWLINE
REPEAT
END
CLOSE
```

References

1. W. Heitler,
   The Quantum Theory of Radiation, Oxford, New York and London, (1954).
2. B. Crawford, Jnr.,
   J. Chem. Phys., 29, 1042, (1958).
3. E.B. Wilson, J.C. Decius and P.C. Cross,
   Molecular Vibrations, McGraw-Hill, New York, (1955).
4. I.M. Mills and D.H. Whiffen,
   J. Chem. Phys., 30, 1619, (1959).
5. B. Crawford, Jnr. and H.L. Dinsmore,
   J. Chem. Phys., 18, 983, 1682, (1950).
6. I.M. Mills, W.L. Smith and J.L. Duncan,
   J. Mol. Spectry., 16, 349, (1965).
7. D.F. Hornig and D.C. McKean,
   J. Phys. Chem., 59, 1133, (1955).
8. D. Steele,
   Quart. Rev. (London), 18, 21, (1964).
9. C.A. Coulson,
   in Proceedings of the Conference on Molecular Spectroscopy, E. Thornton and H.W. Thompson (Editors), Pergamon, London, (1959), p.183.
10. H. Spedding and D.H. Whiffen,
    Proc. Roy. Soc. (London), A238, 245, (1956).
11. D.H. Whiffen,
    Phil. Trans. Roy. Soc. (London), A248, 131, (1955).

12. A.C. Albrecht,

J. Mol. Spectry., 5, 236, (1960).

13. L.M. Sverdlov,

Optics and Spectroscopy, 8, 316, (1960).

14. M.A. Kovner and B.N. Snegirev,

Optics and Spectroscopy, 9, 328, (1960).

15. L.M. Sverdlov,

Optics and Spectroscopy, 10, 33, (1961).

16. C.R. Bailey, J.B. Hale, C.K. Ingold and J.W. Thompson,

J. Chem. Soc., 931, (1936).

17. C.R. Bailey, S.C. Carson and C.K. Ingold,

J. Chem. Soc., 252, (1946).

18. N. Herzfield, C.K. Ingold and H.G. Poole,

J. Chem. Soc., 316, (1946).

19. L. Delbouille,

J. Chem. Phys., 25, 182, (1956).

20. D. Steele and D.H. Whiffen,

Trans. Faraday Soc., 55, 369, (1959).

21. W.B. Person, D.A. Olsen and J.N. Fordemwalt,

Spectrochim. Acta., 22, 1733, (1966).

22. J.L. Hollenberg and D.A. Dows,

J. Chem. Phys., 37, 1300, (1962).

23. R.D. Mair and D.R. Hornig,

J. Chem. Phys., 17, 1236, (1949).

24. S. Brodersen and A. Langseth,

Mat. Fys. Skr. Dan. Vid. Selsk., 1, 1, (1956).

25. J.F. Counsell, J.H.S. Green, J.L. Hales and J.F. Martin,
Trans. Faraday Soc., 61, 212, (1965).

26. J.C. Duinker,
Ph.D. Thesis, University of Amsterdam, (1964).

27. J.C. Duinker and I.M. Mills,
Spectrochim. Acta., 24A, 417, (1968).

28. J.H. Callomon, T.M. Dunn and I.M. Mills,
Phil. Trans. Roy. Soc. (London), A259, 499, (1966).

29. J.R. Scherer,
Spectrochim. Acta., 21, 321, (1965).

30. D. Steele and D.H. Whiffen,
Trans. Faraday Soc., 56, 5, (1960).

31. D. Steele and D.H. Whiffen,
Trans. Faraday Soc., 56, 8, (1960).

32. D. Steele and D.H. Whiffen,
Trans. Faraday Soc., 56, 177, (1960).

33. E. Bright Wilson, Jnr. and A.J. Wells,
J. Chem. Phys., 14, 578, (1946).

34. S.S. Penner and D. Weber,
J. Chem. Phys., 19, 807, 817, (1951).

35. C.H. Townes and A.L. Schawlow,
Microwave Spectroscopy, McGraw-Hill, New York, (1955).

36. J. Overend, M.J. Youngquist, E.C. Curtis and B. Crawford, Jnr.,
J. Chem. Phys., 30, 532, (1959).

37. D. Steele and D.H. Whiffen,
J. Chem. Phys., 29, 1194, (1958).

38. P.J. Hendra, R.D.G. Lane and B. Smethurst,

J. Sci. Inst., 40, 457, (1963).

39. H.M. Randall, D.M. Dennison, N. Ginsburg and L.R. Weber,

Phys. Rev., 52, 160, (1937).

40. I.M. Mills,

Ann. Rep. Progr. Chem. (Chem. Soc. London), 55, 56, (1958).

41. S.L. Gerhard and D.M. Dennison,

Phys. Rev., 43, 197, (1933).

42. E. Teller,

Handbuch u. Jahrb. chem. Physik, 9(II), 43, (1934).

43. R.M. Badger and L.R. Zumwalt,

J. Chem. Phys., 6, 711, (1938).

44. M. Johnston and D.M. Dennison,

Phys. Rev., 48, 868, (1935).

45. H.H. Nielsen,

Rev. Mod. Phys., 23, 90, (1951).

46. W.F. Edgell and R.E. Moynihan,

J. Chem. Phys., 27, 155, (1957).

47. W.F. Edgell and R.E. Moynihan,

J. Chem. Phys., 45, 1205, (1966).

48. A.H. Nahi, E.K. Plyler and R. Thibault,

J. Chem. Phys., 37, 1899, (1962).

49. I. Levin and S. Abramowitz,

J. Chem. Phys., 43, 4213, (1965).

50. J. Aldous and I.M. Mills,

Spectrochim. Acta., 19, 1567, (1963).

51. J.L. Duncan and I.M. Mills,
Spectrochim. Acta., 20, 523, (1964).

52. J.M. Hollas,
Spectrochim. Acta., 22, 81, (1966).

53. G. Herzberg,
Infrared and Raman Spectra of Polyatomic Molecules,
van Nostrand, New York, (1945).

54. H.C. Allen, Jnr. and P.C. Cross,
Molecular Vib-Rotors, Wiley, New York and London, (1963).

55. F. Reiche and H. Rademaker,
Z. Physik, 41, 453, (1927).

56. E. Teller and L. Tisza,
Z. Physik, 73, 791, (1932).

57. J. Overend and M.J. Youngquist,
in Infrared Spectroscopy and Molecular Structure,
M. Davies (Editor), Elsevier, London, (1963), p.345.

58. D.A. Dows and A.L. Pratt,
Spectrochim. Acta., 18, 433, (1962).

59. B. Crawford, Jnr. and F.A. Miller,
J. Chem. Phys., 17, 249, (1949).

60. W.D. Jones,
J. Mol. Spectry., 22, 296, (1967).

61. T.L. Brown,
J. Chem. Phys., 43, 2780, (1965).

62. I.M. Mills, W.B. Person, J.R. Scherer and B. Crawford, Jnr.,
J. Chem. Phys., 28, 851, (1958).

63. R.P. Bell, H.W. Thompson and E.E. Vago,
Proc. Roy. Soc., A192, 498, (1948).

64. W.B. Person and L.C. Hall,
Spectrochim. Acta., 20, 771, (1964).

65. J.H. Meal and S.R. Polo,
J. Chem. Phys., 24, 1119, (1956).

66. J.H. Meal and S.R. Polo,
J. Chem. Phys., 24, 1126, (1956).

67. R.C. Lord and R.E. Merrifield,
J. Chem. Phys., 20, 1348, (1952).

68. I.M. Mills,
J. Mol. Spectry., 5, 334, (1960).

69. N.Q. Chako,
J. Chem. Phys., 2, 644, (1934).

70. S.R. Polo and M.K. Wilson,
J. Chem. Phys., 23, 2376, (1955).

71. J. van Kranendonk,
Physica, 23, 825, (1957).

72. L. Onsager,
J. Am. Chem. Soc., 58, 1486, (1936).

73. W.C. Mullard and J.W. Straley,
J. Chem. Phys., 27, 877, (1957).

74. W.B. Person,
J. Chem. Phys., 28, 319, (1958).

75. E. Hirota,
Bull. Chem. Soc. Japan, 27, 295, (1954).

76. H. Ratajczak and W.J. Orville-Thomas,
Trans. Faraday Soc., 61, 2603, (1965).

77. I.C. Hisatsune and E.S. Jayadevappa,
J. Chem. Phys., 32, 563, (1960).

78. S. Maeda and P.N. Schatz,
J. Chem. Phys., 36, 571, (1962).

79. W.B. Person and L.C. Hall,
Spectrochim. Acta., 20, 771, (1964).

80. M.P. Lisitsa and V.N. Malinko,
Optics and Spectroscopy, 4, 455, (1958).

81. J. Yarwood and W.J. Orville-Thomas,
Trans. Faraday Soc., 62, 3011, (1966).

82. L. Nemes and W.J. Orville-Thomas,
Trans. Faraday Soc., 61, 2612, (1965).

83. S. Tanaka, K. Tanabe and H. Kamada,
Spectrochim. Acta., 23A, 209, (1967).

84. D.H. Whiffen,
Trans. Faraday Soc., 49, 878, (1953).

85. A.D. Buckingham,
Proc. Roy. Soc. (London), A248, 169, (1958).

86. A.D. Buckingham,
Proc. Roy. Soc. (London), A255, 32, (1960).

87. O.F. Kalman and J.C. Decius,
J. Chem. Phys., 35, 1919, (1961).

88. C.J.F. Böttcher,
Theory of Electric Polarization, Elsevier, New York, (1952).

89. J.A. Stratton,

Electromagnetic Theory, McGraw-Hill, New York, (1941).

90. E.L. Stoner,

Phil. Mag., 36, Ser.7, 803, (1945).

91. Th. G. Scholte,

Physica, 15, 437, (1949).

92. S. Ashdown, T.F. Crowdy and D. Steele,

Lab. Prac., 15, 868, (1966).

93. L. Pauling,

The Nature of the Chemical Bond, Oxford, London, (1960) (Third Edition).

94. C.R. Patrick and G.S. Prosser,

Nature, 187, 1021, (1960).

95. J.C.A. Boeyens and J.H. Herbstein,

J. Phys. Chem., 69, 2153, (1965).

96. E. McLaughlin and C.E. Messer,

J. Chem. Soc., (A), 1166, (1966).

97. W.A. Duncan and F.L. Swinton,

Trans. Faraday Soc., 62, 1082, (1966).

98. W.A. Duncan, J.P. Sheridan and F.L. Swinton,

Trans. Faraday Soc., 62, 1090, (1966).

99. D.V. Fenby, I.A. McLure and R.L. Scott,

J. Phys. Chem., 70, 602, (1966).

100. M. Horak and J. Pliva,

Spectrochim. Acta., 21, 911, (1965).

101. C. La Lau,

in Proceedings of the Conference on Molecular Spectroscopy, E. Thornton and H.W. Thompson (Editors), Pergamon, London, (1959).

102. A. Finch, I.J. Hyams and D. Steele,

Trans. Faraday Soc., 61, 399, (1965).

103. A. Finch, P.N. Gates and D. Steele,

Trans. Faraday Soc., 61, 2623, (1965).

104. A. Rollier,

Gazz. chim. ital., 77, 372, (1947).

105. L.J. Andrews and R.M. Keefer,

in Advances in Inorganic Chemistry and Radiochemistry, Vol.3, Academic Press, New York, (1961).

106. K. Hartley and H.A. Skinner,

Trans. Faraday Soc., 46, 621, (1950).

107. P.A.D. de Maine,

J. Chem. Phys., 26, 1192, 1199, (1957).

108. H. Yada, J. Tanaka and S. Nagakura,

Bull. Chem. Soc. Japan, 33, 1660, (1960).

109. J. Yarwood and W. B. Person,

J. Am. Chem. Soc., 90, 594, (1968).

110. E.E. Ferguson and F.A. Matsen,

J. Chem. Phys., 29, 105, (1958).

111. E.E. Ferguson,

Spectrochim. Acta., 10, 123, (1957).

R. H. C.
LIBRARY

112. E.E. Ferguson and F.A. Matsen,

J. Am. Chem. Soc., 82, 3268, (1960).

113. E.E. Ferguson,

J. Chim. Phys., 61, 257, (1964).

114. H.B. Friedrich and W.B. Person,

J. Chem. Phys., 44, 2161, (1966).

115. K.W. Illinger and D.E. Freeman,

J. Mol. Spec., 9, 191, (1962).